BDNF in Developing Aortic Baroreceptors &

Its Role in the Dendritic Morphogenesis of Neurons from

the *Nucleus Tractus Solitarius*

By Jessica L. Martin

A DISSERTATION

Presented to the Neuroscience Graduate Program and
the Oregon Health & Science University School of Medicine
in partial fulfillment of the requirements for the degree of
Doctor of Philosophy

December 2010

School of Medicine

Oregon Health & Science University

CERTIFICATE OF APPROVAL

This is to certify that the PhD dissertation of

Jessica L. Martin

has been approved

_____

Agnieszka Balkowiec

_____

Gary Banker

_____

Beth Habecker

_____

Michael C. Andresen

_____

John Bissonnette

_____

Matthew Frerking

TABLE OF CONTENTS

Acknowledgements

Thank you to Hui-ya (Julia) Hsieh for generating the data showing electrically-stimulated and calcium channel-dependent, endogenous BDNF release from nodose sensory neurons. Thank you to Victoria Jenkins for testing the specificity of the chicken anti-BDNF antibody and performing morphometric analyses of nodose ganglion neurons. Thank you to Alexandra Brown for determining glial cell density in dissociated cultures of the *Nucleus Tractus Solitarius*, as well as assisting in image acquisition.

To Agnieszka Balkowiec: Thank you for giving me the tools, resources, and insights into what it takes to succeed. Through many ups and downs, we have both persevered. Mostly, thank you for giving me the freedom to dream. It is the best part of what I do, so thank you!

To members of my committees – Gary Banker, Mike Andresen, Beth Habecker, Matt Frerking, Pam Lein, and John Bissonnette: Thank you for helping me to grow as a scientist, keeping me on target, honesty, and advice. Your guidance has shaped these projects in so many valuable ways.

To members of the Balkowiec lab present and past – Anke Vermehren-Schmaedick, Victoria Jenkins, Julia Hsieh, Alex Brown, Leila Tarsa, and Heather Scanlin: thank you for advice, support, help, and encouragement. It has been wonderful doing life and science with you.

To a few individuals who provided extra help along the way: Stefanie Kaech and Mike Danilchik for imaging help and guidance; Mike Meredith for statistics guidance; and Sue Aicher for a vast knowledge base of immunohistochemistry.

To my family and friends: Jason Martin, you have been my partner in crime, a source of strength and stability through rocky times, and an inspiration both personally and scientifically; Ian Martin, thank you for being my greatest source of joy; my parents, Jim and Donna Dabler, you have been the greatest source of love, support, and encouragement I could ever ask for; my siblings, Jim Dabler and Vicky Eimer, thank you for your love, support, and encouragement over the years.

Abstract

Cardiorespiratory reflexes are essential to life, maintaining key physiological functions such as breathing and blood pressure. However, the characteristics of these reflexes at birth differ significantly from the characteristics in adults, suggesting a period to refine reflex circuitry. Mechanisms that guide maturation in these pathways are virtually unknown. This lack of understanding is an impediment to discovering the underlying causes of developmental disorders, such as Sudden Infant Death Syndrome, the leading cause of death during the first year of life. Brain-derived neurotrophic factor (BDNF) is one candidate mediator of development in cardiorespiratory pathways and is known to mediate activity-dependent maturation throughout the central nervous system. However, its functional role in developing cardiorespiratory pathways is unknown. My overall hypothesis is that BDNF in cardiorespiratory afferents drives activity-dependent maturation of circuitry in the brainstem *Nucleus Tractus Solitarius* (NTS). The studies in this dissertation support this overall hypothesis. I first characterize BDNF protein distribution and release in the sensory portion of a model cardiorespiratory reflex, the aortic baroreceptor reflex. Then, I assess one possible maturational function of BDNF, dendritogenesis of neurons in the NTS.

Immunoreactivity to BDNF is present in the cell bodies of baroreceptor neurons in the nodose ganglion (NG), their central projections in the solitary tract, and terminal-like structures in the lower brainstem NTS. In addition, native BDNF is released in an activity-dependent manner from cultured newborn NG neurons in response to patterns that mimic the *in vivo* activity of baroreceptor afferents. Thus, these studies show that BDNF is poised to mediate

activity-dependent maturation through the release of BDNF from aortic baroreceptors onto their targets in the NTS.

Coinciding with the maturation of cardiorespiratory reflexes, many structural and functional changes occur within the NTS, including the extension and elaboration of dendritic arbors. The mechanisms guiding dendritic elaboration in the NTS, however, are unknown. Using a dissociate culture model of the NTS, I tested the hypothesis that BDNF mediates dendritic outgrowth and complexity of NTS neurons. Unexpectedly, I discovered a significant contribution of glia in regulating BDNF-mediated dendritic growth. In mixed neuron-glia cultures, BDNF promotes dendritic outgrowth and complexity. However, depleting glia changes the direction of BDNF-mediated effects from promoting to inhibiting NTS dendritogenesis. In addition, I show that the number of glia alone influences dendritic growth of NTS neurons and provide evidence that an unidentified astrocyte-derived diffusible factor inhibits NTS dendritic growth. These findings have important implications for dendritogenesis in the NTS *in vivo,* providing evidence for a functional role of BDNF and showing an unappreciated role of glia in guiding dendritogenesis. Together, these studies further our understanding of maturation in cardiorespiratory pathways and point to BDNF, together with glia, as a significant contributor in guiding these events.

Chapter 1: Introduction

Cardiorespiratory reflexes, including the aortic baroreceptor reflex, are essential to life. They are required to regulate key physiological functions, such as breathing and arterial blood pressure, that maintain bodily homeostasis in spite of a constantly changing environment. However, the characteristics of these reflexes at birth significantly differ from the characteristics in adults, suggesting a period to refine reflex circuitry. The molecular mechanisms guiding circuit development in these reflexes are virtually unknown. By understanding the processes underlying normal development, it becomes possible to discern what goes awry in developmental disorders, such as Sudden Infant Death Syndrome (SIDS), the leading cause of death in babies that is characterized by a failure of several key cardiorespiratory reflexes during sleep. In addition, perturbed developmental events spanning postnatal critical periods are hypothesized to permanently alter the function of these reflexes and may predispose an individual to conditions later in life, such as hypertension (Bavis and Mitchell, 2008). Therefore, a better understanding of how autonomic circuitry develops has potential broader clinical implications for a lifetime.

The work presented in this dissertation is a step toward understanding mechanisms of maturation in cardiorespiratory reflex pathways. In particular, I focus on the neurotrophin brain-derived neurotrophic factor (BDNF), a candidate molecular mediator of development in these pathways. In other areas of the brain, BDNF plays a crucial role in mediating activity-dependent maturation of neural circuits. Given its established role in circuit maturation and the evidence for location of both BDNF and the high-affinity receptor, TrkB, in the afferent portions

of visceral sensory pathways including cardiorespiratory reflex pathways, BDNF is poised to play a crucial role in their maturation. Currently, the functional role of BDNF in these pathways during postnatal maturation is not known.

Overview of the thesis.

In chapter 2, I am providing detailed background information necessary to understand the rationale and implications of the experiments and findings presented in Chapters 3 and 4. The experiments in both of these chapters are aimed at moving closer to understanding the functional role of BDNF in cardiorespiratory pathways with my more general hypothesis being:

BDNF in cardiorespiratory afferents drives activity-dependent maturation of circuitry in the brainstem *Nucleus Tractus Solitarius* (NTS).

In Chapter 3, I characterize BDNF protein expression in the sensory portion of the aortic baroreceptor reflex, which is essential to maintaining blood pressure homeostasis. The rationale behind characterizing BDNF in this specific cardiorespiratory reflex is twofold. First, the aortic baroreflex is an excellent model to study the role of activity because the type and patterns of activity in aortic baroreceptors are very well characterized. Thus, it is very well suited to assessing the role of possible molecular mediators of activity-dependent maturation, such as BDNF. A second advantage is that the peripheral axons of aortic baroreceptors can be isolated and identified by neuronal tracing techniques because of their anatomical separation from other visceral afferents. Specifically, aortic baroreceptors travel unaccompanied in the aortic depressor nerve (ADN) before it joins the vagus nerve, which contains both ascending sensory axons of many different modalities and descending parasympathetic axons. In

experiments described in Chapter 3, I used anterograde neuronal tracing from the ADN to provide compelling evidence that BDNF in viscerosensory afferents is transported to their central synapses with second-order neurons in the NTS; this being a requirement for BDNF-mediated, afferent activity-dependent maturation of neural circuitry in the NTS. Thus, work in chapter 3 lays the foundation for using the aortic baroreflex as a model to study the role of BDNF in the activity-dependent maturation of cardiorespiratory reflexes.

In Chapter 4, I move from characterizing BDNF in aortic baroreceptor afferents to addressing a possible functional role for BDNF in the central targets of visceral sensory afferents, i.e. second-order neurons in the NTS. To date, ascertaining the postnatal functions of BDNF in cardiorespiratory pathways has been hindered because BDNF is required for the survival of visceral afferents. Therefore, general BDNF knock-out mouse models cannot be used to study its role in the postnatal maturation of cardiorespiratory circuitry because visceral afferents are missing altogether. To date, no good selective BDNF knock-out models exist to circumvent the loss of sensory afferents, yet assess the functional role of removing BDNF postnatally after sensory neurons no longer require BDNF for survival. In order to get around this issue, I have taken an *in vitro* approach to assess one possible functional role: regulation of the dendritic growth of neurons in the NTS. My findings indicate that BDNF may play a prominent role *in vivo* in establishing cardiorespiratory neural circuitry through dendritogenesis. Furthermore, I have unexpectedly uncovered a previously unrecognized role of glia in NTS dendritogenesis.

In chapter 5, I piece together what my findings may mean for the maturation of cardiorespiratory reflex pathways *in vivo* and present possible future experiments as well as challenges to moving forward in understanding the mechanisms of postnatal circuit maturation.

Chapter 2: Review of the Literature

This review focuses on the following major topics relevant to my dissertation work: 1) cardiorespiratory control pathways: the sensory component, 2) the aortic baroreflex, 3) BDNF: overview, 4) BDNF and its receptors in the sensory portion of autonomic reflex pathways, 5) dendritic morphology, and 6) glia, with an emphasis on astrocytes. In this chapter, I have provided broad review of each of these topics, including linkages between them whenever appropriate.

Cardiorespiratory control pathways: the sensory component.

Cardiorespiratory reflexes are autonomic reflexes critical to maintaining whole organism homeostasis. Key physiological functions that are regulated by these reflexes include breathing, arterial blood pressure, and cardiac function (Loewy, 1990). My dissertation concerns the first-order sensory neurons with cell bodies in the nodose ganglion (NG) and their central targets, i.e. the second-order neurons in the brainstem *Nucleus Tractus Solitarius* (NTS). I will review pertinent information that is critical to understanding the research design and my findings described in Chapters 3 and 4, as well as the significance of these findings.

General organization and functional properties of viscerosensory afferents and their synaptic connections with NTS second-order sensory neurons. Cardiorespiratory afferents are a sub-division of the broader category of visceral afferents, which also include neurons that innervate such peripheral targets as the gastrointestinal tract. The cell bodies of viscerosensory neurons reside in the nodose, petrosal, and jugular ganglion. Peripheral terminals of these neurons are located in various organs, such as the heart, lungs and large arteries, where they transduce

sensory stimuli to action potentials which, in turn, are conducted to the NTS. Visceral afferents are located mainly in one of two cranial nerves, glossopharyngeal (IX) and vagus (X), through which they enter the brainstem to join the solitary tract in the dorsal medulla. Once in the solitary tract, axons ramify and make synapses, including many that are axo-somatic, with their postsynaptic targets, i.e. the second-order neurons, in the NTS (Andresen and Kunze, 1994)(**Fig. 2-1**).

Visceral afferents fall into one of two broad categories, based on the axon size and the degree of myelination: Adelta (δ) or C-fibers (Brown, 1980; Schild et al., 1994). Aδ fibers are thicker, lightly myelinated, and conduct action potentials at an average rate of ~10 m/s. On the other hand, C-fibers are smaller, unmyelinated and conduct action potentials at a much slower average rate of ~0.5 m/s (Fan and Andresen, 1998). Both Aδ and C-fibers use glutamate as their primary neurotransmitter at synapses with second-order NTS neurons (Talman et al., 1980; Pilowsky and Goodchild, 2002). In addition, these afferents synthesize and release a number of other neurotransmitters/neuropeptides such as ATP and substance P (Pilowsky and Goodchild, 2002). The approximate proportion of fiber types, at least in the aortic baroreceptor population, is around 10% Aδ and 90% C-fibers (Andresen et al., 1978). Interestingly, these two fiber types can be identified by distinct receptors: purinergic receptors (P2X) (Jin et al., 2004) and hyperpolarization-activated cyclic nucleotide-gated ion channel protein 1 (HCN1) (Doan et al., 2004) on Aδ-fibers, and the capsaicin-sensitive receptor, transient receptor potential vanilloid type 1 (TRPV1), on C-fibers (Jin et al., 2004). Afferent signals derived from Aδ and C-fibers do not converge at the same second-order NTS neurons, but rather remain distinct. In fact, minimal convergence of afferent input (three or fewer mono- or poly-synaptic inputs) and almost no divergence of individual afferent axons are observed at second-order neurons,

arguing that second-order NTS neurons faithfully represent their visceral target (McDougall et al., 2009).

Visceral afferent connections with their second-order NTS neurons are very robust and rarely fail at low frequencies of stimulation (Andresen and Yang, 1995; Andresen and Peters, 2008), although synaptic failures become apparent with increasing action potential frequency, especially in C-fibers (Andresen and Peters, 2008). In addition, frequency-dependent depression of synaptic transmission is a common feature of viscerosensory synapses under high frequencies of afferent stimulation (Seller and Illert, 1969; Liu et al., 2000). Glutamate from afferent terminals signals through non-NMDA receptors on second-order neurons (Andresen and Yang, 1990) with a distinct lack of direct NMDA-dependent activation by afferents (Doyle et al., 2002). However, NMDA receptor activation appears to influence second-order neurons through poly-synaptic pathways (Zhang and Mifflin, 1998; Yen et al., 1999).

Organization and properties of the NTS. The NTS is the main integration site for the CNS control of cardiorespiratory reflexes (Andresen and Kunze, 1994). The cell bodies of NTS neurons are organized in a loosely viscerotopic manner, with the neurons receiving cardiorespiratory afferent inputs preferentially located in caudal portions of the nucleus (Loewy, 1990). In addition, the NTS is a collection of neurons exhibiting significant histochemical heterogeneity (Pilowsky and Goodchild, 2002; Appleyard et al., 2005; Appleyard et al., 2007; Bailey et al., 2008; Lin, 2009). This organization hampers studies addressing function within the NTS. For that reason, it remains largely unknown how sensory information arriving in the NTS is processed and targeted beyond the NTS for a specific functional outcome.

A large fraction of NTS neurons (~75%) receive direct peripheral afferent input and are, therefore, classified as second-order. Moreover, only a minority of NTS neurons (~13%) receive

no afferent input, direct or indirect (McDougall et al., 2009). Two distinct populations that are primarily second-order neurons consist of catecholaminergic neurons (also known as the A2/C2 cell group)(Appleyard et al., 2007) and GABA-ergic inhibitory neurons (Bailey et al., 2008), that are identified by their synthetic enzymes, tyrosine hydroxylase (TH) and the glutamic acid decarboxylase 67-kD isoform (GAD-67), respectively.

Development in the NTS. At birth, visceral afferent terminals are present in the NTS (Rinaman and Levitt, 1993; Zhang and Ashwell, 2001; Balland et al., 2006), but their connections with NTS neurons are both morphologically and functionally immature (Kalia et al., 1993a; Vincent and Tell, 1997, 1999; Zhang and Ashwell, 2001). The early postnatal period is marked by dramatic increases in synapse formation (Miller et al., 1983; Rao et al., 1999; Kawai and Senba, 2000; Zhang and Ashwell, 2001; Lachamp et al., 2002), dendritic growth (Kalia, 1992; Kalia et al., 1993a; Vincent and Tell, 1999), and spine density (Vincent and Tell, 1999; Lachamp et al., 2002), as well as electrophysiological maturation of NTS neurons (Kalia et al., 1993a; Vincent and Tell, 1997, 1999; Kawai and Senba, 2000), which includes evidence for significant reorganization of the functional intra-NTS circuitry (Kawai and Senba, 2000). Data concerning the basic membrane properties of NTS neurons suggest that immature NTS neurons are more excitable than their mature counterparts (Vincent and Tell, 1997). This, in turn, would make the immature neurons more responsive to sensory input. It is well established that activity-dependent postnatal maturation relies on sensory input in several other systems in the CNS (Katz and Shatz, 1996; Crair, 1999; Kandler and Gillespie, 2005; Horng and Sur, 2006; Inan and Crair, 2007), and this is likely the case in the NTS as well. When sensory input into gustatory regions of the NTS is markedly reduced in rat pups by a maternal NaCl-restricted diet, significant alterations are observed in the arbors of NTS dendrites (King and Hill, 1993). However, the

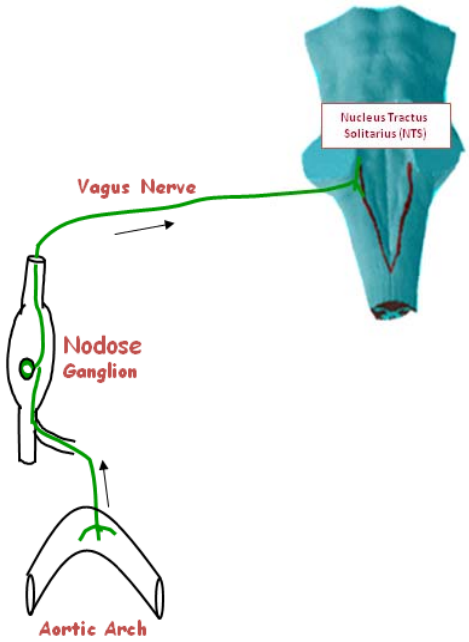

Figure 2-1: Anatomy of the afferent component of cardiorespiratory control pathways.

Sensory transduction begins at a particular target. Depicted here is a baroreceptor afferent whose peripheral terminal innervates the wall of the aortic arch. Blood pressure in the aortic arch is transduced by primary afferent nerve endings sensitive to stretch. Neuron cell bodies are located in the nodose ganglion, which is a collection of a variety of visceral afferent somata, including aortic baroreceptors. The neuronal process continues as part of the vagus nerve, enters the brainstem to join the solitary tract, and terminates on second-order neurons in the *Nucleus Tractus Solitarius* (NTS).

mediators of activity-dependent changes in the NTS have yet to be defined. In this dissertation, I examine BDNF as a candidate mediator of these changes.

The aortic baroreflex.

The aortic baroreflex is a key cardiorespiratory reflex, necessary to maintain short-term blood pressure homeostasis, buffering against rapid changes in blood pressure to ensure stable blood perfusion to vital organs. The primary reflex loop involves the input of peripheral sensory neurons that detect blood pressure, central brainstem integrative regions including the NTS, and ultimately efferent output, the sympathetic and parasympathetic neurons, which regulate two key determinants of blood pressure, i.e. the peripheral resistance and cardiac output (Guyenet, 2006).

At the afferent end of the reflex, peripheral terminals of aortic baroreceptors densely innervate the adventitia of the aortic arch, where blood pressure is sensed by mechanoreceptors that are activated by stretching of the aortic wall. Stretching opens mechanically-gated ion channels that lead to neuron depolarization and may result in action potentials. An increase in blood pressure (or stretching of the aortic wall) results in increased action potential rate, while a decrease in pressure results in decreased action potential rate, thus allowing for a change in pressure in either direction from the set-point to be encoded (Guyenet, 2006).

Like other cardiorespiratory afferents, aortic baroreceptors fall into two broad categories based on fiber myelination, the lightly myelinated Aδ and unmyelinated C-fibers (Brown, 1980). Each of these fiber types exhibit distinct characteristics. Namely, Aδ fibers have lower pressure thresholds for activation and tend to fire bursts of action potentials that are synchronous with the peak systolic blood pressure. C-fibers, on the other hand, have higher

pressure thresholds and tend to fire tonically (Jones and Thoren, 1977; Thoren et al., 1977; Chapleau and Abboud, 1987; Chapleau et al., 1989; Seagard et al., 1993). However, most aortic baroafferents are C-fibers (90%), while only a small minority are Aδ fibers (Andresen et al., 1978).

In rats, the axons of peripheral aortic baroreceptors travel largely unaccompanied in the aortic depressor nerve (ADN) (Sapru and Krieger, 1977; Sapru et al., 1981; Cheng et al., 1997) before joining with the vagus nerve (Ciriello, 1983) that carries the ascending visceral afferents from many different target organs and descending parasympathetic efferents. The cell bodies of aortic baroreceptors reside in the peripheral nodose ganglion (NG), while the central portion of the afferent axon continues into the brainstem, joining the solitary tract, where it travels to make its synaptic connection with a second-order neuron in the NTS (**Fig 2-1**)(Ciriello, 1983; Andresen and Kunze, 1994).

From the NTS, the simplest reflex loops involve projections to the brainstem nuclei nucleus ambiguus (NA), nucleus retroambiguus (RA), and the caudal ventrolateral medulla (CVLM). An increase in arterial pressure provides excitatory drive from the NTS to NA and CVLM. From NA, pre-ganglionic parasympathetic neurons are activated, which in turn activate post-ganglionic parasympathetic neurons that innervate the heart (Guyenet, 2006). On the other hand, excitatory drive to the CVLM activates inhibitory neurons impinging on tonically active, rostral ventral lateral medulla (RVLM) neurons (Pilowsky and Goodchild, 2002; Guyenet, 2006). RVLM neurons output to pre-ganglionic sympathetic neurons in the spinal cord that subsequently drive post-ganglionic sympathetic neurons located in the para- and pre-vertebral ganglia. Post-ganglionic sympathetic neurons involved in the control of blood pressure innervate the heart, major blood vessels, the kidneys, and adrenal medulla (Guyenet, 2006). As

a consequence, increases in blood pressure activate parasympathetic efferents and inhibit sympathetic efferents, triggering a drop in blood pressure through decreased cardiac output and peripheral resistance. Conversely, a decrease in blood pressure releases inhibition to the RVLM and increases sympathetic efferent drive to increase blood pressure through increased cardiac output and peripheral resistance (Guyenet, 2006).

Postnatal development of the aortic baroreceptor reflex. The aortic baroreceptor reflex functions at birth, yet the characteristics of the reflex change dramatically over the first weeks of life, suggesting that significant maturation occurs within the central circuitry controlling the reflex (Segar, 1997). For example, in early postnatal mice, the gain, or sensitivity, of the reflex increases several-fold while simultaneously the set point of the reflex adapts to a gradual increase in blood pressure during the first weeks of life (Ishii et al., 2001). In addition, at early postnatal ages in rats, increases in blood pressure result in decreased heart rate, while decreases in blood pressure do not increase heart rate until the second week of life, suggesting that cardiac sympathetic regulation develops postnatally (Quigley et al., 2005). Furthermore, there is evidence suggesting that there may be critical periods of development that rely on afferent input to these pathways. For example, exposure to intermittent hypoxia in rats during the first month of life, leads to permanently reduced baroreflex sensitivity in adult rats (Soukhova-O'Hare et al., 2006). The precise timing of critical periods and the molecular mediators of development in these pathways are virtually unknown. Given the well-defined input and output relationships of the aortic baroreflex, it potentially provides a good model to study candidate mediators of activity-dependent maturation in cardiorespiratory reflex pathways, such as BDNF.

Brain-derived neurotrophic factor (BDNF).

BDNF is a central theme of this dissertation, thus I provide an overview of the current understanding of BDNF and its receptor signaling. Many of the details go beyond what is required to understand my dissertation research. However, these details provide an important framework for interpreting my research findings in the context of what may be occurring *in vivo*. Many of these details will be revisited in the discussion portion of the dissertation.

BDNF is a member of the neurotrophin family of growth factors (Barde et al., 1982) that in mammals also includes nerve growth factor (NGF), neurotrophin-3 (NT-3), and neurotrophin-4/5 (NT-4/5)(Chao, 2003). BDNF serves many diverse roles in regulating neuronal survival, growth, differentiation, maturation, and various forms of structural and functional plasticity throughout all areas of the nervous system, from embryonic development to adulthood (Thoenen, 1995; McAllister et al., 1999; Huang and Reichardt, 2001; Pezet and McMahon, 2006). BDNF is synthesized as a larger proBDNF protein, 32 kD in size, which can later be cleaved into 14 kD mature BDNF. BDNF is a highly stable protein (Radziejewski et al., 1992), containing three intra-chain disulfide bonds, and exists as a functional, non-covalently linked homodimer (Mowla et al., 2001).

There are two transmembrane receptors for BDNF: 1) tropomyosin-related kinase B (TrkB), the high-affinity receptor for mature BDNF (K_d~10^{-11}M)(Klein et al., 1991), belonging to the Trk receptor tyrosine kinase family (Chao, 2003), and 2) the p75 neurotrophin receptor ($p75^{NTR}$), the low-affinity neurotrophin receptor (mature BDNF K_d~10^{-9}M)(Rodriguez-Tebar et al., 1992), belonging to the tumor necrosis factor receptor superfamily (Chao, 2003). In addition to binding BDNF, TrkB also binds with high-affinity a related mature neurotrophin, Neurotrophin4/5 (NT4/5)(Chao, 2003). Mature BDNF can also bind to other members of the Trk

family of receptor kinases, i.e. TrkA and TrkC, albeit with low affinity (Chao, 2003). $P75^{NTR}$ binds all mature neurotrophins with equally low affinity (K_d~10^{-9}M) (Rodriguez-Tebar et al., 1992; Chao, 1994), and pro-neurotrophins with higher affinity (K_d~10^{-10}M)(Teng et al., 2005).

TrkB and $p75^{NTR}$ activate distinct downstream signaling pathways. Namely, TrkB dimerizes upon ligand binding and trans-autophosphorylates intracellular sites, which leads to the activation of downstream signaling pathways that include the mitogen-activated protein kinase (MAPK), phosphatidylinositol 3-kinase (PI3K), and phospholipase Cγ pathways (Chao, 2003). $P75^{NTR}$, on the other hand, is a cysteine-linked dimer that changes conformation upon ligand binding (Vilar et al., 2009). Subsequently, the receptor recruits adaptor proteins that can activate the downstream signaling pathways, Jun N-terminal kinase (JNK) and NF-κB (Chao, 2003) (**Fig 2-2a**). Adding to the complexity of $p75^{NTR}$, this receptor often interacts with other coreceptors, which may be required to mediate diverse functional outcomes that likely reflect activation of different downstream signaling pathways. Identified coreceptors of $p75^{NTR}$ include sortilin, Trk, NogoR, Neuropilin-1, and Ephrin-A (Schecterson and Bothwell, 2010; Teng et al., 2010).

Signaling through TrkB versus $p75^{NTR}$ often results in opposing biological actions (Lu et al., 2005). For example, BDNF signaling through TrkB induces long-term potentiation in hippocampal pyramidal neurons (Pang et al., 2004), while signaling through $p75^{NTR}$ facilitates long-term depression (Woo et al., 2005). An explanation for the often opposing and context-dependent effects stems from the complexity that continues to be elucidated for both BDNF and signaling through TrkB and/or $p75^{NTR}$. For example, it was discovered that proBDNF may be secreted endogenously (Pang et al., 2004; Yang et al., 2009) and preferentially bind to $p75^{NTR}$ with high affinity (Teng et al., 2005). An additional layer of complexity is that $p75^{NTR}$ can

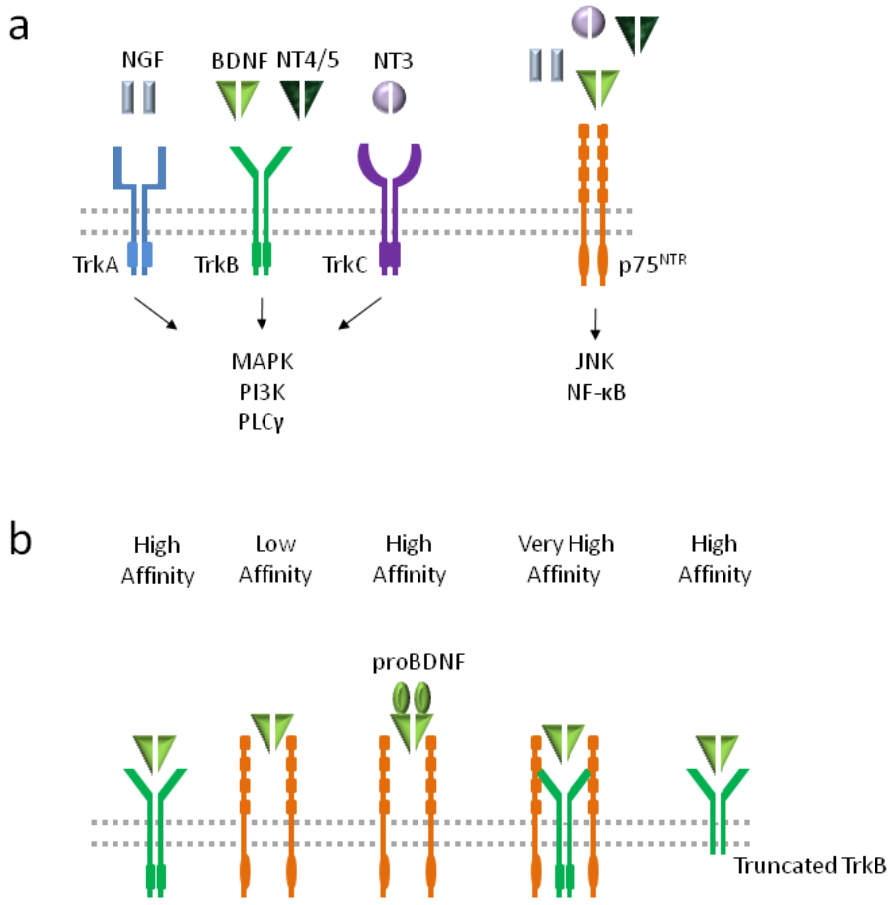

Figure 2-2: Neutrophins and their receptors.

(**a**) The neurotrophin family of growth factors includes NGF, which preferentially binds TrkA; BDNF and NT4/5, which preferentially bind TrkB; and NT3, which preferentially binds TrkC. Intracellular signaling pathways activated upon receptor binding include MAPK, PI3K, and PLCγ. In addition, all mature dimers of neurotrophins bind $p75^{NTR}$, which may lead to activation of JNK and NF-κB pathways. Neurotrophins and $p75^{NTR}$ exist as dimers, while dimerization of Trk occurs following neurotrophin binding. (**b**) Variations of BDNF binding models include classical binding of mature BDNF to TrkB and $p75^{NTR}$, with high and low affinity, respectively. ProBDNF may also be secreted endogenously, binding to $p75^{NTR}$ with high-affinity, often in conjunction with a coreceptor, such as sortilin. Furthermore, $p75^{NTR}$ can interact with TrkB to create very high-affinity binding sites for mature BDNF. Lastly, truncated forms of TrkB that lack the intracellular kinase domain may act to sequester BDNF, thus preventing binding to full-length TrkB, or it may act in concert with $p75^{NTR}$ to activate downstream signaling pathways.

functionally interact with Trk receptors and further increase the binding affinity of mature neurotrophins for Trk receptors (Esposito et al., 2001). Finally, two truncated TrkB isoforms that lack the intracellular kinase domain required for receptor activation are widely expressed (Klein et al., 1990). They were initially thought to scavenge mature BDNF, thereby limiting its interactions with functional, full-length TrkB (Biffo et al., 1995). More recently, however, the truncated TrkB isoform 1 (TrkB.T1) was shown to promote growth of dendritic filopodia in hippocampal neurons through a direct interaction with $p75^{NTR}$, illustrating that this receptor plays other functional roles (Hartmann et al., 2004)(**Fig. 2-2b**). These examples highlight the complexity of BDNF signaling through its receptors, and emphasize that elucidating mechanisms involving BDNF and its signaling must consider these diverse ligand/receptor binding combinations.

BDNF is a molecule that meets the criteria to translate changes in levels of activity into cellular changes, such as dendritic morphology. It is well established that BDNF expression (Lu, 2003) and release (Balkowiec and Katz, 2000; Lessmann et al., 2003) are activity-dependent, and this includes visceral sensory afferents from the nodose ganglion (NG), (Balkowiec and Katz, 2000; Jenkins et al., 2007; Vermehren-Schmaedick and Balkowiec, 2009). BDNF protein is preferentially targeted to the regulated secretory pathway that requires calcium for activity-dependent vesicle release (Lessmann and Brigadski, 2009). In fact, the level and patterns of activity are important for the amount of endogenous BDNF that is ultimately released, with short bursts of high-frequency stimulation being more effective than low-frequency, tonic stimulation (Balkowiec and Katz, 2000). In addition, the receptor, TrkB, is regulated by activity. Both increases in intracellular cAMP and depolarization recruit TrkB from intracellular stores to the cell membrane (Meyer-Franke et al., 1998). Thus, it is not surprising that the BDNF effects on dendritic morphology (McAllister, 2000) and synaptic plasticity (Poo, 2001), for example,

have been shown to be activity-dependent. Chapter 3 further explores the role of activity in releasing endogenous BDNF from nodose ganglion neurons, using known baroreceptor patterns of activity that occur *in vivo*.

BDNF and its receptors in the sensory portion of autonomic reflex pathways.

Evidence for BDNF-mediated afferent activity-dependent maturation at central viscerosensory terminals. There is accumulating evidence to support the hypothesis that BDNF, released in an activity-dependent fashion from visceral sensory afferents, drives maturation of circuitry in the brainstem *Nucleus Tractus Solitarius* (NTS). First, NG neurons continue to express BDNF (Schecterson and Bothwell, 1992; Wetmore and Olson, 1995; Apfel et al., 1996; Zhou et al., 1998) after they have lost at P0 their dependence on BDNF as a target-derived survival factor (Erickson et al., 1996; Brady et al., 1999). Additionally, BDNF is trafficked to central terminals and positioned for release from dense-core vesicles at synaptic terminals in both spinal (Michael et al., 1997) and trigeminal (Buldyrev et al., 2006) sensory systems, thus making it highly likely that this is true in visceral sensory afferents as well. Furthermore, post-synaptic targets of visceral afferents express the high-affinity receptor for BDNF, TrkB (Yan et al., 1997; Balkowiec et al., 2000; Kline et al., 2010). Not only is BDNF and its receptor found in the correct place, but BDNF can be released from a subset of visceral afferents, dissociate nodose ganglion neurons in culture, following patterned electrical stimulation (Balkowiec and Katz, 2000). In addition, exogenous mature BDNF dramatically reduces post-synaptic AMPA currents, in a TrkB-dependent manner, in a large subset of second-order NTS neurons (Balkowiec et al., 2000). Together, these data suggest that primary afferent neurons, in an area of the NTS known to receive cardiorespiratory input, release BDNF onto post-synaptic targets, where it can mediate activity-dependent maturation of second-order NTS neurons.

In addition, it is possible that BDNF released from visceral afferent terminals acts presynaptically on visceral afferent terminals themselves. Neurons in the nodose ganglia express both the mRNA and protein for TrkB and $p75^{NTR}$ (Wetmore and Olson, 1995). Additionally, blocking Trk receptors in brainstem slices while recording from second-order NTS neurons resulted in an increased frequency of mEPSPs, hinting at a possible presynaptic mode of action for endogenous BDNF (Clark et al., 2008). It is currently not known if $p75^{NTR}$ is found postsynaptically on second-order NTS neurons. Other outstanding questions include: 1) which form of BDNF (pro versus mature) may be released, and 2) in what relative quantities? There is evidence supporting that mature BDNF is released endogenously, although this does not exclude the release of proBDNF as well. In brainstem slices, solitary tract evoked EPSPs in second-order NTS neurons are increased in amplitude by Trk blockade (Clark et al., 2008). In summary, BDNF is well-positioned to mediate activity-dependent maturation in viscerosensory pathways. In Chapter 4, I explore one possible maturational role of BDNF, i.e. the dendritogenesis of putative second-order NTS neurons.

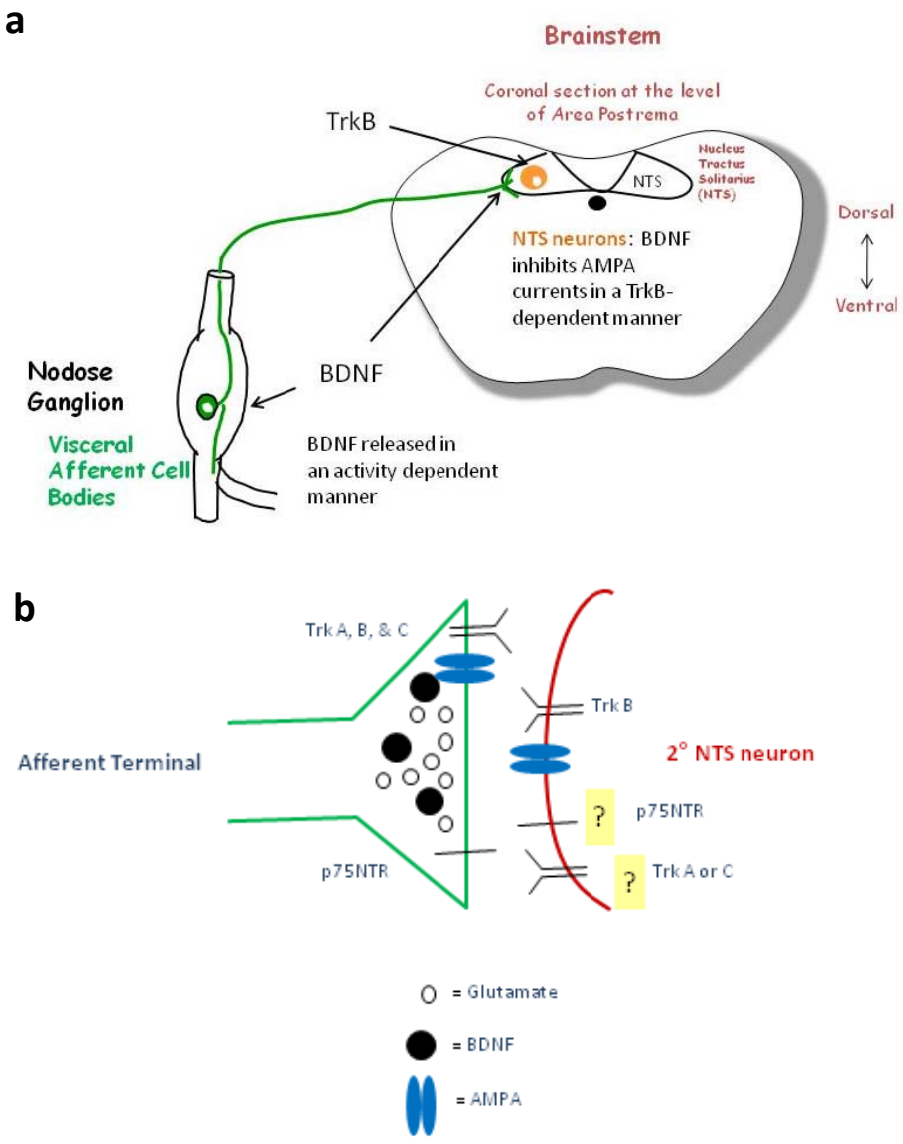

Figure 2-3: BDNF and neurotrophin receptor expression in visceral afferents and second-order NTS neurons.

(**a**) BDNF is expressed in NG neurons and transported to central terminals in the NTS. Functional TrkB is found in second-order NTS neurons. (**b**) Visceral afferent terminals contain BDNF and all Trk receptors. Second-order neurons contain TrkB, yet it is unknown whether they contain p75 or other Trk receptors.

Dendritic morphology.

General features of dendrites. Dendrites are usually branched, tree-like processes extending from the neuronal cell body that receive synaptic inputs. They display thick trunks near the cell body and taper as they extend away from the cell body. Great diversity in dendritic arbor size, shape, and complexity is displayed across the nervous system (Cajal, 1911) and this diversity is ultimately linked to the function that a particular neuron serves within a circuit. For example, cerebellar Purkinje neurons exhibit an incredibly large and complex dendritic tree. This structure enables Purkinje neurons to receive a vast number of synaptic inputs, which underlies this neuron's function to integrate a huge amount of information for a unified axonal output (Kapfhammer, 2004). The size, branching pattern, and position of synapses on dendrites (e.g. proximal vs. distal) ultimately affect the biophysics of both the spatial and temporal summation of synaptic inputs that may lead to an action potential, the cell output. Therefore, structure significantly determines cell function. Synaptic inputs may occur directly on the dendritic shaft but, in addition, dendrites display a variety of synaptic specializations. These include: 1) varicosities, which are enlarged areas of the dendritic shaft, 2) spines, which are protrusions that may take on a sessile, stubby, or mushroom appearance, as well as 3) filopodia. Filopodia are very long, thin protrusions that are rich in actin, highly dynamic, and ubiquitous when synaptogenesis is occurring (Fiala et al., 2008).

The development of dendrites. The elaboration of the dendritic arbor during the postnatal period is a crucial aspect of forming neural circuitry. Both, where the dendritic field is targeted and how branched the arbor becomes determines the types and number of synaptic connections a neuron receives. Typical development proceeds by migration of neurons to their final location in the nervous system, followed by extension of the axon. Subsequently, dendrites begin to extend and elaborate, and synapses form. *In vivo* time lapse imaging has revealed that

dendritic growth is a highly dynamic process involving continual extension and retraction of filopodia (in the time-frame of minutes) with this process slowing as the arbors mature and stabilize (Wu et al., 1999). In fact, filopodia form nascent synapses that will either retract or go on to form mature synapses, and the latter will often stabilize the associated dendritic segment (Niell et al., 2004). This observation supports the synaptotrophic hypothesis of dendritic arborization, which predicts that the formation of synapses promotes the dendritic growth (Cline and Haas, 2008). Finally, there are mechanisms that stop dendritic growth and maintain a stabilized arbor structure. Typically, dendritic arbors remain mostly stable after this initial developmental period, although the formation and retraction of dendritic spines remain plastic throughout life (Majewska et al., 2006).

Determinants of dendritic morphology. The ultimate features of dendritic arbors are guided by a complex interplay among cell intrinsic programs and external cues (Kim and Chiba, 2004; Parrish et al., 2007; Cline and Haas, 2008; Jan and Jan, 2010). The fact that neurons grown in dissociate culture, i.e. isolated from their native environment and inputs, will often form dendritic arbors resembling their arbors *in vivo*, suggests that the general features of dendritic arbors are cell intrinsic. On the other hand, some neuron types, such as the Purkinje neuron, when grown in culture, never display the full dendritic arbor seen *in vivo*. Both of these observations point to a cell-intrinsic program that may be modified depending on the local environment. A large number of factors have been identified that profoundly shape the dendritic arbor and allow dendrites to respond to their local environment for appropriate synapse formation. These cues fall into several broad categories, and include: 1) neural activity, 2) long-range guidance cues that may either attract or repel growing dendrites to/from their appropriate target, 3) short-range cues that may be soluble or contact-mediated and also capable of attracting or repelling, 4) factors that promote growth and/or branching, 5) factors

that inhibit or retract growth and/or branching, and 6) factors that stabilize and maintain dendrites. In many instances, a given cue can perform more than one of these functions, depending on context or cell type. This is the case for BDNF.

The many roles of BDNF in shaping dendrites. BDNF falls into the category of a short-range soluble cue. However, the specific effect that BDNF elicits on dendritic growth is neuron-type specific and context-dependent. For example, in some neuron types, BDNF has been shown to promote dendritic outgrowth and/or branching, while in other neuronal types, its action is inhibitory. A key example comes from the primary visual cortex, pyramidal neurons of layer 4 versus layer 6. Both exogenous and endogenous BDNF causes an increase in the dendritic outgrowth and complexity of basal dendrites of layer 4 neurons grown in a slice culture (McAllister et al., 1995; McAllister et al., 1997). Conversely in layer 6 neurons, endogenous BDNF decreases growth and complexity of basal dendrites (McAllister et al., 1997).

In addition, dendrites may respond differentially within the same cell type, depending on the sub-cellular compartment in which BDNF initiates receptor binding and downstream signaling. An example of this phenomenon comes from the *Xenopus* model of retinal ganglion cells (RGC), whose target is the optic tectum. BDNF application to the retina inhibits RGC dendritic arborization, whereas BDNF depletion in the retina by function blocking antibodies results in enhanced dendritic arborization (Lom and Cohen-Cory, 1999). Conversely, BDNF application at the RGC target in the optic tectum results in enhanced dendritic arborization of RGC neurons, and function blocking antibodies at the RGC target diminish dendritic arborization (Lom et al., 2002). Thus, localized signaling of BDNF may result in qualitatively different outcomes on dendritic growth.

Furthermore, there is evidence that BDNF may play an important role in maintaining the dendritic structure once it is established. In a forebrain-specific BDNF knock-out model, cortical layer 2/3 interneurons extend and elaborate dendritic arbors as in wild-type mice. However, after 3 weeks postnatally, when the dendritic arbor has stabilized in control mice, dendrites in BDNF knock-out mice retract, suggesting that BDNF is necessary for the maintenance of dendritic structure in this cell type (Gorski et al., 2003). To highlight again the opposing roles that BDNF may play depending on neuron-type, BDNF has also been shown to destabilize dendritic arbors rather than preserve them. In cortical pyramidal neurons grown in a slice culture from third postnatal week ferret, BDNF destabilizes dendritic structure, thus allowing for remodeling after the time when these dendritic arbors are normally stable (Horch et al., 1999).

In addition to all of the differential effects of BDNF on dendritic growth described above, BDNF actions tend to be activity-dependent, which is not mutually exclusive with the other effects. There are two complementary scenarios that have been observed for how BDNF mediates its effects in an activity-dependent manner. *In the first scenario*, neuronal activity can cause synaptic release of BDNF, which may act downstream at either the pre- or post-synaptic site, depending on the localization of its receptor. This scenario is well-demonstrated in models where BDNF/NT4-5 scavengers have been employed. In this situation, activity of a circuit remains intact, but in the absence of BDNF, activity-dependent changes in morphology are diminished. For example, in non-pyramidal neocortical interneurons grown in slice culture, both exogenous BDNF and KCl-induced depolarization increase the total dendritic length of these neurons. However, scavenging the released endogenous BDNF/NT4-5 inhibits the KCl-induced changes in dendritic morphology, suggesting that BDNF is the mediator of activity-dependent changes in these neurons (Jin et al., 2003). *In the second scenario*, the action of BDNF depends

on activity within the recipient neuron. Therefore, even in the presence of BDNF, less active neurons will be affected to a lesser extent than more active neurons. This was demonstrated in earlier studies in slice culture, where the dendritic growth and arborization induced by exogenous BDNF in layer 4 pyramidal neurons did not occur in the absence of activity (McAllister et al., 1996).

Dendrites in the NTS. Ramon y Cajal was the first to illustrate the morphological features of neurons in the NTS. Dendrites were described as long, thin, and poorly branched, yet the associated neurons exhibited a variety of cell body shapes (e.g. triangular, fusiform, stellate, spherical, oval). Their shafts ranged from appearing smooth and devoid of spines to possessing moderate numbers of dendritic spines (Cajal, 1911). During the first week of life in rats, dendrites extend from two opposite poles of the soma, orienting to the source of afferent input, which is the solitary tract (Kalia et al., 1993b). Following this directed orientation, dendrites elaborate in all directions, yet are confined to the NTS and the immediately ventral nucleus, i.e. dorsal motor nucleus of the vagus nerve, and rarely cross the midline (Ramon y Cajal, 1897; Kalia et al., 1993b). The mechanisms that underlie this developmental sequence and targeted growth are unknown. Afferent activity is a likely player. The fact that the initial dendritic outgrowth aligns to the solitary tract suggests that a positive cue is coming from the primary afferents. Given the well-known role of BDNF in mediating activity-dependent dendritogenesis, combined with BDNF being positioned for release from primary afferent terminals, BDNF is a strong candidate mediator of dendritogenesis in the developing NTS.

Glia, with an emphasis on astrocytes.

During the course of my studies exploring the role of BDNF in the dendritogenesis of NTS neurons, I discovered that glia, including astrocytes, significantly contribute to the process. Traditionally, glial cells were thought of as a support to neurons, the electrically excitable cells that form the circuitry of the brain. This dogma, however, continues to be shattered as more discoveries suggest that glial cells are equal and essential partners to neurons in terms of nervous system development and function (Barres, 2008). Glial cells of the CNS include astrocytes, oligodendrocytes, and microglia, with astrocytes comprising the largest fraction of CNS glial cells (Eroglu and Barres, 2010). Combined, glial cells outnumber neurons ten to one in the central nervous system (Stevens, 2008). Over a century ago, Ramon y Cajal hypothesized that glial cells play an important role in nervous system function based on their close spatial relationship with neurons (1995). Yet, it is really this last decade when much knowledge and insight has been gained into how glia, together with neurons, may form inseparable functional units. In spite of this, much remains unknown surrounding the function of these cells (Barres, 2008). As documented in chapter 4 of this dissertation, astrocytes play a prominent role in my experimental discoveries. In terms of nomenclature, it is worth pointing out that I refer to "glial cells" when I cannot definitively determine that astrocytes are the underlying cause of an effect that I or others have observed. Regarding other glial cell populations, oligodendrocytes are the myelinating cells of the CNS, while microglia are thought to be the immune cells of the CNS (Barres, 2008; Stevens, 2008). Both oligodendrocytes and microglia undoubtedly play crucial roles in the CNS; however, the remainder of this review focuses on astrocytes since this is the cell type most likely underlying my experimental findings.

Known functions of astrocytes. Traditional support roles assigned to astrocytes include maintaining extracellular ion concentration such as K^+, thus providing a favorable electrolytic

environment that directly impacts neuronal excitability. In addition, astrocytes clear and recycle excess neurotransmitter at synapses to ensure temporally- and spatially- specific neuronal signaling. Another support role attributed to astrocytes is maintaining energy homeostasis of neurons. Astrocytes are capable of taking up glucose from the blood and providing this energy to neurons in an 'on demand' basis, as energy demands may change with neural activity. Thus, astrocytes are thought to serve as a link between neural activity and assimilation of glucose (Halassa and Haydon, 2010). These are arguably essential roles to nervous system function, yet the roles attributed to astrocytes keep growing.

Glial cells are partners in synaptic plasticity. Although these cells do not fire action potentials, they are capable of sensing electrical activity and responding in the form of calcium waves. The newly coined term "tri-partite synapse" refers to the astrocytic processes surrounding both pre- and post-synaptic elements where bidirectional signaling between neurons and astrocytes can occur. Like neurons, astrocytes express many of the same neurotransmitters and neuropeptides, receptors for neurotransmitters and neuropeptides, and transporters. 'Gliotransmitter' refers to neuroactive substances released by astrocytes, such as glutamate, D-serine, and ATP that can directly impact neuronal response (Halassa and Haydon, 2010). In support of a direct role for glia in synaptic plasticity, an interaction between motor neurons and Schwann cells, glial cells of the peripheral nervous system (PNS), was shown to be necessary for long-term plasticity at the neuromuscular junction. Blocking Schwann cell calcium waves and signaling through ATP on neurons prevented the induction of long-term plasticity at the neuromuscular junction (Todd et al., 2010).

Evidence for the role of astrocytes in the maturation of neural circuitry. Most relevant to this dissertation is the emerging evidence that astrocytes significantly contribute to the

development of neural circuitry. The rapid proliferation of astrocytes occurs during the same period as neuronal synaptogenesis and the elaboration of dendritic arbors, while later in postnatal development, the maturation of astrocytes coincides with the stabilization of dendritic arbors and the end of developmental plasticity (Cline, 2001; Eroglu and Barres, 2010). In support of the fact that immature astrocytes differ significantly from mature astrocytes, Muller and Best demonstrated that ocular dominance plasticity could be re-opened in the visual cortices of adult cats by transplanting cultured astrocytes from newborn kittens into adult cortices (Muller and Best, 1989). In effect, this leads to the hypothesis that the developing immature astrocytes contribute to the timing of critical periods, when neural circuitry is established and refined. Possible mechanisms for how astrocytes may mediate development of neural circuitry include bidirectional communication with neurons through soluble factors, contact-mediated mechanisms, and extracellular matrix (ECM) proteins (Wang and Bordey, 2008; Eroglu and Barres, 2010). In the next section, I focus on describing astrocyte-derived soluble factors, which are most relevant to my experimental findings.

Soluble astrocyte-derived factors. Much progress has been made in identifying soluble factors from astrocytes that are specifically required for synaptogenesis in the developing CNS. Astrocyte-derived thrombospondin is crucial in forming structurally normal glutamatergic synapses in cultures of retinal ganglion cells (RGC). However, these synapses are functionally silent. An additional unidentified soluble factor from astrocytes recruits AMPA receptors to the synapse, thus rendering the synapse fully functional (Christopherson et al., 2005). In another example, an unknown astrocyte-derived protein mediates inhibitory synapse formation and axon outgrowth in hippocampal cultures. The authors concluded that the effect was not due to thrombospondin and did not require activity through sodium-dependent action potentials (Elmariah et al., 2005; Hughes et al., 2010). Furthermore, cholesterol bound to apolipoprotein E

is another identified soluble astrocyte-derived factor that strongly promotes synaptogenesis in RGC cultures (Mauch et al., 2001). In a follow-up study, astrocyte-derived cholesterol was shown to be necessary for RGC dendritic development that was ultimately determined to be the rate-liming step for synapse formation (Goritz et al., 2005). These examples highlight a growing list of astrocyte-derived factors that are crucial for synapse formation, and demonstrate that synaptogenic factors often contribute to the morphological changes of neuronal processes as well.

In general, astrocyte-derived factors are well-known to support dendritic growth, yet the identity of soluble factors remains obscure. For example, astrocytes, or the media containing the soluble factors derived from astrocytes, were shown to be necessary for both the survival and the dendritic growth of dissociate hippocampal neurons (Banker, 1980), yet the identity of the factor(s) is still unkown (Barres, 2008). Identified soluble factors that can promote dendritic growth include a class of proteins called bone morphogenic proteins (BMPs) (Withers et al., 2000; Lein et al., 2002). Complementary to BMPs, there are soluble factors inhibiting the actions of BMPs that include noggin and follistatin. These factors act by binding BMPs and preventing a functional interaction with their receptor (Cho and Blitz, 1998). It was previously demonstrated that neuron-glia interactions could influence the levels of BMPs and BMP inhibitors and, thus, control the degree of dendritic elaboration in cultured sympathetic neurons (Lein et al., 2002). With the exception of BMP inhibitors, other soluble factors from astrocytes that are inhibitory to dendritic growth have not been identified.

There is a growing appreciation for astrocyte heterogeneity, which certainly can impact the soluble factors that astrocytes release (Le Roux and Reh, 1994). In fact, it is predicted that glia may be just as diverse as neurons, which is demonstrated by experiments where dendritic

growth of neurons is differentially affected by glia from different brain regions (Zhang and Barres, 2010). For example, mesencephalic dopaminergic neurons have fundamentally different neurite growth properties depending on whether they are plated on their native mesencephalic glia, or glia from the striatum, i.e. their projection region. Native glia support dendritic elaboration similar to dopaminergic neurons *in vivo*, whereas target glia of the striatum result in one long neurite consistent with the axon, yet dendritogenesis is lacking (Denis-Donini et al., 1984). Whether the effects are due to differences in soluble factors, contact-mediated mechanisms, and/or ECM molecules is presently not known. In another example, cultured cortical neurons were grown either in direct contact, or co-cultured in a non-contact system, with glia derived from several distinct brain regions. The degree of dendritic growth varied immensely depending on the source of glia, with the direct contact and the non-contact culture yielding similar results. This suggests that differences in soluble glia-derived factors indeed contribute to dendritic growth in a neuron-dependent manner (Le Roux and Reh, 1994).

Astrocytes and neurotrophins. Glial cells are known to express both neurotrophic factors (i.e. BDNF, NGF, NT-3, NT-4)(Althaus and Richter-Landsberg, 2000) and neurotrophic factor receptors (i.e. $p75^{NTR}$, TrkA, TrkB, TrkC) (Althaus and Richter-Landsberg, 2000; Cragnolini and Friedman, 2008). This raises the possibility for the bidirectional signaling between neurons and glia that involves neurotrophins and their receptors. For example, in hippocampal cultures, an unidentified diffusible factor released by astrocytes promotes inhibitory synapse formation in a mechanism dependent on neuronal BDNF release and signaling through the high-affinity receptor, TrkB. However, neither BDNF nor TrkB expressed by astrocytes were required for this synaptogenic effect (Elmariah et al., 2005). This example highlights that, within a particular brain region, answering any mechanistic questions involving neurons, glia, and neurotrophins will certainly require knowing which receptors and neurotrophins are present when, where, and

at what levels. It is quite likely that the expression profiles within different systems are context-dependent. Within the NTS, it is currently not known whether astrocytes, or other glia, express neurotrophins and/or neurotrophin receptors at any developmental time point.

Astrocytes in the NTS. The density of astrocytes within the NTS is low at birth and gradually increases throughout the first weeks of life. Interestingly, the highest density of labeling using astrocytic markers occurs along the midline and dorsal borders of the rat NTS at all ages examined (Pecchi et al., 2007; Tashiro and Kawai, 2007). The authors also note that, compared to surrounding brainstem regions, the NTS of adult rats has a much greater density of astrocytic processes (Pecchi et al., 2007). Furthermore, a very recent study shows that NTS astrocytes activated through humoral cues, respond with calcium waves, and subsequently signal directly to neurons (Hermann et al., 2009). Evidence that astrocytes directly affect reflex circuitry was demonstrated in the central chemoreceptor region, retrotrapezoid nucleus (RTN). Changes in blood pH, detected by RTN astrocytes, are signaled to RTN neurons, which stimulate breathing. Thus, astrocytes may provide a direct role in reflex function by integrating humoral cues (Gourine et al., 2010).

During the postnatal period, alterations in either the density or numbers of glia may result in structural changes of neurons. One ultrastructural study found that small NTS somata of newborn rats were on average 30% surrounded by glial processes, while two weeks later, the degree of the neuron-glia juxtaposition increased to 70%. The authors found that, during the same period, the density of axo-somatic synapses on small somata significantly decreases, leading the authors to conclude that glia may contribute to a loss of axo-somatic synapses during the first weeks of life (Tashiro and Kawai, 2007). In addition, it was previously shown in postnatal rat gustatory regions of the rostral NTS that dendritic growth and complexity of

neurons, classified based on soma shapes, were differentially modulated by reversibly blocking afferent activity through altering maternal dietary NaCl. Interestingly, in rats whose mothers were deprived of NaCl, the numbers of glia increased in the rostral NTS while the numbers of neurons remained unchanged. Reversing the NaCl deprivation did not reverse the increase in astrocyte density (King and Hill, 1993). These results suggest that a complex interplay between afferent activity and glia shapes dendritic morphology in the NTS.

In light of this possible interaction, several structural changes are observed within the developing NTS of Sudden Infant Death Syndrome (SIDS) victims. It has long been hypothesized that SIDS may result from inappropriate development of the autonomic reflex circuitry, which includes the NTS. Victims of SIDS typically have a significant astrocytic gliosis within the NTS compared to control (Biondo et al., 2004). Moreover, one study found that, in addition to the increase in astrocytes, the normal pruning of synaptic connections that occurs during infant life is lacking in victims of SIDS, thus leading the authors to conclude that maturation of autonomic circuitry may be delayed (Takashima and Becker, 1985). Many questions regarding SIDS remain unanswered, including: Is the commonly observed gliosis a possible cause or just an effect? Studies that would causally link changes in the glial number to structural changes are lacking. Data presented in Chapter 4 of this dissertation suggest that perturbations in the number of glia may profoundly impact structural circuit development, such as dendritogenesis.

Chapter 3:

Brain-derived neurotrophic factor in arterial baroreceptor pathways: Implications for activity-dependent plasticity at baroafferent synapses.

Jessica L. Martin[1,2], Victoria K. Jenkins[1], Hui-ya Hsieh[1], and Agnieszka Balkowiec[1-3]

[1]Department of Integrative Biosciences, [2]Neuroscience Graduate Program, and [3]Department of Physiology and Pharmacology, Oregon Health & Science University, Portland, OR

ABSTRACT

Functional characteristics of the arterial baroreceptor reflex change throughout ontogenesis, including perinatal adjustments of the reflex gain and adult resetting during hypertension. However, the cellular mechanisms that underlie these functional changes are not completely understood. Here, we provide evidence that brain-derived neurotrophic factor (BDNF), a neurotrophin with a well-established role in activity-dependent neuronal plasticity, is abundantly expressed *in vivo* by a large subset of developing and adult rat baroreceptor afferents. Immunoreactivity to BDNF is present in the cell bodies of baroafferent neurons in the nodose ganglion (NG), their central projections in the solitary tract, and terminal-like structures in the lower brainstem *nucleus tractus solitarius* (NTS). Using ELISA *in situ* combined with electrical field stimulation, we show that native BDNF is released from cultured newborn NG neurons in response to patterns that mimic the *in vivo* activity of baroreceptor afferents. In particular, high-frequency bursting patterns of baroreceptor firing, which are known to evoke plastic changes at baroreceptor synapses, are significantly more effective at releasing BDNF than tonic patterns of the same average frequency. Together, our study indicates that BDNF expressed by first-order baroreceptor neurons is a likely mediator of both developmental and post-developmental modifications at first-order synapses in arterial baroreceptor pathways.

INTRODUCTION

The arterial baroreceptor reflex plays a crucial role in cardiovascular homeostasis by controlling arterial blood pressure (Brooks and Sved, 2005; Guyenet, 2006). The afferent limb of the reflex includes mechanosensitive neurons with cell bodies in the nodose-petrosal ganglion complex (NPG), peripheral endings in the cardiac outflow tract, such as the aortic arch, and central projections terminating in the medial *nucleus tractus solitarius* (NTS) of the dorsal medulla (Andresen and Kunze, 1994; Guyenet, 2006). The natural stimulus for these neurons is a distention of the arterial wall by an increase in blood pressure (Guyenet, 2006).

Arterial baroreceptors are active in the fetus, but the functional characteristics of the baroreceptor reflex undergo significant changes during the perinatal period (Segar, 1997). For example, the gain of the reflex increases several-fold between the first and second week of age in mice (Ishii et al., 2001). In fact, the reflex remains plastic throughout adulthood, as is manifested by its ability to reset the operating range of blood pressures while maintaining unchanged reflex sensitivity (Kunze, 1981; Heesch et al., 1984b; Heesch et al., 1984a; Kunze, 1986; Andresen and Yang, 1989; Xie et al., 1991). In addition, increasing frequency of baroreceptor input leads to frequency-dependent depression of the postsynaptic responses in the NTS neurons (Scheuer et al., 1996; Liu et al., 1998; Chen et al., 1999; Liu et al., 2000; Doyle and Andresen, 2001), a form of synaptic plasticity that may influence baroreflex function (Liu et al., 2000). However, the exact molecular mechanisms underlying changes in either the perinatal or adult system are not well understood.

In recent years, brain-derived neurotrophic factor (BDNF), a member of the neurotrophin family of growth factors, has emerged as a key mediator of mechanisms regulating

activity-dependent synaptic maturation and plasticity (Huang and Reichardt, 2001; Poo, 2001). During embryonic development, BDNF is required for the survival of a large subset of NPG neurons, including cardio-respiratory control neurons (Erickson et al., 1996), and specifically arterial baroreceptors (Brady et al., 1999). Namely, BDNF is expressed in the fetal cardiac outflow tract, and acts as a target-derived survival factor for developing baroreceptor afferents (Brady et al., 1999). After birth, when NPG neurons no longer depend on BDNF for survival (Brady et al., 1999), BDNF is expressed by a significant proportion of NPG neurons (Schecterson and Bothwell, 1992; Wetmore and Olson, 1995; Apfel et al., 1996; Zhou et al., 1998) and released from these neurons by activity (Balkowiec and Katz, 2000). There is also evidence suggesting that BDNF is a modulator of visceral sensory transmission (Balkowiec et al., 2000), raising the possibility that BDNF is involved in maturation and/or plasticity in the arterial baroreceptor pathway.

The present study was undertaken to test the following hypotheses: 1) BDNF is present in baroreceptor afferents *in vivo,* and 2) BDNF release from cultured nodose ganglion (NG) neurons is regulated by stimulation patterns that mimic *in vivo* activity of baroreceptor afferents.

MATERIALS AND METHODS

Animals. Postnatal day (P) 0-2, P9, P23 and P30 Sprague Dawley rats (Charles River Laboratories, Wilmington, MA) were used for this study. All procedures were approved by the Institutional Animal Care and Use Committee of the Oregon Health and Science University, and conformed to the *Policies on the Use of Animals and Humans in Neuroscience Research* approved by the Society for Neuroscience.

DiI-labeling of baroreceptor afferents. P2 rats were deeply anesthetized by hypothermia, and either right or both aortic depressor nerves (ADN) exposed in the neck by a ventral midline incision, and isolated from surrounding tissues with Parafilm "M" (Pechiney Plastic Packaging, Menasha, WI). The fluorescent lipophilic dye CM-DiI (Cell Tracker® and Neurotrace® tissue-labeling paste; Invitrogen, Carlsbad, CA) was placed on the uncut nerve, and the region isolated with a fast hardening silicone elastomer (Kwik-Sil; WPI), as previously described (Balkowiec et al., 2000). The animals were then sutured and allowed to recover for either 7, 21 or 28 days. Following the perfusion and before the tissue collection, the position of the dye was verified, and the animals with evidence of dye displacement were excluded from the study.

Preparation of nodose ganglia (NG), brainstems and NG cultures for immunostaining. Rats were euthanized and perfused transcardially with phosphate-buffered saline (PBS), followed by 2% paraformaldehyde in 0.1 M sodium phosphate buffer, in some experiments supplemented with 0.2% parabenzoquinone. NGs and brainstems were dissected and post-fixed with the fixative of the same composition as the one used in perfusion, for 30 min (NGs) or 2 h (brainstems), followed by rinsing in PBS and cryoprotection in 30% sucrose in PBS at 4ºC for at least 24 h. Next, NGs and brainstems were embedded in O.C.T. Tissue-Tek® compound (Sakura Finetek USA, Inc., Torrance, CA) and blocks of tissue were sectioned on a cryostat at 10 μm (NGs) or 30

μm (brainstems). NG sections were collected onto glass slides, whereas brainstem sections were collected into PBS to be processed as free-floating sections. Following tissue cutting, NG and brainstem sections were screened for the presence of DiI in NG somata and the brainstem NTS. Sections were discarded if no DiI was present in the NG or brainstem. Furthermore, sections were discarded if there was evidence of DiI spread beyond the ADN, e.g. DiI fluorescence in a majority of the NG somata, or in neuronal cell bodies in the brainstem dorsal motor nucleus of vagus or nucleus ambiguus. Our overall success rate with the DiI labeling of ADN afferents was approximately 18% (15 of 81 labeled animals across all three time points). Both NG and brainstem sections were collected in a series of two and every other section (i.e. one series) was processed for BDNF immunostaining. For double immunofluorescence in NGs, both series were processed: one for BDNF and HCN1 and the other for BDNF and TRPV1 (VR1, N-terminus), resulting in alternate sections being stained for each marker, i.e. HCN1 and TRPV1. NG cultures for immunostaining were fixed with 2% paraformaldehyde and 0.2% parabenzoquinone in 0.1 M sodium phosphate buffer, pH 7.4, for 30 min at room temperature.

Immunostaining of sections. Sections were (1) incubated for 1 h in a 10% solution of goat serum in dilution buffer (DB; 0.02 M phosphate buffer, 0.5 M NaCl, 0.3% Triton X-100), (2) incubated for 2 h in chicken polyclonal anti-BDNF [1:50 (NGs) or 1:25 (brainstems); Promega, Madison, WI] in DB, applied alone, or in combination with either rabbit polyclonal anti-HCN1 (1:100; Alomone Labs, Jerusalem, Israel) or rabbit polyclonal anti-VR1 (TRPV1), N-terminus (1:500; Neuromics, Edina, MN), (3) washed three times in DB, (4) incubated in secondary antibody diluted in DB with 10% goat serum as specified for the following types of immunostaining: (i) *NG, immunodetection of BDNF only,* 1 h in goat anti-chicken biotinylated IgG (1:200, Vector Laboratories, Burlingame, CA), (ii) brainstem, immunodetection of BDNF only, 2 h in donkey anti-chicken IgG-Cy2 (1:200, Jackson Immunoresearch; West Grove, PA), (iii) NG, double

immunodetection of either BDNF/HCN1 or BDNF/VR1 (TRPV1), 1 h in goat anti-chicken IgG-Alexa 488 (1:1000, Invitrogen, Carlsbad, CA) and goat anti-rabbit IgG-Alexa 647 (1:1000, Invitrogen, Carlsbad, CA), (5) washed three times in PBS, (6) incubated for 30 min in avidin-biotin reagent (ABC) in PBS-0.5M NaCl (1:100, Vectastain *Elite*, Vector Laboratories;), (7) washed for 10 min in PBS-0.5M PBS, (8) washed two times in PBS, (9) incubated for 3-5 min in diaminobenzidine (DAB) solution (in PBS: 0.3 mg/ml DAB, 0.032% $NiCl_2$, 0.0075% H_2O_2), (10) washed three times in PBS, and (11) mounted with Gel Mount (Sigma) or FluorSave (Calbiochem, San Diego, CA). For the fluorescent method (brainstem and double-immunostaining in NG), steps 6-10 were omitted.

Double-immunostaining of cultures for BDNF and Neurofilament, a pan-neuronal marker. Cultures were (1) incubated for 1 h in 1:1 solution of goat serum and PBS-0.1% Triton X-100, (2) incubated for 2 h in chicken polyclonal anti-BDNF (1:100; Promega) alone or combined with mouse monoclonal anti-neurofilament 68 and 160 (1:100; Sigma, St. Louis, MO), diluted in PBS-0.1% Triton X-100 with 10% goat serum, (3) washed one time in PBS followed by two washes in PBS containing 5% goat serum, (4) incubated for 1 h in goat anti-chicken biotinylated IgG (1:200, Vector Laboratories) alone or combined with goat anti-mouse IgG-Cy3 (1:200, Jackson Immunoresearch), diluted in PBS-0.1% Triton X-100 with 10% goat serum, (5) washed in PBS, (6) incubated for 30 min in avidin-biotin reagent in PBS-0.5M NaCl (1:100, Vectastain *Elite*, Vector Laboratories), (7) incubated for 10 min in PBS-0.5M PBS, (8) washed two times in PBS, (9) incubated for 3-5 min in DAB solution, (10) washed once in PBS, and (11) mounted with ProLong® Gold (Invitrogen) or Gel Mount (Sigma).

For immunostaining in both sections and cultures, to minimize a non-specific staining, the anti-BDNF antibody was precleared by overnight incubation with vibratome slices (40 µm) of

a 2% or 4% paraformaldehyde-fixed adult rat cerebellum (approximately 1/3 of cerebellum per 1 ml of the antibody solution). All staining procedures were performed at room temperature.

Testing specificity of the BDNF antibody.

Western blotting. Recombinant human BDNF (Promega) was diluted in loading buffer (130 mM Tris-Cl, 20% glycerol, 4.6% SDS, 5% β-mercaptoethanol, 0.2% bromophenol blue) to yield 2000 ng, 200 ng, and 40 ng samples. Proteins and ladder (SeeBlue Plus2, Invitrogen, Carlsbad, CA) were resolved on a 12% (w/v) SDS-PAGE gel, and electrotransferred to a PVDF membrane. Membranes were incubated in blocking solution (150 mM NaCl, 50 mM Tris-Cl, pH 7.4, with 5% dry milk) for 30 min, then incubated with chicken polyclonal anti-BDNF (1:50 in blocking solution) overnight at 4°C. Following three Tris-buffered saline (TBS, 150 mM NaCl, 50 mM Tris-Cl, pH 7.4) washes, the membranes were incubated with the rabbit anti-chicken IgY-horseradish peroxidase (HRP; 1:1000 in blocking solution, Promega) for 1 hour at 25°C, and washed 3 times in TBS. HRP was activated with chemiluminescent reagents (Western Lightning, Perkin-Elmer, Waltham, MA) for 90 sec, and blue X-ray film (Phenix Research, Candler, NC) was exposed for 2 min.

Preabsorption with BDNF protein. Chicken polyclonal anti-BDNF (Promega, Madison, WI) was preabsorbed by incubation with BDNF-coated beads. Magnetic beads with surface tosyl groups (Dynabead M-280 Tosylactivated, Invitrogen) were coated with BDNF protein (1.25 µg BDNF, R&D Systems, Minneapolis, MN, per 2 x 10^7 beads) according to the manufacturer's instructions, with the exception of using a sodium-phosphate/borate buffer (0.075 M NaH_2PO_4, 0.075 M Na_2HPO_4, 0.1 M H_3BO_4, pH 9.5) during the coating step.

After incubation with beads, no detectable BDNF remained in the solution (unbound to beads), as determined by a sandwich ELISA (BDNF E_{max}^{TM} ImmunoAssay System; Promega), and the estimated density of BDNF bound to beads was approximately 2.4 fg/μm^2. Moreover, after incubation with chicken polyclonal anti-BDNF (see below), BDNF-coated beads exhibited five-fold greater immunoreactivity (measured as the optical density of the reaction product; BDNF E_{max}^{TM} ImmunoAssay System; Promega) than uncoated beads.

Chicken polyclonal anti-BDNF was diluted (1:50) in PBS-powdered bovine serum albumin (BSA, 0.1% w/v, pH 7.4) and precleared with cerebellar slices, as described above for staining cultures. BDNF-coated and uncoated beads were then incubated with the precleared anti-BDNF for 1h at room temperature with rotation. Next, beads were pelleted with a magnet, and the supernatant (containing only the unbound fraction of the antibody) was collected and immediately used to stain NG cultures, as described above.

Specificity of other antibodies used. NG and brainstem sections and NG cultures were stained according to the methods described above, except that primary antibodies were omitted. Under these conditions, the specimens were devoid of staining for all secondary antibodies used (data not shown). Specificity of other primary antibodies used in this study has been previously demonstrated (anti-HCN1, (Doan et al., 2004); anti-TRPV1, (Bennett et al., 2003).

Microscopy, digital imaging, and image analysis. All NG cultures and sections were imaged with an Olympus IX-71 inverted microscope (Olympus America Inc., Center Valley, PA), and images were captured with a Hamamatsu ORCA-ER CCD camera (Hamamatsu, Bridgewater, NJ) controlled by either Wasabi (Hamamatsu) or Olympus Microsuite software (vs. 5.0, Olympus America Inc). In addition, BDNF expression in DiI-labeled baroreceptor terminals in the brainstem was examined using a BioRad Radiance 2100 confocal microscope (BioRad, Hercules,

CA). Confocal images of the two fluorophores, DiI and Cy2, were taken sequentially with a 63x oil-immersion objective with an additional 3x confocal zoom factor as a series of z-stacks of 0.5-0.75 µm thickness. All images were taken from the medial NTS ipsilateral to the DiI placement. Images were analyzed and adjusted for brightness and contrast using ImageJ software (National Institutes of Health, Bethesda, MD).

In order to determine the degree of DiI and BDNF colocalization in the NG somata, all DiI-labeled profiles containing a nucleus from every other section of the NG were selected blinded to BDNF content. Subsequently, the images were overlaid and BDNF content was assessed. BDNF-IR somata exhibited a characteristic perinuclear punctate ring. In a subset of P30 animals, BDNF staining was combined with immunostaining for HCN1 or VR1 (TRPV1, N-terminus). Similar to analysis of BDNF IR alone, DiI-positive NG somata containing a nucleus were analyzed for the presence of BDNF and either HCN1 or VR1.

In order to determine DiI and BDNF colocalization in the brainstem puncta, 25 DiI-labeled puncta were selected throughout the rostro-caudal extent of the medial NTS, ipsilateral to the DiI-labeled ADN, randomly selected, blind to the BDNF content. Images containing DiI and BDNF IR were overlaid, and BDNF IR was assessed.

The cross-sectional area of DiI-labeled P30, unlabeled P0, and unlabeled P30 NG cell bodies was measured in sections single-stained for BDNF (the ABC method) using ImageJ software. Specifically, the cell perimeter was outlined and enclosed area was computed and recorded.

In addition to DiI-labeled cells, the entire NG neuron population was sampled, and BDNF content, along with the cross-sectional area, were assessed in the right side P0 and P30 ganglia

from three rats each. Every 10th NG section (approximately 100 μm apart from each other) was digitally imaged, and each cell that contained a nucleus was assessed for its BDNF content and the cross-sectional area. For each age, all data from the three rats were subsequently pooled and plotted as frequency histograms of cross-sectional areas. The cell size distribution was compared between BDNF-IR and BDNF-non-IR cells in the sample of the entire NG population.

Preparation of NG cultures. P0-P1 (3-48 h old) and P9 rat pups were euthanized by intraperitoneal injection of Euthasol (0.1 mg/kg) and decapitated. NGs were rapidly and aseptically dissected from each animal in ice-cold Ca^{2+}/Mg^{2+}-free Dulbecco's phosphate-buffered salt solution (Mediatech, Herndon, VA). The ganglia were next digested in 0.1% crystallized trypsin-3X (Worthington Biochemical Corp., Lakewood, NJ), followed by 0.2% collagenase (Sigma), 30 min each, at 37°C in a humidified atmosphere of 5% CO_2 and 95% air. Both enzymes were dissolved in Ca^{2+}/Mg^{2+}-free Hanks' balanced salt solution (Mediatech) which had been pre-incubated for at least 2 h at 37°C in a humidified atmosphere of 5% CO_2 and 95% air. Following the enzymatic treatment, NGs were rinsed twice: first in 0.1% soybean trypsin inhibitor (Worthington) dissolved in Ca^{2+}/Mg^{2+}-containing Dulbecco's phosphate-buffered salt solution (Mediatech), and next in plating medium, both at room temperature. The tissue was next transferred to the plating medium and triturated through fire-polished Pasteur pipettes of decreasing tip diameter. Dissociated NG cells were plated in UV-sterilized, 96-well, flat bottom ELISA plates (MaxiSorp™, Nalge Nunc Int., Naperville, IL) pre-coated with anti-BDNF capture antibody (BDNF E_{max}™ ImmunoAssay System, Promega; for BDNF ELISA *in situ*; (Balkowiec and Katz, 2000), and/or in 24-well tissue culture-treated polystyrene plates (Corning Inc., Corning, NY) on poly-D-lysine (0.1 mg/ml; Sigma) and laminin (0.4 μg/ml; Sigma)-coated glass coverslips (for immunocytochemistry). NG cultures were grown in Neurobasal-A plating medium (Invitrogen) supplemented with B-27 serum-free supplement (Invitrogen), 0.5 mM L-glutamine

(Invitrogen), 2.5% fetal bovine serum (HyClone, Logan, UT), 1% Penicillin-Streptomycin-Neomycin antibiotic mixture (Invitrogen), and in some experiments, 2.5% Nystatin (Sigma), for 3 days at 37°C in a humidified atmosphere of 5% CO_2 and 95% air.

Electrical field stimulation. Following the initial 3-day incubation, NG cultures were stimulated in 96-well plates as recently described by our laboratory (Buldyrev et al., 2006). Specifically, the wells were fitted with paired Ag/AgCl electrodes (0.25 mm wire diameter; one pair per well), connected in parallel (four wells per set) to one of four independent outputs of the stimulator (MultiStim System; Digitimer; Welwyn Garden City, Hertfordshire, UK). The stimulation pattern delivered by each of the outputs was controlled by the 8-channel programmable pulse generator Master-8-cp (AMPI, Jerusalem, Israel). Four additional wells were also fitted with pairs of electrodes, but were not connected to the stimulator and served as controls. The plate was put back to the incubator, and the neurons were stimulated with biphasic rectangular pulses of 0.5 ms duration and amplitude of 80-120 mA per well, delivered at various patterns (see Results).

Drug treatment. Cultures were treated with the drugs for 30 min prior to electrical stimulation, at 37 °C in a humidified atmosphere of 95% air / 5% CO_2. ω-Conotoxin GVIA (Sigma) was dissolved in distilled water and used at the final concentration of 1 μM, and nimodipine (Sigma) was dissolved in ethanol and used at the final concentration of 2 μM.

Measurement of BDNF release. BDNF protein was measured with a modified sandwich ELISA, termed ELISA *in situ*, as previously described (Balkowiec and Katz, 2000). Specifically, 96-well ELISA plates were UV-sterilized for 20 min and coated with anti-BDNF monoclonal capture antibody (BDNF E_{max}^{TM} ImmunoAssay System, Promega) at 4°C for 12-18 h. Next, plates were washed and blocked, followed by two 1-h (or longer) incubations with culture medium to

remove any residue of the ELISA washing solution. Then, NG cultures were prepared as described above, plated in anti-BDNF-coated wells, and grown for three days. The BDNF E_{max}^{TM} ImmunoAssay System (Promega) was used according to the protocol of the manufacturer, except that the concentration of the anti-BDNF monoclonal and anti-human BDNF polyclonal antibody was 3 μg/ml and 2 μg/ml, respectively, and the dilution of the anti-IgY-HRP antibody was 1:100. All reagents used prior to cell plating were sterilized with a 0.2 μm syringe filters (Millex® GP, Millipore, Carrigtwohill, Ireland). BDNF samples used to generate standard curves were incubated in the same plate as the NG cell culture. Following cell stimulation and a 1-h post-stimulus incubation, plates were extensively washed to remove all cells and cell debris, and the anti-human BDNF polyclonal antibody was applied, followed by subsequent steps according to the manufacturer's protocol. Absorbance values were read at 450 nm in a plate reader (V_{max}^{TM}, Molecular Devices, Sunnyvale, CA).

Calculations and statistical analysis:

BDNF localization studies. The percentage of BDNF-IR NG somata or brainstem puncta within the DiI-labeled (putative baroreceptor) population was calculated for each animal. The mean percentages of BDNF-IR DiI-containing profiles were compared among three time points, i.e. P9, P23 and P30, using a one-way ANOVA, followed by Tukey's posthoc test. Furthermore, an independent sample, two-tailed *t*-test was used to make the following comparisons: (i) the mean percentage of BDNF-IR NG somata in the entire population of NG neurons at P0 *versus* P30, (ii) the mean percentage of BDNF-IR neurons between the entire NG population and the DiI-containing NG at P30, and (iii) the mean percentage of BDNF-IR profiles between DiI-containing somata in the NG and DiI-containing puncta in the medial NTS at P30. Data are expressed as mean ± standard error. $P < 0.05$ was considered significant.

BDNF release studies. BDNF levels were calculated from the standard curve prepared for each plate, using SOFTmax PRO® vs. 4.3 software (Molecular Devices). The standard curves were linear within the range used (0-500 pg/ml) and the quantities of BDNF in experimental samples were always within the linear range of the standard curve. Data are expressed as mean ± standard error. Samples were compared using ANOVA followed by Duncan's multiple comparison procedure, and $P < 0.05$ was considered significant.

RESULTS

Brain-derived neurotrophic factor (BDNF) is abundantly expressed in aortic baroreceptor neurons *in vivo.*

A subset of developing visceral sensory neurons from the nodose-petrosal ganglion complex (NPG) expresses BDNF as early as embryonic day 16 (Brady et al., 1999). BDNF mRNA and protein have also been detected in a subset of adult NPG neurons (Schecterson and Bothwell, 1992; Wetmore and Olson, 1995; Apfel et al., 1996; Zhou et al., 1998). However, the functional identity of the BDNF-expressing population is, for the most part, unknown. Thus far, only the tyrosine hydroxylase-expressing subpopulation of chemoafferent neurons has been identified as containing a portion of the BDNF-positive neurons (Brady et al., 1999). Therefore, we tested the hypothesis that BDNF is also found in aortic baroreceptor neurons, whose cell bodies are located in the nodose ganglion (NG), using BDNF immunohistochemistry.

We first conducted several control experiments to verify the specificity of the BDNF antibody. Recombinant human BDNF protein was applied to an SDS-PAGE gel and immunoblotted with the BDNF antibody. The 27-kDa BDNF protein was monomerized by reducing agents in the loading buffer, yielding a monomer of approximately 13 kDa. The 2000 ng and 200 ng samples of BDNF were detected, but not the 40 ng sample, using the Western blot technique (Fig. 1 A). Consistent with this result, we were not able to detect BDNF in the NG, in which total levels of BDNF are in the picogram range, as confirmed by ELISA (data not shown). The specificity of the BDNF antibody was further assessed with a modified preabsorption assay. BDNF protein was covalently linked to magnetic beads and then incubated with the BDNF antibody, providing a novel way to separate BDNF-antibody complexes from unbound antibody.

The supernatant, potentially containing any antibody that did not bind to the BDNF-coated beads, was used to stain NG cultures. Cultures stained with antibody preabsorbed with BDNF immobilized on beads (Fig. 1 B, 'preabsorbed') showed markedly reduced BDNF IR compared to cultures stained with the antibody incubated with uncoated beads (Fig. 1 B, 'control'). Furthermore, the pattern of staining in NG sections and the caudal brainstem matches results obtained using different anti-BDNF antibodies (Ichikawa et al., 2007).

The peripheral processes of aortic baroreceptor neurons travel largely unaccompanied (Sapru and Krieger, 1977; Sapru et al., 1981; Cheng et al., 1997) in the aortic depressor nerve, thus allowing us to isolate aortic baroreceptor neurons for neuronal tracing studies. The right side aortic depressor nerve was pre-labeled at P2 with the fluorescent tracer CM-DiI. Following 7, 21 and 28 days *in vivo*, sections of ipsilateral NGs from P9 (n=6 rats), P23 (n=3 rats) and P30 (n=5 rats), respectively, were processed for BDNF immunohistochemical staining (Fig. 2 A, B). All DiI-labeled somata also containing a nuclear profile were identified in every other section of the ganglion, and BDNF immunoreactivity was assessed for every DiI-labeled profile meeting these criteria.

At P9, an average of 46.3 ± 8.1 DiI-labeled profiles were found, and among these, 26.7 ± 5.1 were BDNF-IR (n = 6 NG). At P23, an average of 35.7 ± 7.8 DiI-labeled profiles were found, and 12.7 ± 4.2 of these cells were BDNF-IR (n = 3 NG). Similarly at P30, an average of 30.2 ± 5.5 DiI-labeled profiles were found, and 12 ± 2.2 of these cells showed BDNF IR (n = 5 NG). The percentage of neuronal somata that contain BDNF IR significantly decreases between P9 and P23 ($P<0.01$) but, subsequently, remains unchanged between P23 and P30, in the DiI-labeled putative baroreceptor population (Fig. 2 C). These data indicate that BDNF is expressed by a majority of baroreceptor afferents during early postnatal development, and the number of

BDNF-IR baroafferents remains high even after the period of postnatal maturational changes in the baroreceptor reflex.

BDNF immunoreactivity is present in baroreceptor afferents of all sizes.

Baroreceptor afferents are divided into two broad categories: larger, myelinated (Aδ) and smaller unmyelinated (C) fibers, each serving a distinct function in the baroreceptor reflex (Jones and Thoren, 1977; Thoren et al., 1977; Chapleau and Abboud, 1989; Chapleau et al., 1989; Seagard et al., 1993). In order to begin addressing the question of whether BDNF is associated with a specific subtype of baroreceptor afferents, we first examined the cell size distribution of BDNF-IR, compared with BDNF-non-IR, DiI-labeled cells from P30 NG. For this analysis, we used the same cell population that was selected for counting percentages of BDNF-IR baroafferents. A total of 60 BDNF-IR and 91 BDNF-non-IR were identified in 5 ganglia, and the cross-sectional area of each cell was determined as described in the 'Materials and Methods' section. Our data indicate that the BDNF-IR subpopulation of baroafferents is not limited to neurons of a specific size range and, instead, spans the entire range of cell sizes found for the DiI-labeled aortic baroreceptors, including the least abundant myelinated A-fibers that are associated with the largest cell bodies. In fact, when comparing among various cell sizes, the proportion of BDNF-IR cells is greater in larger neurons (Figure 3 A).

For comparison, we examined the cell size distribution of BDNF-IR and BDNF-non-IR cells in the entire population of P30, as well as P0, NG neurons. Sections of three P30 and three P0 right-side ganglia single-stained for BDNF (ABC method; Fig. 3 B, C, insets) were used for the analysis. One-thousand-six-hundred-thirteen neurons from three P30 ganglia were measured, including 1047 BDNF-IR cells. Similar to the cell size distribution of BDNF-IR baroreceptors, BDNF-IR NG afferents, sampled from the whole NG population at P30, are distributed across the

entire size range (Fig. 3 B). This result indicates that the distribution pattern of BDNF expression among baroreceptor afferents is shared with other subpopulations of NG neurons at this age. We also examined P0 NG neurons and, here too, BDNF IR was present in all cell sizes found in this age group (1675 BDNF-IR cells out of 2540 cells sampled from 3 ganglia; Fig. 3 C). In both P0 and P30 ganglia, the proportion of BDNF-IR cells is greater in neurons of larger cross-sectional area. These data suggest that the distribution of BDNF expression among various subpopulations of NG neurons does not change during the postnatal maturational period. In addition, the percentage of BDNF-IR cells in the entire NG neuron population does not significantly change between P0 (66%) and P30 (65%). Moreover, the overall mean percentage of BDNF-IR baroreceptor somata at P30 (40%) is significantly lower compared to the mean percentage of BDNF-IR somata in the entire NG population (65%; $P<0.01$). This indicates that the developmental decline in BDNF expression observed for the baroreceptor population (Fig. 2 C) is not a general phenomenon that affects the NG population as a whole.

BDNF immunoreactivity is present in large subsets of HCN1- and TRPV1- expressing baroreceptor afferents.

To further explore the functional identity of BDNF-IR baroreceptor afferents, we next turned to histochemical markers selective for specific subpopulations of NG afferents. Doan and colleagues (2004) have found the hyperpolarization-activated cyclic nucleotide-gated ion channel protein 1 (HCN1) to be expressed in myelinated, but not unmyelinated, baroreceptor terminals. Therefore, we first examined BDNF IR in HCN1-IR DiI-labeled NG neurons (putative baroreceptor afferents) from P30 animals. Out of 84 DiI-labeled cells, 18 expressed HCN1 IR, and 8 showed double HCN1/BDNF IR. These data indicate that HCN1-IR cells constitute

approximately 21% of the DiI-labeled population, and nearly a half of them show BDNF IR, similar to HCN1-non-IR cells (Fig. 4 A, Table 1).

A marker selective for unmyelinated NG afferents is the vanilloid receptor TRPV1 (Jin et al., 2004). Moreover, functional TRPV1 channels are present exclusively in unmyelinated, C-type aortic baroreceptors (Reynolds et al., 2006). Therefore, we used TRPV1, combined with BDNF immunostaining in order to examine BDNF expression in unmyelinated baroafferents. We find that one-half of baroafferents identified by the DiI labeling of the aortic depressor nerve express TRPV1 (28 out of 51 DiI-labeled cells; Table 1). From those cells, almost 60% exhibit BDNF IR (Fig. 4 B, Table 1). Within the TRPV1-non-IR baroreceptor population, on the other hand, only one-third contains BDNF IR. Together, these results are consistent with our cell size distribution analysis indicating that BDNF is present in both small unmyelinated, and large myelinated baroafferents.

BDNF immunoreactivity is present in the central projections of baroreceptor afferents in the brainstem.

During development, nodose-petrosal ganglion (NPG) neurons are dependent on target-derived BDNF for survival (Erickson et al., 1996), but this dependence is lost by the first postnatal day (Brady et al., 1999). Consequently, BDNF expressed by postnatal baroreceptor neurons is likely to play other roles, such as promoting maturation and/or modulating the function of baroreceptor synapses in the medial *nucleus tractus solitarius* (NTS) of the lower brainstem. In support of this possibility, BDNF has previously been shown to be anterogradely transported in the central axons of dorsal root ganglion sensory neurons (Zhou and Rush, 1996). Therefore, we next asked whether BDNF is present in the central afferent tract as well as the central terminal field of baroreceptor neurons in the NTS. For these studies, we used the same

DiI-labeled P30 rats (i.e. 28 days post-labeling) that were used in the studies of BDNF distribution in baroreceptor cell bodies described above. P9 and P23 rats, which represent shorter DiI-transport times (i.e. 7 and 21 days, respectively) were not used in this analysis.

Using confocal microscopy, we examined the distribution of BDNF IR in the central projections of baroreceptor afferents in five P30 brainstems. Specifically, we examined the solitary tract, which contains the central axons of NPG neurons, and the medial NTS, the major central target of baroreceptor afferents (Andresen and Kunze, 1994). In all P30 brainstems examined, strong BDNF IR was observed in the solitary tract (Figure 5 A, B), suggesting that BDNF is transported to central terminals in visceral afferent neurons. BDNF IR was also present in DiI-labeled synaptic terminal-like puncta in the medial NTS (Fig. 5 C, D). The distribution of BDNF in the central projections of baroreceptor afferents closely matched the BDNF distribution in the cell bodies of these neurons for each of the 5 animals examined (Fig. 5 E). Moreover, out of a total of 125 DiI-labeled terminal-like puncta identified in the NTS from 5 brainstems, 56 (44.8%) were also BDNF-IR. This percentage closely matches the percentage of BDNF-IR DiI-labeled cell bodies in the NG (Fig. 5 E), suggesting that BDNF is faithfully transported to the central targets. Due to a relatively long time course of DiI transport, it was not possible to examine BDNF distribution in specifically identified baroafferent terminals at time points earlier than P30. However, we have found BDNF immunoreactivity in the solitary tract and the medial NTS as early as P1 (data not shown). Together, our data suggest that BDNF is likely to play a role at first-order baroreceptor synapses during both postnatal maturation and adult plasticity.

Bursting patterns of electrical stimulation known to induce plasticity in baroreceptor pathways are significantly more effective at releasing BDNF from nodose ganglion neurons than tonic patterns of the same average frequency.

Expression of BDNF in baroafferent axons and terminal-like structures in the brainstem strongly suggests that BDNF is released at first-order baroreceptor synapses. In order to help establish physiological conditions under which BDNF is released from arterial baroreceptors, we examined the effects of stimulation patterns that mimic different levels of baroafferent activity *in vivo* on the release of native BDNF from dissociate cultures of NG neurons (Fig. 6 A), which included the baroafferent population (Fig. 6 B). We focused our study on patterns of baroreceptor activity known to evoke plastic changes at baroreceptor synapses, and asked whether the magnitude of BDNF release is regulated by these patterns. Seven stimulation protocols, each delivering the same overall number of pulses (20,000), were applied: 4 protocols of continuous stimulation, i.e. at 6 Hz, 12 Hz, 24 Hz and 48 Hz, were compared with 3 protocols of bursting patterns, i.e. 2 pulses at 36 Hz (mean frequency 12 Hz); 4 pulses at 72 Hz (mean frequency 24 Hz), and 8 pulses at 144 Hz (mean frequency 48 Hz), applied at 6 Hz, a frequency corresponding to a rat heart rate, as previously described by Liu *et al.* (Liu et al., 2000). Following the initial 3-day culture period, sister NG cultures were stimulated using the protocols described above and schematically depicted in Figure 6 C and D.

All stimulated cultures exhibited a significant increase in BDNF release compared to unstimulated controls. However, stimulation with patterns known to induce plastic changes in baroreceptor pathways was markedly more effective at releasing BDNF compared to tonic stimulation at the same average frequency (Fig. 6 C, D). Moreover, the amount of released BDNF was regulated by inter-pulse frequency during phasic, but not tonic, stimulation (Fig. 6 D).

Together, the data indicate that the mechanisms regulating BDNF release from NG neurons discriminate among not only different frequencies but also patterns of stimulation, such that the release is facilitated selectively by high-frequency bursting patterns.

Patterned stimulation-evoked release of BDNF from nodose ganglion neurons requires both L- and N-type calcium channels.

Our earlier studies demonstrated that electrical stimulation-evoked BDNF release from NPG neurons is abolished by tetrodotoxin (TTX), an inhibitor of voltage-gated sodium channels (Balkowiec and Katz, 2000). Also, we have previously shown that activity-dependent BDNF release from both sensory and hippocampal neurons requires calcium mobilization from intracellular stores (Balkowiec and Katz, 2002; Buldyrev et al., 2006). The same studies revealed that the relative contribution of different calcium channels to activity-dependent BDNF release is cell type-specific (e.g. hippocampal vs. trigeminal ganglion cells;(Balkowiec and Katz, 2002; Buldyrev et al., 2006). Therefore, we next sought to determine which subtypes of voltage-activated calcium channels are involved in BDNF release from NG neurons.

Pretreatment of NG cultures with an L-type channel antagonist Nimodipine (2 μM) inhibited BDNF release by 25.8% during 1 h of 24-Hz continuous stimulation (Fig. 7). For the same stimulation paradigm, pretreatment with 1 μM ω-Conotoxin GVIA, an N-type calcium channel antagonist, inhibited BDNF release by 64 % (Fig. 7). Simultaneous application of both Nimodipine (2 μM) and ω-Conotoxin GVIA (1 μM) resulted in an abolition of BDNF release (Fig. 7). These data indicate that activity-dependent release of native BDNF from NG neurons is controlled by calcium entry through both N- and L-type calcium channels, with a much stronger contribution by N-type calcium channels.

DISCUSSION

The current study provides the first direct evidence that BDNF is present in a large subset of arterial baroreceptor afferents, including their central axons in the brainstem solitary tract and terminal-like puncta in the *nucleus tractus solitarius* (NTS). BDNF is expressed in both A- and C-type baroreceptor afferents, during and after the period of postnatal maturational changes, indicating a potential for this neurotrophin to play a role in the plasticity of various baroreceptor reflexes activated under differing sensory inputs. BDNF release from nodose ganglion (NG) neurons is regulated by patterns that mimic baroreceptor activity *in vivo*, such that phasic baroreceptor firing patterns are markedly more effective at releasing BDNF than tonic patterns of the same average frequency. Furthermore, the release is largely dependent on activity of N-type voltage-gated calcium channels, known to be primarily expressed at synaptic terminals of NG neurons.

The arterial baroreceptor reflex, together with other cardiorespiratory reflexes, undergoes considerable maturational changes during the early postnatal period (Merrill et al., 1995; Segar, 1997; Mazursky et al., 1998; Merrill et al., 1999; Ishii et al., 2001; Arsenault et al., 2003). Within the first two postnatal weeks in mice, the baroreflex gain increases nearly 4-fold to almost reach the adult value (Ishii et al., 2001). Several lines of evidence indicate that the first weeks of postnatal life bring significant changes to the NTS circuitry, which is the central target of cardiorespiratory afferents. These changes include morphological and electrophysiological maturation of NTS neurons and synaptic connections (Kalia, 1992; Denavit-Saubie et al., 1994; Vincent and Tell, 1997; Smith et al., 1998; Rao et al., 1999; Vincent and Tell, 1999; Kawai and

Senba, 2000). Furthermore, changes in the NTS likely result in changes in reflex function as a whole. However, very little is known about molecular mechanisms that govern these changes.

The present study demonstrates that a large subset of baroreceptor neurons from both early postnatal and young adult rats expresses BDNF, the neurotrophin with a well-established role in developmental and adult plasticity of synaptic connections (Huang and Reichardt, 2001), including sensory pathways (Malcangio and Lessmann, 2003). Using young adult rats, we show that BDNF is present not only in baroreceptor cell bodies, but also their central projections. Unfortunately, our experimental approach using DiI tracing could not provide direct evidence for BDNF expression in the central projections of early postnatal baroreceptor neurons for technical reasons (i.e. inadequate time for the dye transport). However, the fact that BDNF is abundantly expressed in the early postnatal solitary tract as well as areas of the NTS known to receive baroafferent input, together with the evidence for the abundant expression of BDNF in early postnatal baroreceptor cell bodies, make the existence of BDNF in central axons and terminals of early postnatal baroafferents highly likely.

Previous studies, including a recent study from our laboratory, show that a significant fraction of BDNF within central axon terminals of sensory neurons is localized to dense-core vesicles (Michael et al., 1997; Buldyrev et al., 2006). These data, combined with the current findings, strongly suggest that BDNF is released at baroafferent synapses in the NTS by activity, indicating a potential role of BDNF in developmental and adult plasticity of baroreceptor pathways. This notion is supported by the fact that second-order sensory neurons in the NTS express the high-affinity receptor for BDNF, TrkB (Balkowiec et al., 2000). Moreover, very recent studies from other laboratories indicate that microinjections of the BDNF neutralizing antibody

to the medial NTS lead to significant decreases in mean arterial blood pressure (Clark et al., 2008), suggesting a direct role of BDNF in baroafferent transmission in the NTS.

Baroreceptor afferents constitute a morphologically and functionally heterogenous population, with two major types of cells: thinly myelinated Aδ, associated with bursting patterns of baroreceptor activity, and unmyelinated C-type, distinguished by more tonic discharge patterns (Chapleau and Abboud, 1989; Chapleau et al., 1989; Seagard et al., 1993). In an attempt to identify the subpopulation of baroreceptor neurons that expresses BDNF, we performed a thorough analysis of cell size distribution and colocalization studies with HCN1, a marker of A-type baroafferents (Doan et al., 2004) and TRPV1, a marker of capsaicin-sensitive C-type baroafferents (Jin et al., 2004). All lines of evidence indicate that BDNF is expressed by significant fractions (40-60%) of both A- and C-type baroreceptors. This raises the possibility that BDNF is involved only in select baroreflexes, or mobilized under certain physiological conditions. Since BDNF expression is regulated by activity, the BDNF-non-IR subpopulation could simply represent the "silent", or less active, fraction of baroreceptor afferents. In support, BDNF protein is upregulated in DOCA-salt hypertensive rats compared to aged-matched controls (Jenkins et al., 2007). Similarly, the developmental decline in the number of BDNF-expressing baroafferents could be a result of changes in neuronal activity among various subpopulations of baroreceptor neurons. The cell size distribution analysis revealed that the proportion of BDNF-IR cells is greater in large, A-type, baroafferents, known to preferentially discharge with bursting patterns. This is consistent with another observation from this study that the magnitude of BDNF release from NG neurons is significantly higher in response to bursting, compared to tonic patterns of activation.

It is not possible at the present time to measure BDNF released exclusively from the baroreceptor population of NG neurons. For that reason, we chose to examine the effects of baroreceptor patterns of stimulation on BDNF release from dispersed NG neurons. Although NG cultures contain, in addition to baroafferents, other functionally distinct populations of sensory neurons, baroreceptor afferents retain BDNF expression *in vitro* (Fig. 3B) and, therefore, are very likely to contribute to the detected BDNF release. Moreover, previous studies strongly suggest that baroreceptor afferent pathways do not differ from other NG afferent pathways with respect to stimulus-response characteristics at first-order synapses in the NTS (Mifflin, 1997; Bailey et al., 2006).

Our results show that the stimulus-evoked BDNF release from NG neurons is largely dependent on N-type calcium channels. In turn, N-type channels are present predominantly at synaptic terminals of NG neurons, as previously demonstrated (Mendelowitz et al., 1995). Although our *in vitro* model of activity-dependent BDNF release does not allow for a direct determination of the subcellular sites of the release, these data are consistent with the hypothesis that BDNF release occurs at central terminals of baroreceptor afferents.

Our data indicate that the mechanisms regulating BDNF release from NG neurons discriminate among not only different frequencies but also patterns of stimulation, such that the release is enhanced during high-frequency bursts delivered at the heart rate frequency. These data are consistent with previous studies of BDNF release from other neuronal populations, including dorsal root ganglion (Lever et al., 2001) and hippocampal (Balkowiec and Katz, 2002) neurons. It is well established that many baroreceptor afferents provide a bursting input to the NTS that is synchronous with the systolic phase of the cardiac cycle (Chapleau and Abboud, 1989; Chapleau et al., 1989; Seagard et al., 1993). Moreover, the pattern of baroreceptor

activity determines the magnitude of the reflex response independently of the mean frequency of baroreceptor discharges, with pulsatile activation leading to central facilitation of the reflex (Chapleau and Abboud, 1987, 1989). Therefore, there is a possibility that BDNF, released in large quantities from a subpopulation of baroreceptor afferents during their pulsatile activation, contributes to the baroreflex facilitation. In support of this possibility, we found that BDNF is expressed in a significant fraction of larger, A-type baroafferents, which are characterized by bursting patterns of activity. We also determined that BDNF is expressed in baroreceptor afferents beyond the period of postnatal maturational changes. Consequently, BDNF is likely to play a role in adult plasticity of selected baroreflexes.

In addition to baroreflex facilitation, phenomena representing other forms of synaptic plasticity at baroreceptor synapses have been described. For example, the magnitude of postsynaptic responses in NTS neurons is regulated by the frequency of the presynaptic input. Specifically, increasing the frequency of baroreceptor input leads to depression of postsynaptic responses in NTS neurons (Scheuer et al., 1996; Liu et al., 1998; Chen et al., 1999; Liu et al., 2000; Doyle and Andresen, 2001), the phenomenon known as 'frequency-dependent depression' (FDD), which may influence the function of the baroreceptor reflex (Liu et al., 2000). Several mechanisms have been implicated to contribute to FDD, including alterations in presynaptic mechanisms (Schild et al., 1995; Chen et al., 1999), desensitization of non-NMDA receptors (Schild et al., 1995; Zhou et al., 1997), an adenylate cyclase-mediated regulatory mechanism (Schild et al., 1995), activation of presynaptic metabotropic glutamate receptors (Liu et al., 1998), activation of mu-opiate receptors (Hamra et al., 1999), and frequency-dependent depression of endocytosis (Pamidimukkala and Hay, 2001). In the present study, the patterns known to evoke very pronounced FDD were most effective at releasing BDNF. Previously, we demonstrated that exogenous BDNF acutely inhibits AMPA currents in second-order sensory

neurons in the NTS (Balkowiec et al., 2000). These data, in conjunction with the evidence that glutamate receptors mediate baroreceptor afferent transmission in the NTS (Guyenet et al., 1987; Andresen and Yang, 1990; Drewe et al., 1990; Gordon and Leone, 1991; Lawrence and Jarrott, 1994; Zhang and Mifflin, 1995; Aylwin et al., 1997; Andresen et al., 2001; Gordon and Sved, 2002; Schreihofer and Guyenet, 2002; Guyenet, 2006), indicate that BDNF may be involved in the mechanisms of FDD.

In conclusion, the present study identifies BDNF as a likely mediator of activity-dependent modifications at first-order synapses in arterial baroreceptor pathways, including postnatal maturation of the baroreceptor reflex. These data may be relevant to understanding the pathomechanisms of developmental disorders of the cardio-respiratory system, such as Sudden Infant Death Syndrome (SIDS).

ACKNOWLEDGEMENTS

A.B. would like to thank Dr. David M. Katz of Case Western Reserve University, Cleveland, OH, for his invaluable support at initial stages of the project development. The authors express their gratitude to Dr. Michael Danilchik for help with the confocal microscopy portion of this study. This work was supported by grants from the American Heart Association (0230095N) and the National Heart, Lung, and Blood Institute of the National Institutes of Health (HL076113) to A.B.

TABLES & FIGURES

Table 1

	DiI-labeled Cell Bodies (Putative Baroafferents) %	BDNF-IR DiI-labeled Cell Bodies (Putative Baroafferents) %
HCN1-IR	21.36 ± 0.85	43.75 ± 6.25
HCN1-non-IR	78.64 ± 0.85	48.48 ± 0.09
TRPV1-IR	51.47 ± 6.02	58.26 ± 1.74
TRPV1-non-IR	48.53 ± 6.02	31.37 ± 1.96

Table 1: Quantification of BDNF-IR DiI-labeled cell bodies of NG neurons (putative baroafferents) within HCN1- and TRPV1-IR and non-IR subpopulations.

Somata that were analyzed for HCN1 IR or TRPV1 IR were further assessed for BDNF IR. Data are derived from two nodose ganglia (NG) of two P30 rats that were pre-labeled with DiI applied to the aortic depressor nerve at P2. Double immunofluorescent staining was performed on alternate sections of the same NG for HCN1-IR and BDNF-IR or TRPV1-IR and BDNF-IR, respectively. All DiI-positive somata containing a nucleus were assessed.

Figure 1

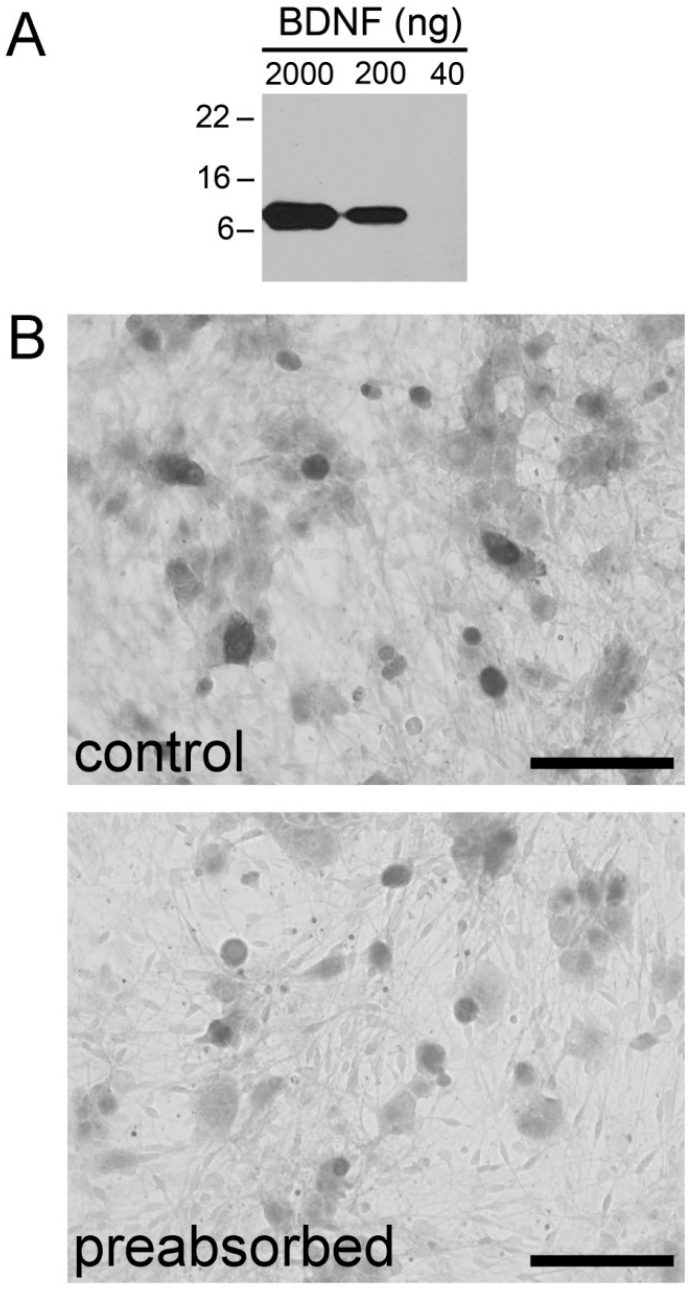

Figure 1: Chicken anti-BDNF polyclonal antibody preabsorbed with BDNF protein is ineffective in detecting endogenous BDNF in NG neurons.

A, The results of Western blotting performed using 2000 ng, 200 ng, and 40 ng samples of recombinant human BDNF protein and the chicken anti-BDNF antibody. BDNF was reduced to approximately 13-kDa monomers by boiling in loading buffer containing 4.6% SDS and 5% β-mercaptoethanol. *B,* A dissociate 3-day culture of newborn rat NG neurons, immunostained with the BDNF antibody in control conditions (control) and following preabsorption with BDNF bound to magnetic beads. Scale bar, 100 μm.

Figure 2

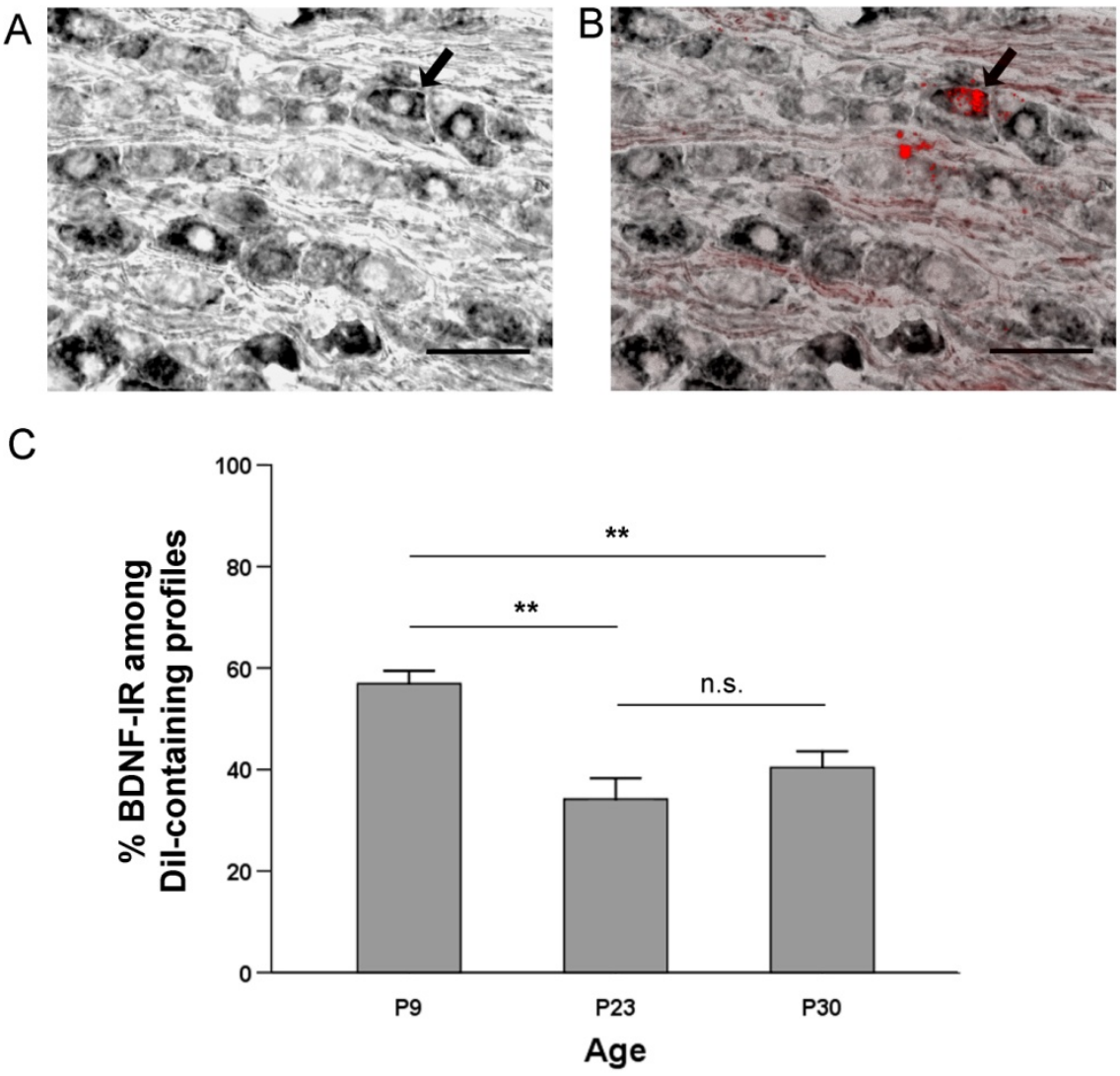
A
B
C
% BDNF-IR among
DiI-containing profiles
100
80
60
40
20
0
**
**
n.s.
P9
P23
P30
Age

Figure 2: Cell bodies of putative baroafferent neurons in the nodose ganglion show abundant BDNF immunoreactivity from postnatal development into adulthood.

A, A section through the right nodose ganglion immunostained for BDNF (ABC method) from a postnatal day (P) 23 rat in which CM-DiI was placed on the right aortic depressor nerve at P2. *B*, DiI fluorescence overlay of the same section. Arrows indicate a BDNF-positive neuron which is also labeled with DiI, suggesting its baroreceptor origin. Scale bar, 50 µm. *C*, Mean percentage of BDNF-IR cells within the DiI-labeled NG somata (putative baroafferents) in P9 (n=6), P23 (n=3), and P30 rats (n=5); ** $p<0.01$, n.s. = not significant.

Figure 3

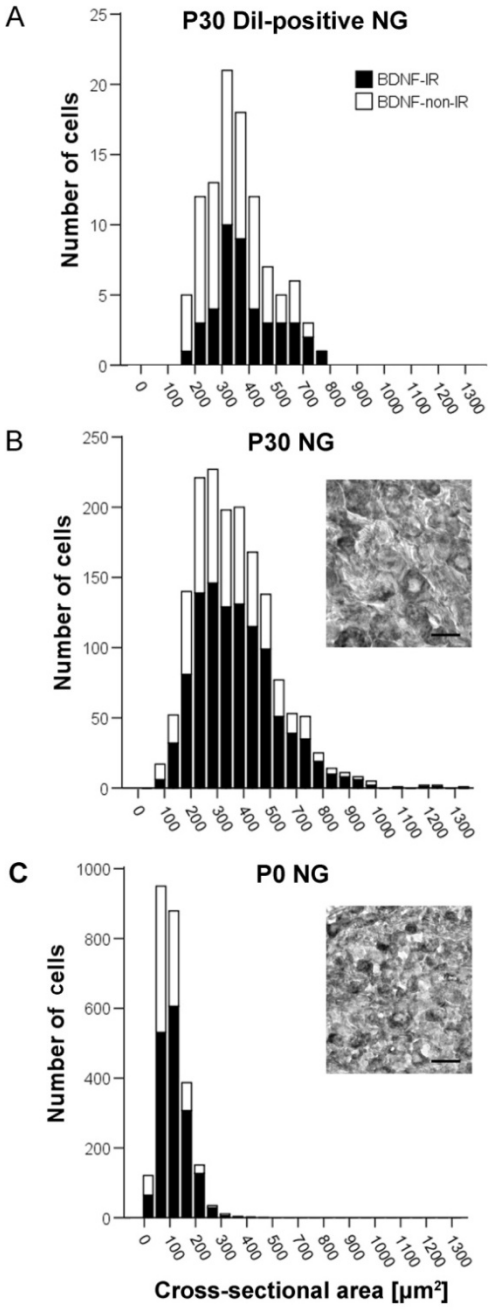
A
P30 DiI-positive NG
BDNF-IR
BDNF-non-IR
Number of cells
B
P30 NG
Number of cells
C
P0 NG
Number of cells
Cross-sectional area [µm²]

Figure 3: BDNF IR is present in baroafferent neurons of all sizes.

A, Frequency distribution of the cross-sectional areas of DiI-positive somata from three P30 rats sampled from every other section through the NG. Frequency distribution of the cross-sectional areas of P30 (*B*) and P0 (*C*) NG somata taken from ganglion sections spaced approximately 110 µm apart. The data represent the combined number of cells obtained from three ganglia. *Insets*, example images of a section of P30 (*B*) and P0 (*C*) NG immunostained for BDNF (ABC method). Scale bar, 25 µm. Black bars, BDNF-IR; white bars, BDNF-non-IR. Sum of black bar and white bar represents the entire population sampled.

Figure 4

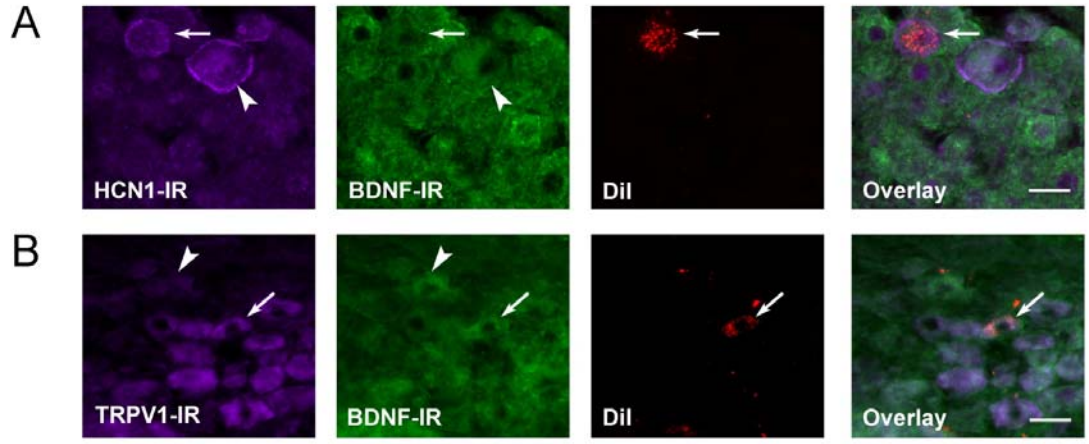

Figure 4: BDNF-IR is present in two distinct populations of NG neurons: lightly myelinated A-fibers (HCN1-IR) and unmyelinated C-fibers (TRPV1-IR).

Double immunofluorescence of HCN1 IR (*A*) or TRPV1 IR (*B*) and BDNF IR in a P30 rat, in which the neuronal tracer DiI was placed on the ADN at P2. In *A,* The arrow indicates a putative baroafferent neuron containing HCN1 IR, but negative for BDNF IR. The arrowhead points to an NG cell that is HCN1 immunoreactive, as well as BDNF immunoreactive. HCN1 IR is characterized by a bright, cell membrane staining in medium to larger neurons. In *B*, the arrow points to a putative baroafferent neuron positive for TRPV1 and BDNF. The arrowhead indicates an NG cell that is TRPV1-non-IR, but positive for BDNF.

Figure 5

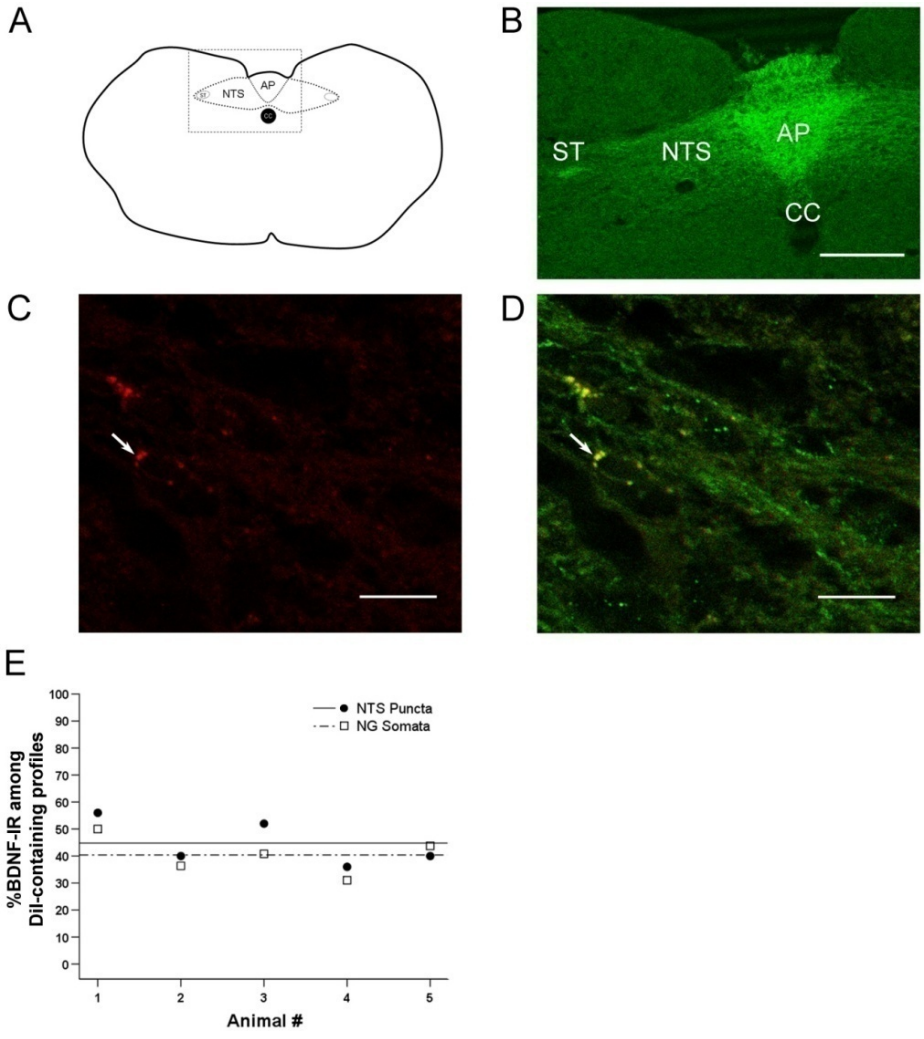
A
NTS
AP
CC
B
ST
NTS
AP
CC
C
D
E
%BDNF-IR among DiI-containing profiles
NTS Puncta
NG Somata
Animal #
100
90
80
70
60
50
40
30
20
10
0
1
2
3
4
5

Figure 5: BDNF immunoreactivity (-IR) is present in the terminal field of nodose ganglion visceral sensory neurons in the nucleus tractus solitarius (NTS), including putative baroafferents.

A, Schematic of a cross-section through the caudal brainstem. AP, area postrema; NTS, *nucleus tractus solitarius*; ST, solitary tract; CC, central canal. Box represents the field of view seen in *B*. *B*, Laser scanning confocal image through the caudal brainstem of a postnatal day (P) 30 rat showing strong BDNF IR in the NTS, which contains terminations of nodose ganglion (NG) neurons, including baroreceptor afferents. BDNF IR is also present in the ST, suggesting that BDNF is transported in NG afferents to their terminals in the NTS. Scale bar, 250 μm. *C*, High magnification laser scanning confocal image showing terminal-like puncta of DiI-positive, putative baroafferent neurons (red). *D*. Overlay of DiI (red) and BDNF IR (green). Arrows indicate a punctum in which DiI and BDNF IR colocalize (yellow). Scale bar, 10 μm. *E*, The percentage of BDNF-IR somata (open squares) and medial NTS puncta (filled circles) shown for individual P30 animals analyzed. Percentages of BDNF IR calculated for NG somata closely match the percentages obtained for NTS puncta, further supporting the hypothesis that BDNF expressed in the cell bodies of baroreceptor neurons is faithfully transported to afferent terminals in the brainstem. The mean percentage of BDNF-IR profiles within the putative baroafferent population does not significantly differ between NG somata (dashed line) and NTS puncta (solid line) across individual animals, $p=0.41$.

Figure 6

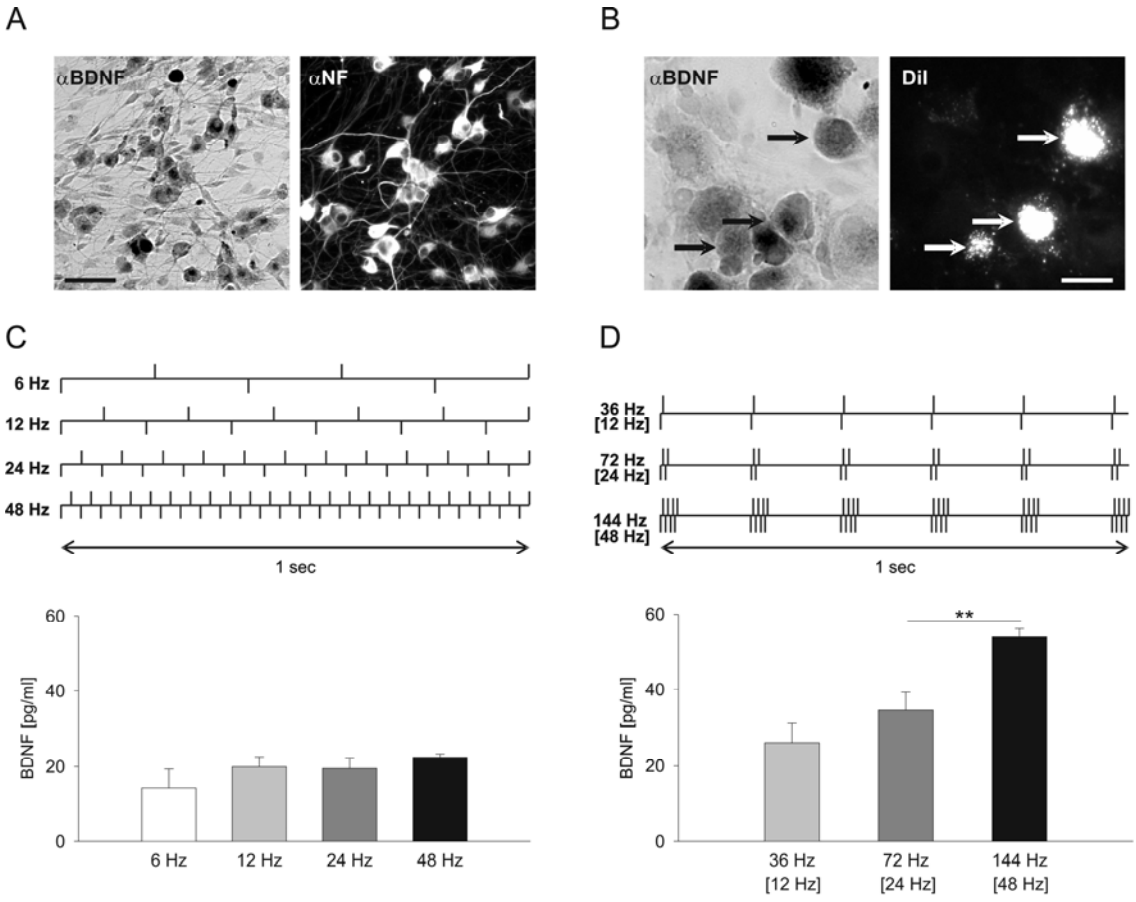
A
αBDNF
αNF
B
αBDNF
DiI
C
6 Hz
12 Hz
24 Hz
48 Hz
1 sec
BDNF [pg/ml]
60
40
20
0
6 Hz
12 Hz
24 Hz
48 Hz
D
36 Hz
[12 Hz]
72 Hz
[24 Hz]
144 Hz
[48 Hz]
1 sec
BDNF [pg/ml]
60
40
20
0
**
36 Hz
[12 Hz]
72 Hz
[24 Hz]
144 Hz
[48 Hz]

Figure 6: Endogenous BDNF is released from newborn nodose ganglion (NG) neurons in vitro by physiological patterns of baroreceptor activity.

A, A representative example of a dissociate 3-day culture of newborn rat NGs, double-immunostained for BDNF (αBDNF) and Neurofilament (αNF). Scale bar, 60 µm. *B*, BDNF-immunoreactivity (αBDNF) in a dissociate 1-day culture of NGs from postnatal day (P) 9 rats, in which both aortic depressor nerves were pre-labeled with the fluorescent tracer CM-DiI (DiI) at P2. Arrows indicate three BDNF-positive neurons (αBDNF, black arrows) that are also DiI-labeled (DiI, white arrows), indicating their putative baroreceptor origin. Scale bar, 15 µm. *C*, *D, top*, Schematic representation of stimulation patterns delivered to sister 3-day cultures of newborn NG neurons. *C*, *D, bottom*, Mean above control levels of BDNF released during electrical field stimulation delivered continuously at 6 Hz (55.6 min), 12 Hz (27.8 min), 24 Hz (13.9 min) or 48 Hz (6.95 min; *C*), or as bursts of 2, 4 or 8 pulses, with intraburst/[average] frequencies of 36 Hz/[12 Hz], 72 Hz/[24 Hz] and 144 Hz/[48 Hz], respectively (*D*). The total number of delivered pulses was the same for all stimulation protocols. A total of three independent experiments, each containing four cultures per stimulation pattern, were performed; ** $p<0.01$.

Figure 7

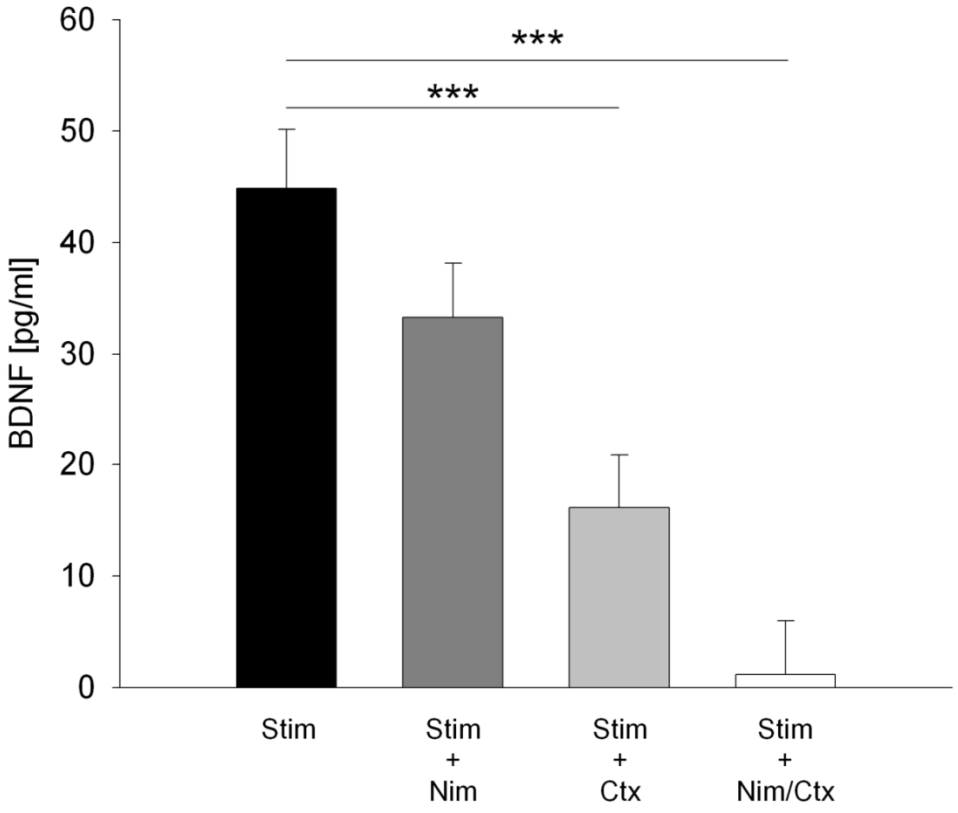

Figure 7: Release of endogenous BDNF evoked by patterned electrical stimulation of newborn NG neurons requires calcium influx through L- and N-type channels.

Mean above vehicle-control levels of BDNF released in sister cultures of newborn NG neurons during one hour of continuous electrical field stimulation at 24 Hz in the absence (Stim; n=18) or presence of voltage-activated calcium channel antagonists: 2 μM Nimodipine, an L-type channel antagonist (Stim + Nim; n=12), 1 μM ω-Conotoxin GVIA, an N-type channel antagonist (Stim + Ctx; n=13), or both applied simultaneously (Stim + Nim/Ctx; n=7); *** $p<0.001$.

Chapter 4:

Glia determine the course of BDNF-mediated dendritogenesis and provide a soluble inhibitory cue to dendritic growth in the brainstem.

Jessica L. Martin[1,2], Alexandra L. Brown[1], and

Agnieszka Balkowiec[1-3]

[1]Department of Integrative Biosciences, [2]Neuroscience Graduate Program, and [3]Department of Physiology and Pharmacology, Oregon Health & Science University, Portland, OR

ABSTRACT

Glia are increasingly being realized as essential players in neuronal circuit maturation, including dendritogenesis. A well-established extrinsic cue guiding dendritogenesis is brain-derived neurotrophic factor (BDNF). However, the specific effects that BDNF elicits on dendritic growth are context-dependent and it is currently unknown if any aspect of BDNF-mediated dendritogenesis is regulated by glia. In the present study, we used neonatal rat brainstem *nucleus tractus solitarius* (NTS) neurons *in vitro* to examine the role of BDNF and glia in dendritic development of neurochemically-identified subpopulations of NTS neurons. In the presence of abundant glia, BDNF promotes NTS dendritic outgrowth and complexity, with the magnitude of the BDNF effect dependent on neuronal phenotype. However, upon glia depletion, BDNF switches from promoting to inhibiting NTS dendritogenesis. Astrocyte-conditioned medium (ACM), while promoting hippocampal dendritogenesis, inhibits NTS dendritic outgrowth, the effect that is abolished by heat-inactivation of ACM. Together, these results point to novel roles of glia that carry important implications for dendritogenesis *in vivo*. Previously documented dramatic increases in NTS glial proliferation in victims of sudden infant death syndrome (SIDS) underscore the importance of our findings and the need to better understand the role of glia and their interactions with BDNF during neuronal circuit maturation.

INTRODUCTION

An immense variety of dendritic morphologies is displayed across the nervous system (Cajal, 1911). Yet, how dendritic arbors form is not well understood. It is thought that the ultimate features of dendritic arbors are guided by a complex interplay among cell intrinsic programs and external cues (Kim and Chiba, 2004; Parrish et al., 2007; Cline and Haas, 2008), and one well-established external cue is the neurotrophin, brain-derived neurotrophic factor (BDNF) (McAllister, 2000; Dijkhuizen and Ghosh, 2005). The specific effect that BDNF elicits on dendritic morphology is far from straightforward. BDNF increases dendritic growth and complexity of basal dendrites in layer 4 visual cortical pyramidal neurons (McAllister et al., 1995; McAllister et al., 1997). Yet, in layer 6 pyramidal neurons, BDNF decreases the dendritic complexity and growth of basal dendrites (McAllister et al., 1997). In fact, numerous other examples exist showing that BDNF can both promote and either reverse or inhibit dendritic growth depending on not only the cell type, but also on the sub-cellular localization of receptor activation (Lom and Cohen-Cory, 1999; Lom et al., 2002), the type of signaling activated downstream of BDNF (Ohira and Hayashi, 2009), as well as other features, such as developmental time point (Gorski et al., 2003).

In addition, astrocytes are emerging as important determinants of proper circuit formation (Freeman, 2006; Barres, 2008), and this includes recent evidence for astrocyte-assisted dendritic morphogenesis (Procko and Shaham, 2010). Whether any interactions exist between BDNF and astrocytes to influence the overall dendritic arbor is currently unknown. In hippocampal cultures, an unidentified diffusible factor released by astrocytes promotes inhibitory synapse formation in a mechanism dependent on neuronal BDNF release and signaling through TrkB, the high-affinity receptor for BDNF (Elmariah et al., 2005). The latter suggests a complex interplay between neurotrophins and glia that likely represents a more

general phenomenon. This begs the question: are some aspects of these context-dependent and often differential effects of BDNF on dendritic morphology determined by glia?

Our previous studies show that BDNF is poised to participate in afferent-dependent development and plasticity of the brainstem *nucleus tractus solitarius* (NTS; (Martin et al., 2009), which is an integral part of autonomic reflex pathways essential for bodily homeostasis (Andresen and Kunze, 1994). In spite of the vital importance of NTS circuitry, very little is known of mechanisms guiding the extensive maturational changes that take place in this system during the early postnatal period (Kalia et al., 1993b; Segar, 1997; Vincent and Tell, 1997, 1999; Kawai and Senba, 2000; Lachamp et al., 2002).

In the present study, we have tested the hypothesis that BDNF regulates dendritic outgrowth and complexity of NTS neurons in a cell type-specific and glia-dependent manner, using dissociate cultures of neurochemically-identified neuronal populations. We show that BDNF switches from promoting to inhibiting NTS dendritogenesis following glia depletion. Moreover, astrocyte-conditioned medium exerts a potent inhibitory effect on the dendritic growth of NTS neurons, while promoting dendritogenesis of hippocampal neurons. These data have important implications for the possible pathogenesis of the sudden infant death syndrome (SIDS).

MATERIALS AND METHODS

Animals. Sprague-Dawley rats (Charles River Laboratories) were used in these studies. All procedures were approved by the Institutional Animal Care and Use Committee of the Oregon Health and Science University.

Primary dissociate cultures of the NTS region. Postnatal day (P) 2-3 Sprague-Dawley rat pups were euthanized with an intraperitoneal injection of Euthasol (0.1 mg/kg) and decapitated. Whole medullas were rapidly and aseptically dissected from each animal into ice-cold Ca^{2+}/Mg^{2+}-free Dulbecco's phosphate-buffered salt solution (PBS; Mediatech). Subsequently, a block dissection of the *nucleus tractus solitarius* (NTS) was performed as previously described (Fitzgerald et al., 1992). Briefly, the NTS block was obtained by making one cut at the commissural NTS and the other at the level of obex. Next, area postrema, and cuneate and gracile nuclei were all cut out of the block with a fine scalpel blade. Every attempt was made to limit the block to the NTS, but due to the nature of the block dissection, some adjacent areas may have been included. Tissue blocks were minced using a scalpel blade, and placed into 0.1-0.15% crystallized trypsin 3x (Worthington Biochemical Corporation) that was dissolved in pre-equilibrated Ca^{2+}/Mg^{2+}-free Hank's balanced salt solution (CMF-HBSS, Mediatech) for 30 min in a tissue culture incubator (37°C; humidified 95% air / 5% CO_2). Next, tissue was rinsed in 0.1% soybean trypsin inhibitor (Worthington) dissolved in Ca^{2+}/Mg^{2+}-containing Dulbecco's PBS (Mediatech), followed by a rinse in plating medium, both at room temperature. Plating medium consisted of Neurobasal-A (NBA, Invitrogen), supplemented with B-27 (Invitrogen), fetal bovine serum (FBS; 10%, HyClone), L-glutamine (2 mM, Invitrogen), and an antibiotic mixture of penicillin, streptomycin, and neomycin (PSN, Invitrogen). Tissue was placed in 2 mL of plating medium and dissociated through approximately four fire-polished Pasteur pipettes of decreasing tip diameter. Larger debris was allowed to settle for approximately 5 min and the

supernatant was transferred to a new tube. The final cell density was adjusted to approximately 500,000 viable cells/mL based on hemacytometer cell counts in Trypan blue-stained samples. In order to reduce the number of glia at plating, cells were first pre-plated two times onto 15 mm diameter, untreated glass coverslips (Fisher Scientific) in 24-well tissue culture plates (Corning, 250,000 cells per well) for 30 min each, in the tissue culture incubator. After pre-incubation on untreated glass to allow binding of glia, the medium containing unattached cells was removed from the wells and plated into 24-well plates fitted with poly-D-lysine-coated (0.1 mg/mL, Sigma-Aldrich) glass coverslips (15 mm diameter, Fisher Scientific). After 24 hrs post-plating, all cell medium was replaced with medium of the same composition, excluding FBS (i.e., serum-free neuronal maintenance medium). For glia-depleted conditions, cytosine β-D-arabinofuranoside (AraC; 5 μM, Sigma-Aldrich) was added to the serum-free maintenance medium to prevent glial cell proliferation.

BDNF treatment. BDNF (Promega) from a freshly thawed stock solution (100 μg/mL in PBS, stored at -80°C) was diluted in the neuronal maintenance medium with or without AraC, to a final concentration of 200 ng/mL, as in a previous study of similar nature (Singh et al., 2008). Cultures were switched to either BDNF- or PBS (control)-containing medium at 4 days *in vitro* (DIV) and maintained for three days until fixed on the 7^{th} DIV.

Primary dissociate hippocampal cultures. Hippocampi were dissected from embryonic day (E) 20 Sprague-Dawley rats as previously described (Banker and Cowan, 1977). Tissue was enzymatically treated and dissociated as described for the *primary dissociate cultures of the NTS region*, except that 0.1% trypsin was applied for 15 min. The final cell density was adjusted to approximately 100,000 viable cells/mL. Cells were then plated into wells of a 24-well tissue culture plate (50,000 cells/well) containing glass coverslips (12 mm diameter, Fisher Scientific) that were pre-coated with poly-D-lysine (0.1 mg/mL).

Astrocyte cultures and preparation of ACM. Primary astrocyte cultures of either the NTS region or cortex were prepared from P2-P3 Sprague-Dawley rats using a protocol adapted from a previously described procedure (McCarthy and de Vellis, 1980). Briefly, tissue was dissected and treated with enzyme as described for the *primary dissociate cultures of the NTS region*. Following enzyme treatment, tissue was dissociated in Dulbecco's Modified Eagle's Medium (DMEM, Invitrogen) supplemented with 10% FBS and PSN that was pre-equilibrated in the tissue culture incubator. Cells were plated into 12.5 cm^2 tissue culture flasks (BD Biosciences) at a density of 1.0-1.2 x 10^6 viable cells per flask. Cultures were maintained in the tissue culture incubator, replacing the medium every 2-3 days until cultures reached confluency (10-16 days). Once cultures were confluent, flasks were sealed and shaken for 18-20 hrs on an orbital shaker (250 rpm at 37°C). The next day, flasks were rinsed and trypsinized (0.25% trypsin dissolved in 2mL of pre-equilibrated CMF-HBSS) for 2 min to lift the astrocyte-enriched cell monolayer. Cells were rinsed two times in medium before their final re-suspension in 4-6 mL of medium and reseeding into 8-12 wells of a 24-well tissue culture plate. Re-seeded cultures typically reached confluency 3-5 days later and consisted of >95% astrocytes (the fraction of cells with DAPI-stained nuclei that shows GFAP-immunoreactivity). Prior to generating ACM, astrocyte cultures were switched to serum-free neuronal maintenance medium. Every 1-2 days, ACM was collected and pooled from all wells of the astrocyte cultures to be used immediately.

ACM treatment of cultures and heat-inactivation of ACM. NTS cultures were treated with NTS ACM, cortical ACM, or control medium. Control medium was the neuronal maintenance medium (please see *primary dissociate culture of the NTS region* for details) that was pre-incubated in untreated 24-well tissue culture plates for the same amount of time that ACM was generated by astrocytes. All media were supplemented with AraC (5 μM) to prevent glial cell proliferation. For ACM heat-inactivation studies, NTS ACM and control medium were incubated for 30 min in a

55°C water bath followed by equilibration in the tissue culture incubator prior to being supplemented with AraC and used on cultures. The cultures were treated with freshly generated ACM or control every 24 hrs between 4 DIV and 7 DIV, when the cultures were fixed.

For hippocampal cultures, the entire medium was replaced with NTS ACM, cortical ACM, or control medium 3 hrs after plating. The treatment was repeated approximately every 24 hrs until cultures were fixed at 5 DIV. This experiment was performed side-by-side with NTS cultures that were treated with NTS ACM from the same pool.

Immunocytochemistry. Cultures were fixed and immunostained according to our previously published procedures (Martin et al., 2009), except that all primary antibodies were incubated 18-24 hrs at 4°C. The following primary and secondary antibody pairs were used: i) Chicken anti-MAP2 (1:5,000; Millipore) with Goat anti-chicken Alexa 488 (1:500; Invitrogen); ii) Rabbit anti-TH (1:1,000; Pel-Freez; Chan and Sawchenko 1995) with Goat anti-rabbit Alexa 647 (1:500; Invitrogen); iii) Mouse anti-GAD67 (1:1,000; Millipore, clone1G10.2; Fong et al., 2005) with either Goat anti-mouse Cy3 (1:500; Jackson Immunoresearch) or Goat anti-mouse Alexa 647 (1:500; Invitrogen); iv) Guinea pig anti-VGlut2 (1:20,000; Millipore; Rosin et al., 2006) with Goat anti-guinea pig Cy3 (1:500; Jackson Immunoresearch); and v) Rabbit anti-GFAP (1:1000; Dako) with Goat anti-rabbit Cy3 (1:500; Jackson Immunoresearch).

In some instances, following secondary antibody application, DAPI (300 nM in PBS, Invitrogen) was applied to coverslips for 10 min at room temperature, followed by three, 5-min rinses in PBS. All coverslips were mounted in either ProLong Gold anti-fade reagent (Invitrogen) or Fluormount-G (Southern Biotech). No signal was detected for secondary antibodies when primary antibodies were omitted. We also tested the specificity of the secondary antibodies by applying a primary antibody, but replacing the appropriate with an inappropriate secondary

antibody that was normally used to detect an excluded primary antibody. This control was devoid of signal as well.

Microscopy, Imaging, and Image Analysis. Images of cells in culture were acquired using an Olympus IX-71 inverted microscope through a 20x objective (NA = 0.4) with a Hamamatsu ORCA-ER CCD camera controlled by Olympus Microsuite software (v. 5.0). For NTS cultures triple-immunostained against TH, GAD67, and MAP2, neurons (MAP2-ir) were divided into three separate phenotypes: 1) TH-ir; 2) GAD67-ir; and 3) TH-non-ir/GAD67-non-ir, since TH-ir and GAD67-ir did not overlap. In a subset of experiments, a combination of antibodies against TH, VGlut2, and MAP2 was used, and neurons with the VGlut2-ir/TH-non-ir phenotype were selected for analysis. For all conditions tested, and each neurochemical phenotype, all neurons present on a coverslip, or a maximum of 30 randomly chosen neurons, were imaged. Cells were excluded from the analysis if: 1) vacuoles were apparent in the cell bodies, 2) all dendritic processes were shorter than 10 µm, or 3) the dendritic arbors overlapped with dendrites of other neurons. In some instances, a process showed strong MAP2-ir only in the proximal segment, with an abrupt loss of MAP2-ir signal, followed by what morphologically appeared to be the axon. In these instances, the segment showing strong MAP2-ir was included in the analysis if its length exceeded 10 µm. In order to quantify dendritic arbors, the NeuronJ plug-in (Meijering et al., 2004) for ImageJ software (v. 1.44f, NIH) was used to trace dendrites and acquire three parameters for each neuron: number of primary dendrites, total dendritic length, and number of branch tips. For all neurons of a given phenotype, each dendrite parameter was averaged to acquire the mean per coverslip. A typical experiment consisted of at least three independent cultures prepared on different dates, with each culture containing 2-3 biological replicates (coverslips).

In order to assess the number of glial cells present in the NTS cultures, out of all images taken for MAP2-ir in neurons, 15 images (the total area of 2.5 mm^2) were selected such that they were evenly distributed across the coverslip. Contrast was enhanced in order to detect the background of glial cells and all glial cells were counted, followed by computing their average density (number per cm^2). This method of analysis was verified with cultures triple-stained specifically for GFAP, MAP2, and DAPI. Two investigators (J.L.M. and A.L.B.) independently confirmed that the average density of glial cells obtained using the MAP2 background method did not significantly differ from the density of cells with DAPI-stained nuclei that were not MAP2-ir.

For purified astrocyte cultures used to generate ACM, five images (the total area of 0.8 mm^2) were randomly sampled from a coverslip labeled for GFAP-ir, DAPI, and MAP2-ir. To determine the purity of astrocytic cultures, DAPI and GFAP-ir images were overlaid, and the percentage of cells with DAPI-positive nuclei that showed GFAP-ir was calculated. MAP2-ir was used to confirm a lack of neurons. Cultures were used only if more than 95% of cells with DAPI-stained nuclei were GFAP-ir, and a typical culture contained over 98% of astrocytes. In addition, the average density of astrocytes was computed and expressed per cm^2.

Statistical Analysis. One-way ANOVA followed by Tukey's post-hoc test was used to detect significant differences between groups when more than a single comparison was made. For studies involving BDNF treatment and glial depletion, a two-way ANOVA was used in order to determine whether a significant interaction occurred between the two factors. In all other instances, where a single comparison was made, an independent sample *t*-test was used. In all cases using ANOVA and *t*-test, data followed a normal distribution and had equal variances. When normality and/or variance equality was not met, Kruskal-Wallis test with pair-wise comparisons was performed. All data, unless otherwise specified, are expressed as mean ±

SEM, and $p<0.05$ was considered significant. PASW Statistics software (v. 18) was used for all statistical tests, except regression analysis, which was performed with GraphPad Prism (v. 5.02).

RESULTS

The NTS culture model

In order to test our specific hypotheses on the role of BDNF and glia in morphological maturation of NTS neurons, we developed a low-density dissociate culture model. Two neuronal populations, i.e. the catecholaminergic (Appleyard et al., 2007) and GABAergic (Bailey et al., 2008), have previously been shown to be primarily second-order, i.e. receive direct synaptic input from visceral afferents, which express and release BDNF (Martin et al., 2009). In our study, both populations were identified immunocytochemically by their specific markers, tyrosine hydroxylase (TH) and glutamic acid decarboxylase 67-kD isoform (GAD67), respectively. For each culture, antibodies against TH and GAD67 were combined with antibodies recognizing microtubule-associated protein 2 (MAP2), a general somatodendritic marker. Using this approach, we have found that, within the MAP2-ir population, there was no overlap between TH-ir and GAD67-ir neurons (Fig. 1A), which is consistent with previous *in vivo* data (Stornetta and Guyenet, 1999). Moreover, because TH-ir and GAD67-ir do not overlap, a distinct third population of neurons was possible to analyze: the MAP2-ir population that lacks both TH-ir and GAD67-ir (TH-non-ir/GAD67-non-ir; Fig. 1A). In our cultures, among all MAP2-ir cells, 29.86 ± 1.7%, 51.46 ± 2.0% and 18.6 ± 1.0% were TH-ir, GAD67-ir, and TH-non-ir/GAD67-non-ir, respectively (Fig. 1B). Furthermore, we have determined that, for each of the three subpopulations, the average number of neurons per coverslip was not affected by experimental conditions, including BDNF treatment and the number of glial cells (Table 1). Thus, it is highly unlikely that our data on dendritic morphogenesis are attributable to changes in neuron numbers within individual phenotypes, e.g. a phenotypic switch.

BDNF selectively increases dendritic length and complexity of TH-ir and TH-non-ir/GAD67-non-ir neurons, but not GAD67-ir neurons

Within the first three days after birth in the rat NTS, dendrites extend from two opposite poles of the soma and are oriented to follow the direction of the solitary tract (Kalia et al., 1993b), which is the source of afferent input (Andresen and Kunze, 1994). In subsequent days, the dendrites continue extending and elaborating in all directions (Kalia et al., 1993b). Mediators of dendritic maturation in the NTS are unknown. One well-known mediator of afferent activity-dependent dendritic changes in other CNS regions is the neurotrophin BDNF (McAllister et al., 1996; Landi et al., 2007). In fact, BDNF is prominent in visceral afferents and their central terminals in the NTS (Martin et al., 2009; Kline et al., 2010), while its high-affinity receptor, TrkB, is found in NTS neurons (Balkowiec et al., 2000; Kline et al., 2010). Thus, BDNF is strategically positioned to mediate dendritic morphogenesis in viscero-sensory pathways in the NTS.

We reasoned that if BDNF, released from visceral afferent terminals, is a dendritic morphogen for the postsynaptic NTS neurons, exogenous BDNF applied to cultured NTS neurons, grown in isolation from the afferent source of BDNF, would increase the outgrowth and complexity of their dendritic arbors. To test this hypothesis, we grew mixed neuron-glia NTS cultures for a total of 7 days, and treated with either BDNF (200 ng/mL) or vehicle control during the final three days. We imaged MAP2-ir neurons in each culture and assessed the presence of TH- and GAD67-ir within the MAP2-ir population. To determine the effects of BDNF on dendritic growth and complexity, we quantified the number of primary dendrites, the total dendritic length, and the number of branch tips for each neuron. In support of our hypothesis, TH-ir neurons showed a significant increase in the average total dendritic length (Fig. 2B), the average number of branch tips (Fig. 2C), and a small, but significant increase in the average

number of primary dendrites per neuron (Control, 1.98 ± 0.08, n=180 vs. BDNF-treated, 2.39 ± 0.08, n=191, one-way ANOVA followed by Tukey's post-hoc comparison, p=0.002).

On the other hand, GAD67-ir neurons showed no significant change in the average total dendritic length (Fig. 2B), the average number of branch tips (Fig. 2C), or the total number of primary dendrites in response to BDNF (Control, 2.28 ± 0.07, n=203 vs. BDNF-treated, 2.48 ± 0.07, n=225, one-way ANOVA followed by Tukey's post-hoc comparison, p=0.2).

Lastly, TH-non-ir/GAD67-non-ir neurons showed qualitatively the same response to BDNF treatment as TH-ir neurons, but its magnitude was much greater (Fig. 2A, B, C; and the number of primary dendrites: Control, 2.33 ± 0.1, n=110 vs. BDNF-treated, 3.16 ± 0.1, n=138, one-way ANOVA followed by Tukey's post-hoc comparison, p<0.001).

These findings support our hypothesis that BDNF acts on subpopulations of NTS neurons to increase the length and complexity of dendritic arbors during the early postnatal period. Moreover, these data reveal differential sensitivities to BDNF-mediated dendritic growth among the three neurochemically-distinct populations.

The glial cell density determines the course and magnitude of BDNF-mediated dendritogenesis

An increasing appreciation of neuron-glia interactions has emerged within recent years (Barres, 2008), and this holds true in autonomic regions of the CNS (Gourine et al., 2010), including the NTS (Hermann et al., 2009). Throughout the first postnatal weeks, the number of astrocytes rapidly increases in the NTS (Pecchi et al., 2007). Thus, glia may play a crucial role in developing autonomic pathways and, therefore, are an important experimental consideration. In our initial experiments, we used mixed neuron-glia cultures to show that, consistent with our hypothesis, BDNF increases dendritic growth in sub-populations of NTS neurons. However, we cannot rule out the possibility that the response to BDNF is dependent, directly or indirectly, on glial cells. To begin teasing out these possibilities, we next asked whether the effect of BDNF on

dendritic outgrowth remains the same when glial cells are significantly depleted from the culture.

In order to address this question, we examined sister cultures characterized by diminished glial cells (Median values: Vehicle, 12 x 10^3 glia/cm^2 vs. BDNF-treated, 10 x 10^3 glia/cm^2, Kruskal-Wallis pairwise comparison, p=0.8, n=8 cultures). The numbers of glial cells in these cultures were significantly lower compared to cultures with unmodified glial cell density (Kruskal-Wallis pairwise comparison, p<0.01, Median value for cultures with unmodified density of glia: both Vehicle *and* BDNF-treated, 78 x10^3 glia/cm^2, p=1.0, n=8 cultures). Fascinatingly, depleting glial cells completely reversed the direction of the response of dendritic length and complexity to BDNF. Namely, when the number of glial cells was diminished (Fig. 3A; TH-ir, Supplementary Figure 1; TH-non-ir/GAD67-non-ir, Supplementary Figure 3), BDNF caused a significant decrease in the average total dendritic length in all three neuronal populations (Fig. 3A, B). The average number of branch tips was significantly decreased in TH-ir and TH-non-ir/GAD67-non-ir (Fig. 3C). In addition, the TH-non-ir/GAD67-non-ir population responded with a decreased average number of primary dendrites per neuron (Control, 3.06 ± 0.1, n=158 vs. BDNF-treated, 2.63 ± 0.1, n=158, one-way ANOVA followed by Tukey's post-hoc comparison, p=0.016; Fig. 3A). Thus, the response to BDNF treatment depends on the glial density (two-way ANOVA: TH-ir neurons, p<0.001, TH-non-ir/GAD67-non-ir neurons, p<0.001). Moreover, upon depleting glia, GAD67-ir neurons (Supplementary Figure 2), whose dendritic morphology was not affected by BDNF in the presence of high-density glia (Fig. 2B, C), showed a significant decrease in the average total dendritic length (Fig. 3B). However, the average number of branch tips (Fig. 3C) and the average number of primary dendrites per neuron (Control, 2.64 ± 0.07, n=228 vs. BDNF-treated, 2.64 ± 0.07 n=232, one-way ANOVA followed by Tukey's post-hoc comparison, p=1.0) remained unaffected in this population.

Dendritic outgrowth and complexity of NTS neurons decrease with increasing glial cell density

While determining the effects of BDNF on NTS dendritic growth in the presence or relative absence of glial cells, we discovered that the glial cells themselves exert a potent inhibitory effect on dendritic growth and complexity in all three populations of NTS neurons (Fig. 2 vs. Fig. 3, Control; Table 2, one-way ANOVA followed by Tukey's post-hoc comparison, all p-values <0.01). Based on this observation, we hypothesized that the density of glial cells in a culture can predict the overall dendritic length. Thus, for each neuron phenotype, we took advantage of the natural variability in the densities of glial cells among individual cultures and plotted the mean density of glial cells *versus* the mean total dendritic length per neuron for each culture well. For all neuron types, a negative linear relationship is observed between the logarithm of the density of glial cells and the mean total dendritic length per culture (TH-non-ir/GAD67-non-ir neurons, Fig. 4; TH-ir neurons, r^2=0.47, n=20 cultures, p<0.01; GAD67-ir neurons r^2=0.46, n=17, p<0.01). Thus, the number of glial cells alone influences the overall dendritic length.

A diffusible factor derived from astrocytes reduces dendritic outgrowth and complexity of NTS neurons

We next aimed to determine which glial cell type in the culture is mediating the inhibitory effect on NTS dendritic growth and how the effect may be mediated. Under both abundant (Fig. 5A) and depleted (Fig. 5B) glial cell conditions, the predominant cell type in our culture model is astrocytes (abundant glia, 89.0 ± 1.3% vs. depleted glia, 87.3 ± 1.5%, independent sample *t*-test, p=0.5, n= 3 cultures). We observed that, even when astrocytes are significantly depleted from the culture, dendrites still tend to come into contact with astrocytes

(Fig. 5B), which would support a contact-mediated mechanism of growth inhibition, with astrocytes providing a stop signal. However, arguing against this scenario is our observation that neuronal processes in astrocyte-abundant conditions grow over and past their first astrocytic contacts (Fig. 5A). Together, these observations led us to hypothesize that the reduced dendritic growth in NTS neurons is mediated by astrocytes through a diffusible factor.

In order to test this hypothesis, we treated NTS cultures that were depleted of glial cells with medium collected from purified astrocyte cultures from the NTS (astrocyte-conditioned medium, ACM) or with non-conditioned control medium. We reasoned that if a diffusible factor from astrocytes were responsible for the reduced dendritic length and complexity, ACM treatment in the relative absence of astrocytes (glial cell-depleted conditions) should mimic the effect of glial cells, i.e. lead to a decreased dendritic length and complexity compared to the unconditioned medium-treated control neurons.

For this analysis, we focused on the strongest responding cell phenotype, i.e. the TH-non-ir/GAD67-non-ir population. Consistent with our hypothesis, ACM significantly reduced the total dendritic length (Fig. 5C), the number of branch tips (Fig. 5D), and the total number of primary dendrites per neuron (Control = 2.57 ± 0.73, n=254 vs. NTS ACM-treated = 2.18 ± 0.68, n=218 neurons, independent samples, *t*-test, $p<0.001$). These data indicate that the glia-dependent suppression of NTS dendritic morphogenesis is mediated by astrocyte-derived diffusible factor(s).

Since the TH-non-ir/GAD67-non-ir neurons constitute a significant portion of all neurons in culture, yet only defined by the absence of TH- and GAD67-ir, we sought to further characterize this population. A large fraction of NTS neurons is glutamatergic, and a selective marker of glutamatergic neurons is the vesicular glutamate transporter type 2 (VGlut2; Stornetta et al., 2002). In order to determine the fraction of TH-non-ir/GAD67-non-ir neurons

that contains VGlut2-ir, the following triple-immunocytochemistry protocols were applied to sister cultures: 1) TH, GAD67 and MAP2; 2) TH, VGlut2 and MAP2; and 3) GAD67, VGlut2 and MAP2. Since TH-ir and GAD67-ir do not overlap, and VGlut2-ir and GAD67-ir have a negligible overlap (1.6% ± 2.0%), the fraction of TH-non-ir/GAD67-non-ir neurons that expresses VGlut2 (VGlut2/TH-non-ir) was calculated by subtracting the percentage of VGlut2-ir/TH-non-ir cells (immunocytochemistry protocol 2) from the percentage of TH-non-ir/GAD67-non-ir cells (immunocytochemistry protocol 1). The results of this analysis show that a majority of TH-non-ir/GAD67-non-ir neurons express VGlut2 (Fig. 6) and, therefore, are likely to be glutamatergic. Moreover, the fact that VGlut2 is expressed by nearly all TH-ir, but virtually none of GAD67-ir neurons (Fig. 6) is consistent with previous studies of NTS neurons *in vivo* (Stornetta et al., 2002). In addition, our data indicate that VGlut2-ir/TH-non-ir neurons exhibit a similar response to treatment with ACM as TH-non-ir/GAD67-non-ir neurons (Fig. 8).

Astrocyte-conditioned medium from NTS astrocytes, which inhibits NTS dendritogenesis, promotes dendritic outgrowth and complexity of hippocampal neurons

Our finding that ACM treatment reduces the dendritic length and complexity of NTS neurons is contrary to the canonical dendritic outgrowth-promoting response to ACM treatment exhibited by other CNS neurons (Banker, 1980). Therefore, we next asked whether the ACM derived from NTS astrocytes would retain its inhibitory effect on cultured hippocampal pyramidal neurons that have previously been shown to increase neurite growth in response to ACM derived from cortical astrocyte cultures (Banker, 1980). We grew hippocampal cultures from embryonic day 20 rats for 5 days, and treated them with ACM derived from purified astrocyte cultures from the NTS region, ACM derived from purified cortical astrocyte cultures (positive control), or non-conditioned medium (negative control). Compared to non-conditioned control medium (Fig. 7A), ACM from both cortical (Fig. 7B) and NTS (Fig. 7C)

astrocytes induced marked dendritic outgrowth and complexity in hippocampal neurons, with non-discernable differences between the effects of both ACM types. This result reveals that the effects of astrocyte-derived diffusible factor(s) are neuron type-specific.

Heat-inactivation reverses the inhibitory effect of ACM on dendritic morphogenesis in NTS neurons

We next aimed to hone in on the diffusible factor(s) that are mediating the inhibitory effect on NTS dendritic morphogenesis. We exposed both ACM and control media to a mild heat-inactivation protocol (55°C, 30 min) that is commonly used to inactivate immune proteins that are found in serum, while leaving more stable proteins, such as growth factors, intact. Each day beginning on the 4th day *in vitro* (DIV), glia-depleted NTS cultures were treated with: ACM, control medium, heat-inactivated ACM, or heat-inactivated control medium. Cultures were fixed on the 7th DIV and immunostained for TH, VGlut2, and MAP2. All VGlut2-ir/TH-non-ir that were also MAP2-ir were identified and imaged. Next, all dendritic parameters that have previously been described were attained using MAP2-ir. Consistent with our earlier results, ACM significantly diminished the total dendritic length of VGlut2-ir/TH-non-ir neurons compared to control medium. Notably, heat inactivation of ACM completely abolished its inhibitory effect, while the effects of heat-inactivated control medium did not significantly differ from non-heat-inactivated control medium (Fig. 8). Therefore, we conclude that an astrocyte-derived diffusible factor underlying the inhibitory effect on the total dendritic length of NTS neurons is a heat-labile factor and, thus, likely a peptide or protein. The lack of heat stability argues against neurotrophins as likely candidate mediators since they are highly heat stable.

DISCUSSION

In the current study, using NTS neurons as a model, we show for the first time that the number of glia determines the course of dendritic morphogenesis mediated by BDNF. Consistent with previous studies in other parts of the brain, the BDNF-mediated dendritic growth is dependent on NTS neuron phenotype. We also show a novel, inhibitory effect of astrocyte-conditioned medium (ACM) on NTS dendritic arborization that is abolished by heat-inactivation of ACM. Significantly, the same ACM promotes outgrowth of hippocampal pyramidal dendrites, as in earlier studies.

Our finding that BDNF has differential effects on the dendritic growth of phenotypically distinct NTS neurons adds to the growing body of evidence that BDNF acts in a context-dependent manner. McAllister and colleagues were the first to show that BDNF could either increase or decrease basal dendritic growth of cortical pyramidal neurons depending on whether they were located in layer 4 or 6 (McAllister et al., 1995; McAllister et al., 1997), respectively. More recently, a global deprivation of BDNF in the CNS through a targeted deletion of BDNF in post-mitotic neurons reveals that BDNF induces postnatal dendritic elaboration in a brain region-selective manner. Namely, BDNF is required for the dendritic growth of striatal neurons, while hippocampal neurons are almost entirely unaffected (Rauskolb et al., 2010). This finding was recapitulated in dissociate cultures from both striatum and hippocampus that were treated with BDNF. Based on these observations, the authors concluded that sensitivity to BDNF may be dependent on a neuron-intrinsic program (Rauskolb et al., 2010). Our present findings support this notion since the dendritic characteristics of neurons with three distinct phenotypes grown in the same culture are differentially affected by BDNF. However, we also find that the presence of glia may modulate this intrinsic program.

In addition, our finding that dendrites of distinct neuronal populations are differentially modulated by BDNF treatment provides a framework for how an afferent-derived signal could result in shaping the neural circuitry of functionally distinct neuron types. It was previously shown in gustatory regions of the postnatal rat NTS that dendritic growth and complexity of neurons classified based on soma shapes were differentially modulated by reversibly blocking afferent activity through altering maternal dietary NaCl (King and Hill, 1993). It is well established that activity powerfully drives dendritogenesis and, in some cases, BDNF is the transducer of these activity-dependent changes. For example, blocking endogenous BDNF signaling abolishes activity-dependent dendritic remodeling in the *in vivo* retina (Landi et al., 2007). In fact, our previous data provide several lines of evidence that BDNF is poised to mediate afferent activity-dependent maturation in the NTS (Martin et al., 2009). Combined with our current findings that exogenous BDNF mediates phenotype-dependent responses of dendritic growth in NTS neurons, it is imperative to examine dendritogenesis in these distinct neuronal populations in the NTS *in vivo* following BDNF knockdown in early postnatal visceral afferents. In addition, reversibly blocking afferent drive, such as through maternal dietary NaCl combined with manipulating BDNF, would likely be a useful model to explore the role of BDNF-mediated activity-dependent maturation of visceral sensory pathways.

We find for the first time that, within the same neuron phenotype, the direction and magnitude of BDNF-mediated dendritic morphogenesis are determined by the number of glia. This finding is supported by previous studies that reveal complex neuron-glia interactions involving BDNF and/or TrkB (Djalali et al., 2005; Elmariah et al., 2005). For example, the postsynaptic clustering of GABA receptors in hippocampal neurons that is induced by a diffusible astrocyte-derived factor is prevented in neurons lacking BDNF or TrkB. This suggests that a diffusible astrocytic factor is required to form the inhibitory postsynaptic elements by

modulating neuronal BDNF release and signaling through TrkB (Elmariah et al., 2005). In another study, BDNF added to glia-depleted cultures of serotonergic neurons from the raphe nucleus increases the number of primary dendrites, whereas simultaneously adding the astrocytic calcium-binding protein, S100β, inhibits the BDNF-mediated dendritic outgrowth (Djalali et al., 2005). These data combined with our current findings highlight the need to understand neuron-glia interactions in mechanisms of neurotrophin action since both of these factors are established potent mediators of developmental events.

Finally, we have found a previously unknown effect of diffusible factor(s) present in astrocyte-conditioned medium (ACM). Namely, NTS ACM reduces dendritic outgrowth of NTS neurons while promoting the outgrowth of hippocampal pyramidal neuron dendrites. Thus, the canonical dendritic growth-promoting response to astrocytic factors (Banker, 1980; McAllister, 2000) appears to be not universal but, instead, neuron type- and/or context- specific, with consequences for how we approach and interpret mechanisms of neuronal circuit formation in different parts of the brain.

Time and again, diffusible, astrocyte-derived factors have been shown to promote dendrite growth (Powell et al., 1997; McAllister, 2000). Inhibitory actions due to diffusible factors have rarely been described (Lein et al., 2002) and, in most cases, it is unclear whether there is a true inhibitory factor or simply a lack of growth-promoting factor (Denis-Donini et al., 1984; Ballas et al., 2009). In our experiments, heat-inactivating the ACM completely abolished the inhibitory effect, strongly suggesting that the unknown factor is indeed inhibitory.

Our knowledge of diffusible factors released from astrocytes is growing, yet many of them remain to be identified. For example, the growth-promoting effect of astrocyte-derived factors on hippocampal neurons was first described three decades ago (Banker, 1980), yet the factor(s) remain unknown (Barres, 2008). Potential candidates include the soluble bone

morphogenic protein (BMP) inhibitors, such as follistatin and noggin, that act by sequestering soluble, dendritic growth-promoting BMPs (Cho and Blitz, 1998). In sympathetic neurons, neuron-glia interactions influence the balance of BMPs and BMP inhibitors during the period of dendritic elaboration, with BMPs up-regulated and BMP inhibitors down-regulated, respectively (Lein et al., 2002). Another group of candidate molecules are astrocyte-derived factors that affect synaptogenesis, such as thrombospondins (Christopherson et al., 2005) and cholesterol (Mauch et al., 2001). Critical questions that need to be addressed include determining whether the factor(s) that promote hippocampal dendritogenesis are the same or distinct from the factor(s) that inhibit NTS dendritic outgrowth, as well as what are the receptors and/or downstream signaling pathways that may be involved.

Besides their importance to the CNS development as a whole, our data bring up many intriguing implications for dendritogenesis in the *in vivo* NTS. It is well established that during the first week of postnatal development in rats, dendrites extend from two opposite poles of the soma, orienting to the source of afferent input, i.e. the solitary tract (Kalia et al., 1993). This observation is consistent with afferent input guiding initial dendritic growth, with BDNF being strategically positioned to serve this role (Martin et al., 2009). Following this initial directed orientation, dendrites elaborate in all directions yet are confined to only one side of the NTS and the immediately ventral nucleus, i.e. dorsal motor nucleus of vagus nerve (Kalia et al., 1993). At birth, while there are few astrocytes within the NTS, a high astrocyte density exists along its midline and dorsal borders (Pecchi et al., 2007). Over the course of the first weeks of postnatal life, astrocytes differentiate/proliferate and invade the NTS itself (Pecchi et al., 2007). The unique spatial distribution of astrocytes, combined with our current finding that astrocytes provide a diffusible inhibitory signal to dendritogenesis, suggest that midline/dorsal astrocytes may prevent growing dendrites from extending into inappropriate regions.

Finally, our findings have profound implications for both the normal and pathological neurodevelopment. During normal CNS development, glial cells are rapidly proliferating concurrently with dendritogenesis and synaptogenesis. Our current findings suggest that, if either the numbers and/or timing of glial cell proliferation deviate from their normal course, the formation of neural circuitry could be fundamentally altered. In the developing NTS, significant astrocytic gliosis has been documented in infants whose death was linked to SIDS (Biondo et al., 2004). Whether the gliosis is a cause or an effect is presently unknown, but it is believed that SIDS victims exhibit abnormal autonomic reflex responses during sleep. The fact that the NTS plays a crucial role in integration of autonomic reflexes (Andresen and Kunze, 1994), together with our present findings, suggests that gliosis contributes to abnormal development of autonomic circuitry that can result in SIDS. In light of the ubiquitous nature of glial proliferation and BDNF-mediated activity-dependent maturation, our findings have CNS-wide implications and highlight the need for a better understanding of interactions between neurotrophins and glia during development.

TABLES AND FIGURES

Figure 1

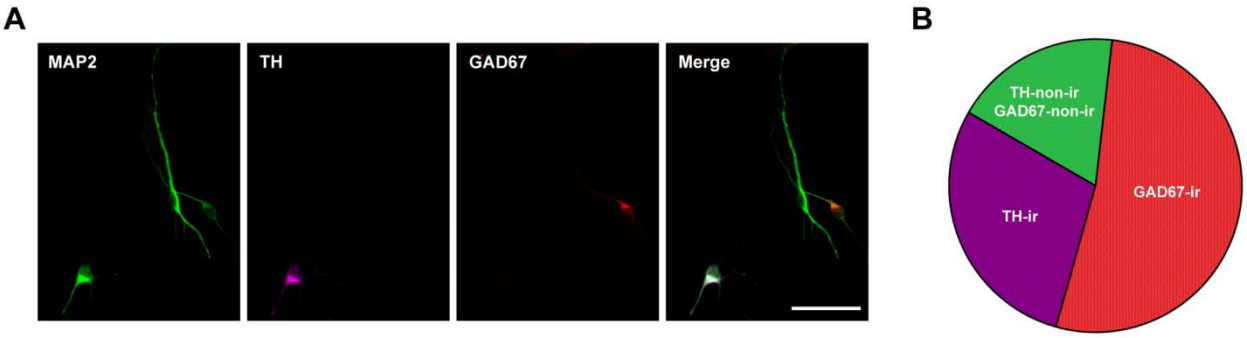

Figure 1: The Nucleus Tractus Solitarius (NTS) dissociate culture model exhibits three immunocytochemically distinct and non-overlapping neuronal subpopulations.

(A) Micrographs of a single field of an NTS culture which was triple-immunostained for microtubule-associated protein type 2, a general somatodendritic marker (MAP2, green), tyrosine hydroxylase, a marker of catecholaminergic neurons (TH, purple), and glutamic acid decarboxylase 67-kD isoform, a marker of GABAergic neurons (GAD67, red). The merged image shows both TH- and GAD67-immunoreactive neurons, in addition to a neuron which does not express either marker (Merge, green). Scale bar, 50 µm. (B) Diagram showing a relative distribution of the three phenotypically distinct neuronal subpopulations within NTS cultures: TH- immunoreactive (-ir, purple), GAD67-ir (red), and TH-non-ir/GAD67-non-ir (green). Data are from seven independent cultures, the total of 3377 neurons (TH-ir, 29.86 ± 1.7%; GAD67-ir, 51.46 ± 2.0%; TH-non-ir/GAD67-non-ir, 18.6 ± 1.0%).

Table 1

		Abundant non-neuronal cells (No AraC)		Depleted non-neuronal cells (AraC)	
		Average number of cells per coverslip ±SEM	% of all MAP2-ir neurons ±SEM	Average number of cells per coverslip ±SEM	% of all MAP2-ir neurons ±SEM
TH-ir	Control	39.3 ±6.0	36.5% ±4.3%	37.0 ±4.8	25.8% ±3.0%
	BDNF [200 ng/mL]	37.0 ±4.8	30.0% ±2.5%	35.0 ±2.6	29.9% ±1.7%
GAD67-ir	Control	57.9 ±12.1	48.2% ±5.3%	70.3 ±10.8	54.3% ±3.8%
	BDNF [200 ng/mL]	66.1 ±9.9	51.3% ±4.1%	59.1 ±8.3	52.5% ±2.1%
TH-non-ir GAD67-non-ir	Control	17.1 ±3.5	15.3% ±1.7%	23.1 ±2.9	18.6% ±2.0%
	BDNF [200 ng/mL]	22.9 ±2.5	18.8% ±2.0%	26.0 ±5.0	22.0% ±2.0%

Table 1: The cell surival and the neuron phenotype fractions are not affected by either glial density or BDNF.

TH-ir neurons p=0.4, GAD67-ir neurons p=0.8, TH-non-ir/GAD67-non-ir neurons, p=0.3; independent samples Kruskal-Wallis test, from seven independent cultures.

Figure 2

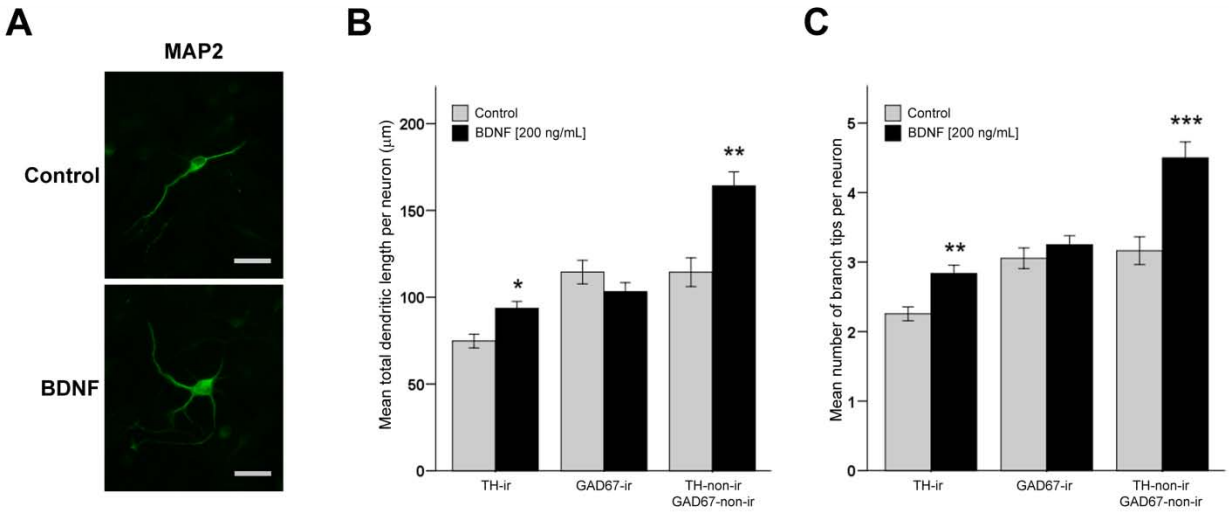

Figure 2: In mixed neuron-glia cultures, NTS neuron phenotypes display differential responses on dendritic outgrowth and complexity due to BDNF treatment.

(A) Representative TH-non-ir/GAD67-non-ir NTS neurons grown under glia-abundant conditions and treated with vehicle (top panel, Control) or 200 ng/mL BDNF (bottom panel, BDNF). Scale bars, 25 µm. Mean total dendritic length (B) and mean number of branch tips (C) per neuron in TH-ir, GAD67-ir and TH-non-ir/GAD67-non-ir populations of NTS neurons grown in control (grey bars) or BDNF-treated (black bars) cultures with abundant glia; *$p<0.05$, **$p<0.01$, ***$p<0.001$, one-way ANOVA with Tukey's post-hoc comparison; TH-ir, control n=180, BDNF n=191; GAD67-ir, control n=203, BDNF n=225; TH-non-ir/GAD67-non-ir, control n=110, BDNF n=138, from five independent cultures.

Figure 3

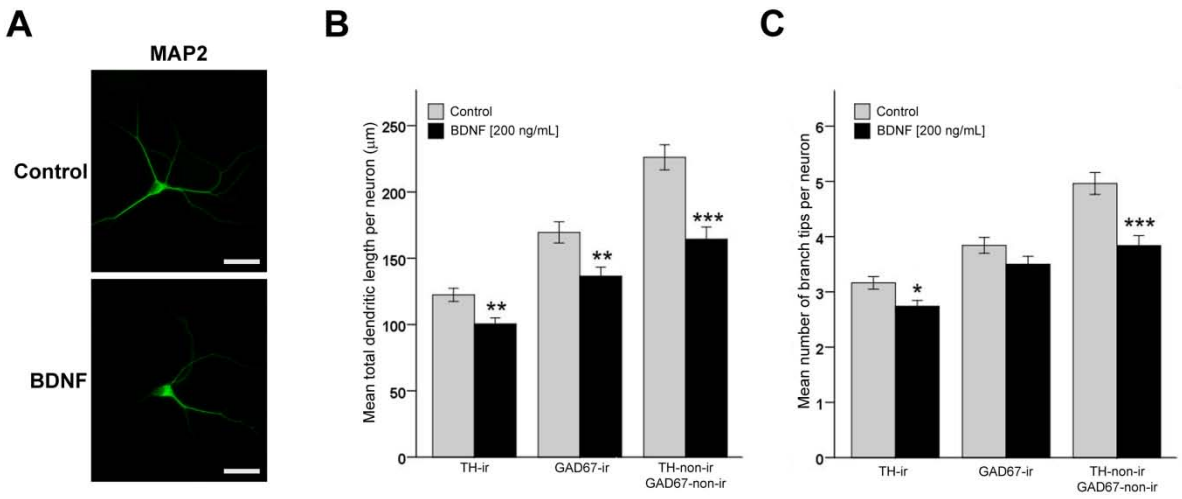

Figure 3: Depleting glia from NTS cultures reverses the direction of BDNF-mediated dendritogenesis.

(A) Representative TH-non-ir/GAD67-non-ir neurons grown in glia-depleted cultures and treated with vehicle (top panel, Control) or 200 ng/mL BDNF (bottom panel, BDNF). Scale bars, 25 µm. Mean total dendritic length (B) and mean number of branch tips (C) per neuron in TH-ir, GAD67-ir and TH-non-ir/GAD67-non-ir populations grown in control (grey bars) or BDNF-treated (black bars) glia-depleted cultures; *p<0.05, **p<0.01, ***p<0.001, one-way ANOVA with Tukey's post-hoc comparison; TH-ir, control n=183, BDNF n=196; GAD67-ir, control n=228, BDNF n=232; TH-non-ir/GAD67-non-ir, control n=158, BDNF n=158, from five independent cultures.

Table 2

	Total dendritic length (μm)	Number of branch tips	Number of primary dendrites
TH-ir	47.58 ±6.28 ***	0.91 ±0.16 ***	0.58 ±0.11 ***
GAD67-ir	64.48 ±8.90 ***	0.94 ±0.18 ***	0.36 ±0.10 **
TH-non-ir/ GAD67-non-ir	111.69 ±13.24 ***	1.80 ±0.30 ***	0.74 ±0.16 ***

Table 2: Depleting glia dramatically increases dendritic length and complexity of NTS neurons compared to conditions with abundant glia, regardless of neuron phenotype.

Results presented are mean differences between untreated control in glia-depleted cultures (**Fig 3**) and untreated control in abundant glia cultures (**Fig 2**); **p<0.01, ***p<0.001, one-way ANOVA with Tukey's post-hoc comparison; TH-ir neurons, depleted glia n=183, abundant glia n=180; GAD67-ir neurons, depleted glia n=228, abundant glia n=203; TH-non-ir/GAD67-non-ir neurons, depleted glia n=158, abundant glia n=110, from five independent cultures.

Figure 4

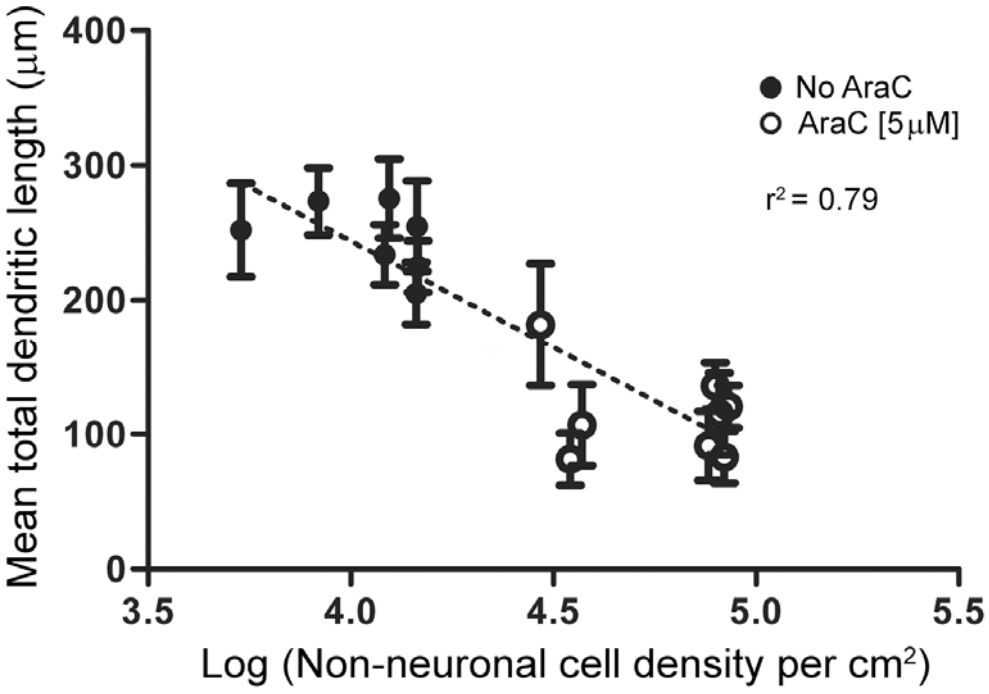

Figure 4: Increasing glial cell density results in decreased total dendritic length of NTS neurons.

Mean dendritic lengths of TH-non-ir/GAD67-non-ir neurons per culture expressed as a function of the logarithm of the average glial cell density in the same culture. The cultures were prepared without (closed circles) or with (open circles) addition of 5 μM AraC, which inhibits glial proliferation; linear regression, r^2=0.79, p<0.001, n=15 cultures.

Figure 5

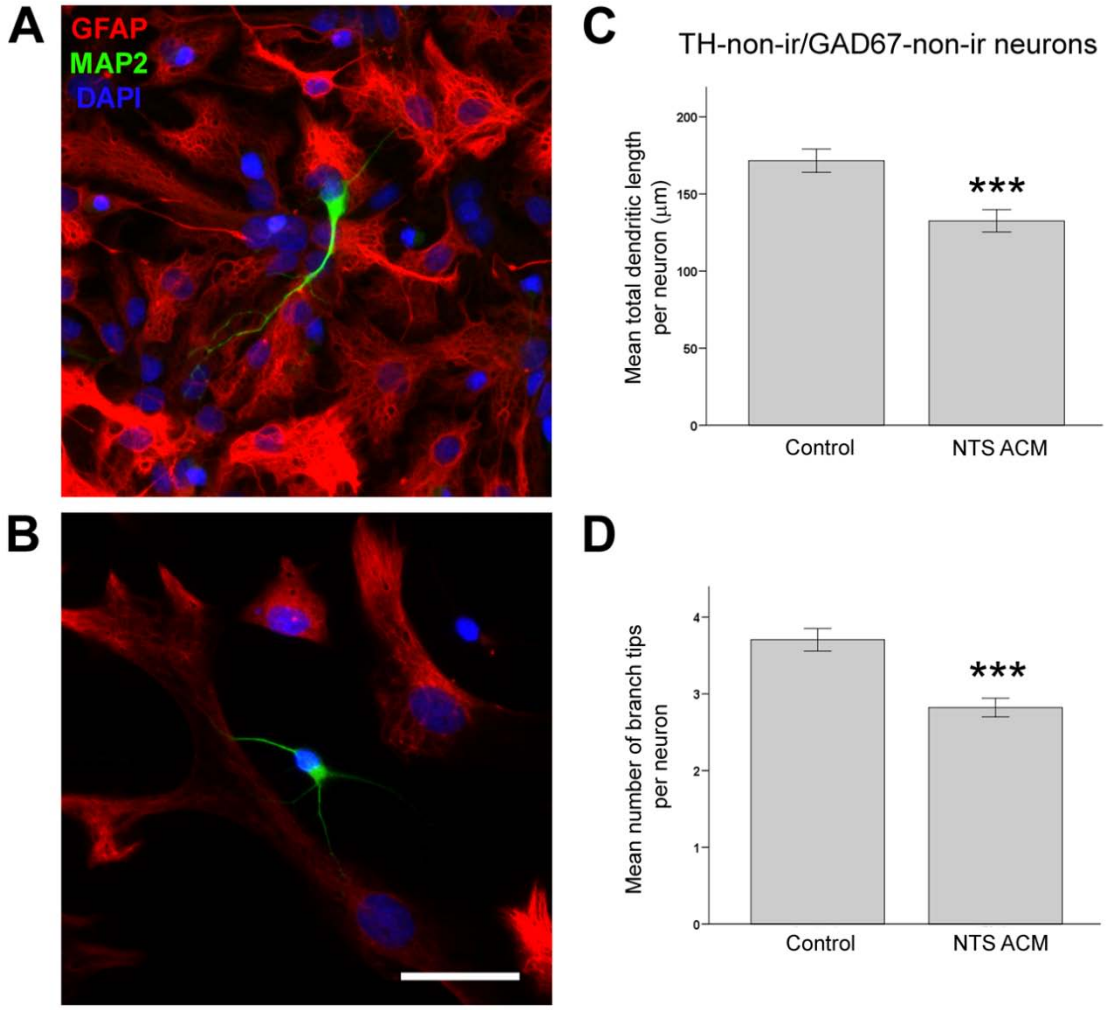

Figure 5: Astrocytes are the predominant glial cell in NTS cultures, and astrocyte-conditioned medium (ACM) inhibits dendritic outgrowth of NTS neurons.

Representative examples of NTS cultures with abundant (A) and depleted (B) glial cells, immunocytochemically stained for the astrocytic marker GFAP (red), the somatodendritic neuronal marker MAP2 (green), and DAPI (blue), which labels all cell nuclei. Even though neuronal processes contact GFAP-immunoreactive astrocytes in glia-depleted conditions (B), processes tend to grow past the first astrocytic contact in abundant glia conditions (A); scale

bar, 50 µm. Mean total dendritic length (C) and mean number of branch tips (D) per neuron within the TH-non-ir/GAD67-non-ir population grown in glia-depleted cultures treated for 3 days with control medium (Control) or ACM derived from purified NTS astrocyte cultures (NTS ACM); ***$p<0.001$, independent sample *t*-test; Control, n=254; NTS ACM, n= 218 neurons, from four independent cultures.

Figure 6

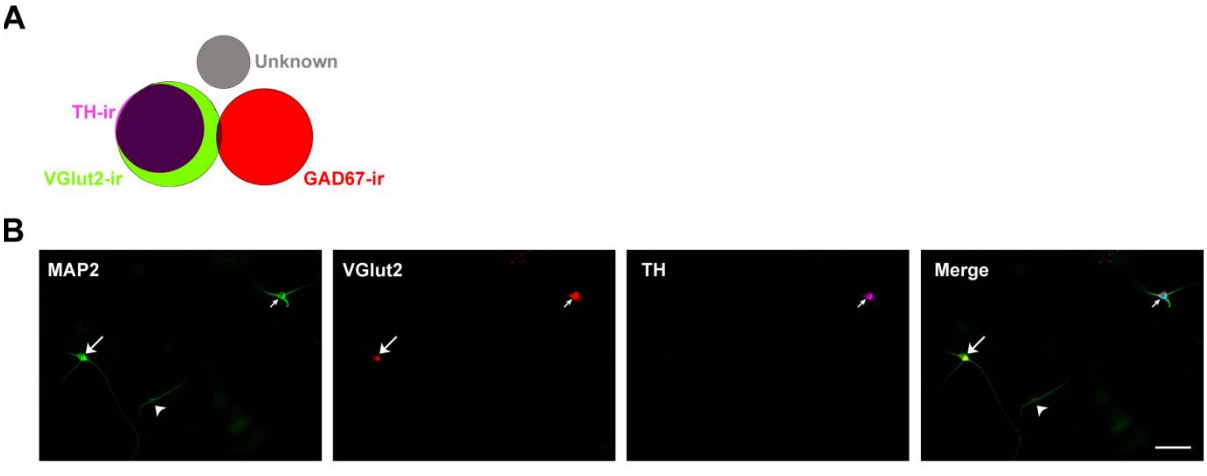

Figure 6: The vesicular glutamate transporter type 2 (VGlut2) is expressed by a significant proportion of NTS neurons, including a large fraction of TH-non-ir/GAD67-non-ir neurons.

(A) Venn diagram representing the population breakdown of NTS neurons, based on triple-immunocytochemistry protocols applied to sister cultures. Nearly all (97.8% ± 1.0%) TH-ir neurons (purple) are also VGlut2-ir. On the other hand, VGlut2-ir is absent from virtually all GAD67-ir neurons (red). Among TH-non-ir/GAD67-non-ir neurons, 62.0% ± 5.7% are characterized by immunoreactivity to VGlut2 (green). The remaining neurons (13.9% ± 4.0% of all neurons) do not express any of the three markers (grey, Unknown). Data are derived from three independent cultures. (B) Micrographs of a single field of an NTS culture triple-immunostained for TH, VGlut2, and MAP2 demonstrating three neurochemically distinct neurons: VGlut2-ir/TH-non-ir (large arrow), TH-ir/VGlut2-ir (small arrow), and TH-non-ir/ VGlut2-non-ir (arrowhead); scale bar, 50 µm.

Figure 7

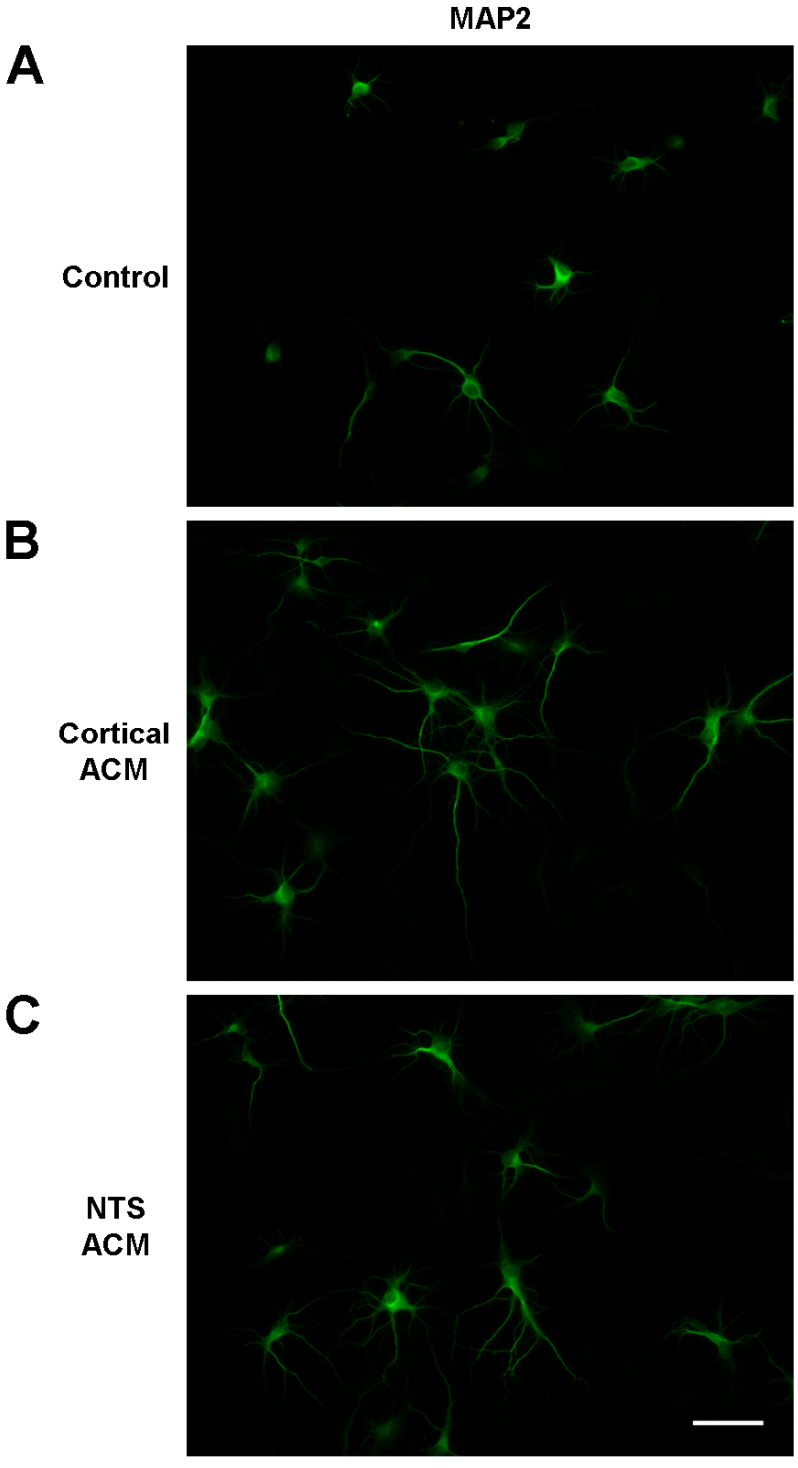

Figure 7: Hippocampal neurons dramatically increase dendritic length and complexity in response to astrocyte-conditioned medium (ACM).

Representative examples of hippocampal neurons (MAP2-immunoreactive) grown in a dissociate culture and treated for 4 days with either control medium (A) or astrocyte-conditioned medium (ACM) derived from cortical (B) or NTS (C) purified astrocyte cultures; scale bar, 50 μm.

Figure 8

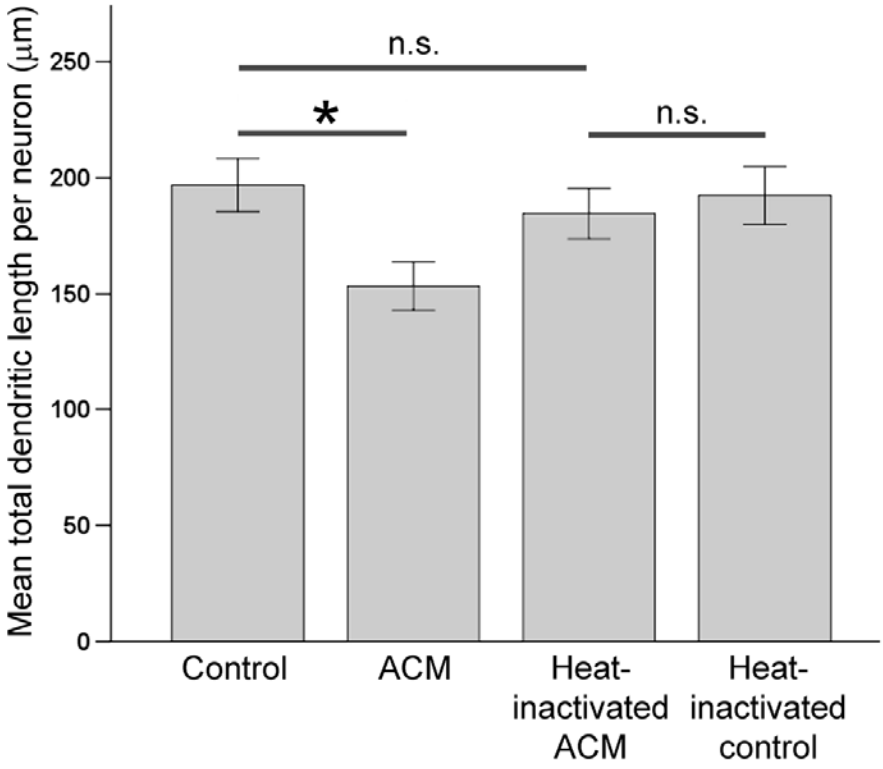

Figure 8: Heat-inactivation of astrocyte-conditioned medium (ACM) derived from purified NTS astrocyte cultures reverses the inhibitory effect on total dendritic length in VGlut2-ir/TH-non-ir neurons.

Mean total dendritic length per neuron of VGlut2-ir/TH-non-ir NTS neurons treated for 3 days with intact control medium (Control), ACM, heat-inactivated ACM, and heat- inactivated control medium; *$p<0.05$, n.s., not significant, one-way ANOVA with Tukey's posthoc comparison; Control n=130, ACM n=129, Heat-inactivated ACM n= 131, Heat-inactivated control n=82 neurons, from three independent cultures.

Supplementary Figure 1

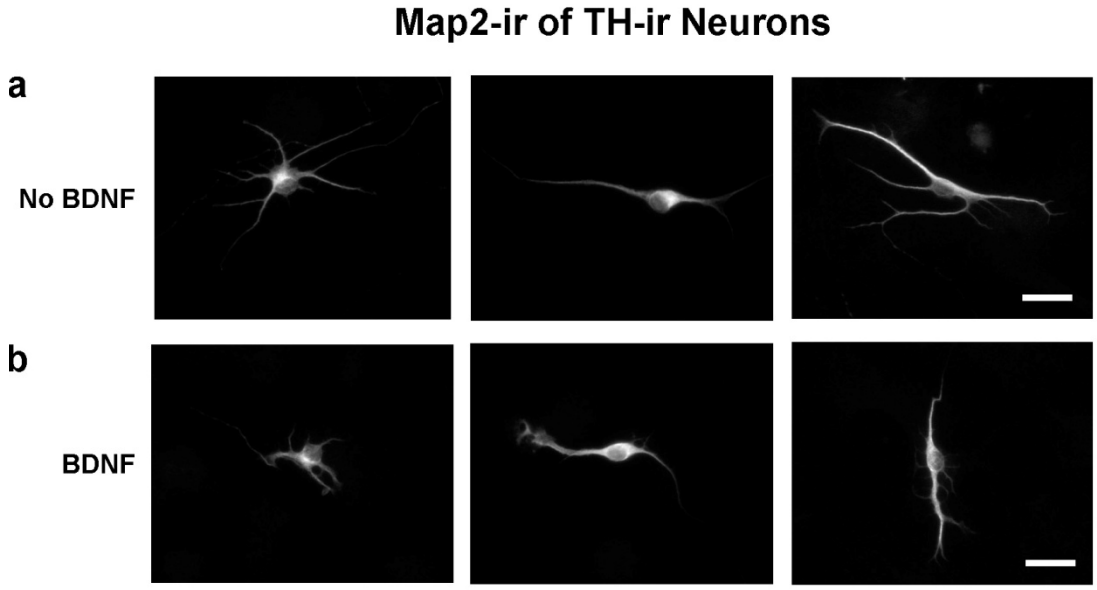

Supplementary Figure 1: Example TH-ir neurons from glia-depleted NTS dissociate cultures labeled with the general somatodendritic marker, MAP2. (**a**) Control, (**b**) Treated with 200 ng/mL BDNF. Scale bars, 25µm.

Supplementary Figure 2

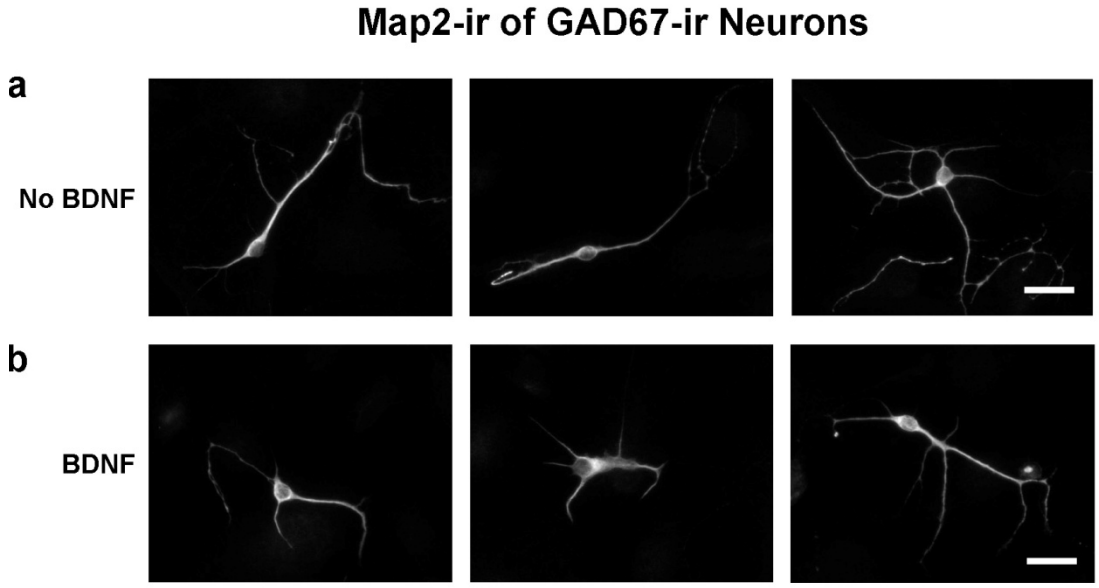

Supplementary Figure 2: Example GAD67-ir neurons from glia-depleted NTS dissociate cultures labeled with the general somatodendritic marker, MAP2. (**a**) Control, (**b**) Treated with 200 ng/mL BDNF. Scale bars, 25µm.

Supplementary Figure 3

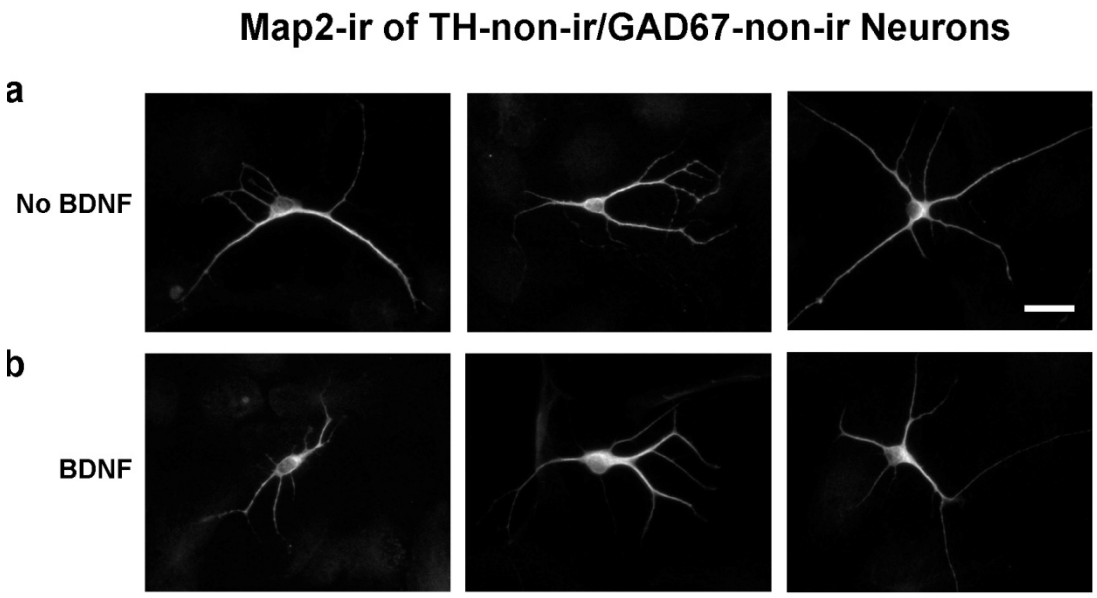

Supplementary Figure 3: Example TH-non-ir/GAD67-non-ir neurons from glia-depleted NTS dissociate cultures labeled with the general somatodendritic marker, MAP2. (**a**) Control, (**b**) Treated with 200 ng/mL BDNF. Scale bars, 25µm.

Chapter 5: Discussion and Conclusions

The findings that I present in the previous two chapters move us closer to understanding the maturational function of BDNF in visceral afferent pathways, yet many issues remain unresolved and new questions abound. Moreover, in an unexpected twist of experimental events, I have uncovered a previously unrecognized contribution of glia to the *in vitro* dendritogenesis of neurons from the *Nucleus Tractus Solitarius* (NTS). In this chapter, I first discuss issues raised by my *in vitro* findings on the dendritogenesis of putative second-order neurons with possible strategies to uncover the mechanistic underpinnings. Next, I discuss implications for the organization of NTS circuitry in view of the effects of BDNF, glia, and their potential interactions. Finally, I come full circle to my overall hypothesis: BDNF in visceral afferents mediates activity-dependent maturation of NTS circuitry. While the findings described in Chapters 3 and 4 support this hypothesis, a lot of work remains to fully address it by translating to the *in vivo* setting. Thus, along the way, I discuss the challenges and possible strategies to directly test this hypothesis *in vivo*.

The effects of BDNF and glia in NTS cultures – strategies to identify mediators and mechanisms. In Chapter 4, I have taken an *in vitro* approach to probe for a possible functional role of BDNF in the maturing NTS – the dendritogenesis of putative second-order neurons. By isolating the NTS neurons in culture, I have removed afferent-driven activity and presumably the primary source of BDNF, as unilateral vagotomy significantly reduces BDNF in the ipsilateral NTS (Clark et al., 2008). Adding back exogenous BDNF under the more tightly controlled culture environment allowed me to test if BDNF was capable of mediating dendritogenesis. Indeed, the

fact that BDNF mediates a change in the dendritic structure of most NTS neurons supports the overall hypothesis that afferent-derived BDNF may elicit functional changes in second-order NTS neurons *in vivo*. It was unforeseen, however, that the effect of BDNF depends on the density of glia within the culture. This may be particularly relevant to the *in vivo* postnatal development, since glia are rapidly proliferating and maturing during the early postnatal period (Pecchi et al., 2007). At this point, it is unclear what the direct target of BDNF is within the culture. It is highly likely that BDNF acts directly on NTS neurons, given that they express the BDNF receptor TrkB and BDNF can elicit a TrkB-dependent inhibition of AMPA currents in a high fraction of NTS neurons (Balkowiec et al., 2000; Kline et al., 2010). At present, it is not known if NTS neurons express $p75^{NTR}$ or truncated TrkB. Furthermore, it is also unknown if any of the glia express TrkB, $p75^{NTR}$, or truncated TrkB, although it is highly likely to be the case since glia are known to express both neurotrophins and their receptors (Althaus and Richter-Landsberg, 2000; Cragnolini and Friedman, 2008). In fact, my preliminary findings using immunocytochemistry directed against TrkB, indicate that some glia likely express TrkB. If it is true that glial cells express functional receptors for BDNF , then this raises the possibility for actions of BDNF on glia that affect neurons indirectly. For example, BDNF may bind TrkB receptors present on glia, and this would cause glia to release a soluble factor that affects NTS dendrites. Pinning down the ultimate mechanism will require knowing which receptors and neurotrophins are present where, under what conditions (abundant vs. depleted glia), and their respective levels (**Fig 5-1**). As noted earlier in Chapter 2 (BDNF sub-section), the possible combinations of neurotrophins and their receptors provide great potential to mediate an array of diverse effects.

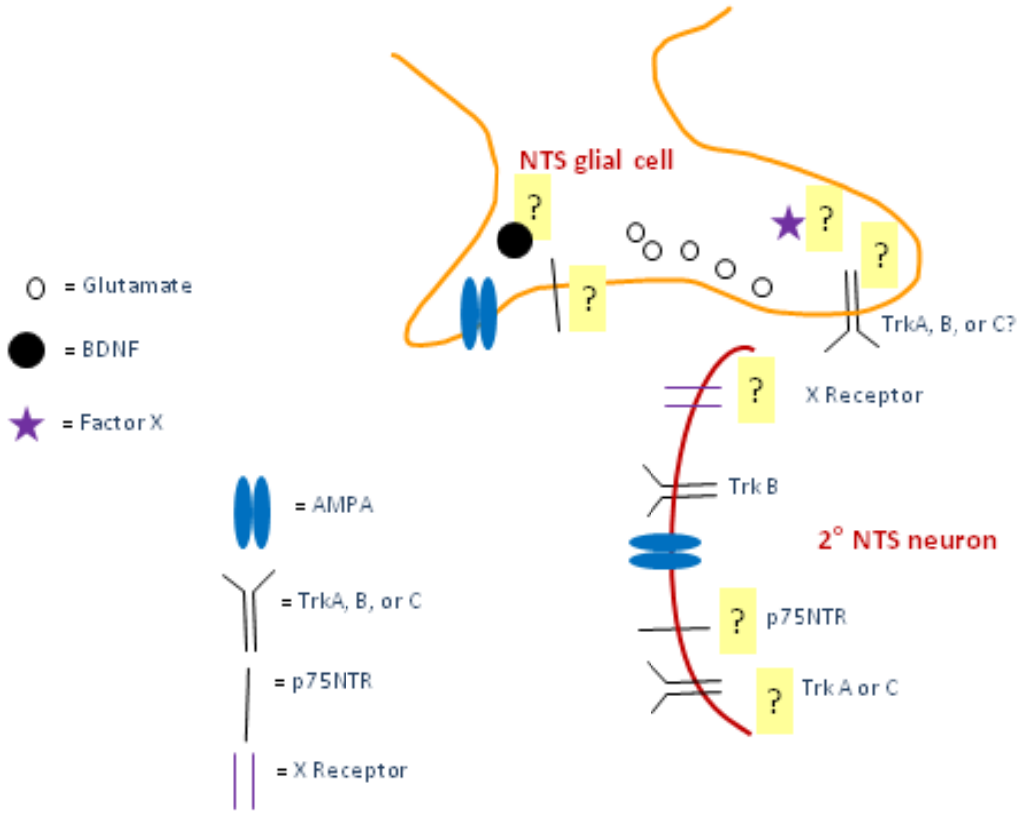

Figure 5-1

NTS culture schematic - localization of confirmed and potential neurotrophins, neurotrophin receptors, and one possible indirect mediator of dendritic growth.

Attempting to narrow the possible mechanisms likely requires a multi-pronged strategy. I would first attempt to characterize the localization of Trk and $p75^{NTR}$ receptors in cultures containing abundant, compared to depleted glia. This could be accomplished through an immunocytochemical approach using two different combinations of antibodies: 1) TrkB, glia-selective, and neuron-selective (e.g. focus on a responding population such as TH-ir) and 2) $p75^{NTR}$, glia-selective, and neuron-selective. The advantage of this approach is that it allows specific cell localization if a positive signal is present, and antibody specificity is assured. The disadvantage is that both negative and positive results must be interpreted with caution. Neurotrophins and their receptors are notorious for functional levels of protein being below the detection threshold of antibody-based methods, and for non-specific antibody binding. An additional, more sensitive approach would be to test both mixed cultures with abundant and depleted glia as well as purified astrocyte cultures using quantitative RT-PCR for mRNAs of Trks, $p75^{NTR}$, and neurotrophins. The advantage is that this method has high sensitivity to detect very small levels of mRNA and their relative abundance. Therefore, it should reveal whether any of the cultures express these genes for these proteins. Furthermore, comparisons between the different culture conditions (abundant glia, depleted glia, purified astrocyte cultures) may provide additional clues as to receptor regulation under these different conditions. However, there are several disadvantages to this approach. First of all, levels of mRNA do not necessarily reflect functional protein levels (e.g. cell surface TrkB). It also does not answer which cell types contain the mRNAs. The best case scenario would be to compare purified astrocyte cultures with the mixed neuron/glia conditions and determine if purified astrocytes, for example, contain any of the mRNAs that mixed neuron-glia cultures contain. The problem, however, is that interactions between neurons and glia may ultimately influence expression of these genes in astrocytes, and therefore give an inaccurate read-out of expression that may not extrapolate to

mixed culture models. In light of this, single cell quantative RT-PCR may be an option. Based on what the combined immunocytochemistry and quantitative RT-PCR reveal will hopefully determine a more directed approach to answer mechanistic question using a combination of pharmacological agents (K252a which preferentially blocks Trk tyrosine kinases), function blocking antibodies (against p75 and Trk), and selective protein knock-down strategies using microRNA (e.g. TrkB in astrocytes).

It is highly intriguing that, at least in TH-ir and TH-non-ir/GAD67-non-ir neurons, the abundance or depletion of glia reverse the direction of BDNF-mediated dendritic growth. Given the known opposing effects of activation through Trk and $p75^{NTR}$ (Lu et al., 2005), it is reasonable to speculate that glia influence the relative ratios of Trk and $p75^{NTR}$ in TH-ir and TH-non-ir/GAD67-non-ir neurons. Whether this is a feasible hypothesis will be determined by strategies aimed at identifying neurotrophin and neurotrophin receptor localization described above.

In addition, I discovered that astrocytes alone strongly influence dendritic growth in NTS neurons through an unidentified soluble inhibitory factor(s). The “holy grail” is determining the identity of the soluble factor(s). A logical first step would be to test on glia-depleted cultures exogenously applied, known diffusible factors from astrocytes that influence neuron function, such as thrombospondin (Christopherson et al., 2005) and cholesterol (Mauch et al., 2001). If either of these factors reduces dendritic growth, then strategies, such as treatment with scavenging antibodies, could be aimed at depleting endogenously released thrombospondin or cholesterol in astrocyte-conditioned medium (ACM) and subsequently testing on glia-depleted cultures. If one of these factors is the mediator of dendritic inhibition, then I would expect the

ACM depleted of the putative factor would reverse the inhibitory effect of control ACM on dendrites.

Other candidate molecules to consider are complement proteins. Mild heat-inactivation of the ACM completely reversed the inhibitory effect of ACM on NTS dendritogenesis. Interestingly, the heat-inactivation protocol I used has traditionally been used to heat-inactivate serum before its use on cell cultures. The idea was to remove less stable complement proteins, while keeping more stable growth factors intact. In fact, complement proteins were previously shown to mediate developmental synaptic pruning (Stevens et al., 2007), giving some credence to complement proteins as candidate mediators of dendritic inhibition in NTS neurons. If testing a few putative candidate mediators is not fruitful, however, more thorough biochemical analyses are required. Confirming that it is a protein and knowing its size, charge density, and glycosylation, would narrow the possible options. A recent study identified over 150 molecules secreted by astrocytes (Keene et al., 2009). Therefore, narrowing the possible options is essential to discovering the identity of the diffusible factor(s).

A final point to make on my findings in Chapter 4 is that, currently, there are two independent findings that may be linked, yet this idea has not been tested. First, I found that the number of glia influence the direction of BDNF-mediated dendritic growth of NTS neurons. Second, I found that a diffusible factor from astrocytes is inhibitory to NTS dendritic growth in neurons. It will be important to determine if the glia-dependent BDNF effect is mediated by the astrocyte-derived diffusible inhibitory factor. This could be tested by comparing glia-depleted vs. glia-abundant NTS cultures, treated with either ACM or control media, in the presence or absence of BDNF.

Implications for NTS dendritogenesis and the importance of testing *in vivo.* My *in vitro* findings in Chapter 4 reveal that glia likely play an essential role in the postnatal maturation of NTS circuitry *in vivo*. Although the culture model provides compelling insight into the possible function of glia, BDNF, and their interactions during development, there are several reasons why extrapolation from the culture model is limited.

Heterogeneity of glia is quite plausible in the NTS region. In fact, glia are hypothesized to exhibit as many different types as there are neuron types in the CNS (Zhang and Barres, 2010). In the dissociate culture model, all cell types from the region are interspersed and the original three dimensional positioning of cells is lost. Thus, it is possible that glia along the borders and midline regions of the NTS, for example, are different than glia located within the NTS borders. It is intriguing that astrocytes are densely found along the dorsal and midline borders of NTS from birth (Pecchi et al., 2007). If we combine this observation with the fact that NTS astrocytes inhibit dendritic growth in culture and dendrites tend not to spread beyond the immediate dorsal and midline borders of the NTS *in vivo*, it is hypothetical that astrocytes in these regions serve to prevent growing dendrites from spreading into inappropriate regions. Strong inhibitory factors derived from glia located in the NTS proper, where dendrites elaborate extensively *in vivo*, seem unlikely, though not impossible. Given the known heterogeneity of glia from different brain regions (Zhang and Barres, 2010), it is possible that different types of glia are distributed differentially within and around the NTS. Testing these ideas will require the three dimensional structure to be preserved.

Another related point is that glia located along the midline of the CNS are shown time and again to be crucial in axon guidance. For example, many cues have been identified that either prevent, or permit, growing axons from crossing, or to cross, the midline, such as in the

spinal cord. In general, much less is known about cues guiding dendrite growth (Kim and Chiba, 2004). However, many of the cues that have been shown to mediate axon guidance also regulate dendritic growth, such as semaphorin 3a. In fact, semaphorin 3a was shown to simultaneously repel axons and attract dendrites within the same neuron (Polleux et al., 2000). Thus, the midline glial cells, which are interspersed in the culture model, may provide some of the same cues for dendritic growth, as have been already identified for axon growth. Testing this idea, too, will require preservation of the three dimensional structure of the NTS.

The intact NTS is crucial to test the role of BDNF in guiding dendritic growth, as well. One hypothesis of mine relates to the timing of astrocyte proliferation within the borders of NTS that significantly increases during the first weeks of life, coinciding with dendrite elaboration (Kalia et al., 1993b; Pecchi et al., 2007). In the culture model, I observed that BDNF reduces dendritic growth when glia are depleted, while BDNF increases dendritic growth when glia are abundant. Second-order neurons of the NTS already contain functional synapses at birth and BDNF from visceral afferents can act at most second-order neurons. One possibility is that the density of astrocytes within the NTS is a developmental switch for dendritic growth (at least in TH- and non-GAD-ir/non-TH-ir populations). In the relative absence of glia, such as at birth, I would predict that BDNF would inhibit dendritic outgrowth of NTS neurons. However, when glia begin differentiating and increasing in number, this could provide a developmental switch that allows BDNF-exposed neurons to elaborate dendrites.

Furthermore, combining the heterogeneous response of different NTS cell types with the fact that likely not all second-order NTS neurons receive BDNF input from visceral afferents (Chapter 3) implies that there may be different outcomes for different cell types when it comes

to BDNF. This could certainly be an explanation for some of the heterogeneity of neurons and possibly provide clues as to how neurons within the NTS are connected.

A final thought on why it is essential to test the role of BDNF, glia, and their interactions in a more intact system is that NTS neurons likely receive BDNF in a spatially restricted manner, i.e. BDNF-containing afferents form synapses with second-order neurons at well defined sites (many on the soma). In the culture model, BDNF equally bathes all neuronal compartments (dendrites, soma, axon). Yet, based on *in vivo* data from *Xenopus*, BDNF signaling from either the dendritic or axonal compartment elicits opposite effects on dendritic growth (Lom and Cohen-Cory, 1999; Lom et al., 2002). Furthermore, a very recent study identified that, within cultured hippocampal neurons, acute versus gradual BDNF application resulted in markedly different duration of TrkB signaling, leading to different functional outcomes (Ji et al., 2010). Thus, timing of BDNF may be equally important to spatial distribution. Last, but certainly not least, the *in vivo* model would allow us to test these ideas in the presence of activity, an essential factor in and of itself for the maturation of CNS circuitry (Katz and Shatz, 1996; Cline and Haas, 2008).

Does BDNF from visceral afferents mediate activity-dependent maturation of the NTS and cardiorespiratory reflexes *in vivo*?

The ideal solution to address this question requires selectively removing BDNF from visceral afferents while keeping activity intact. This is currently not possible since precise genetic targets selective for visceral afferents are unknown. In the event that such an animal model existed, I would begin testing this hypothesis in several ways. First, I would establish an assay for maturation in the NTS and a functional/behavioral assay to measure maturation of cardiovascular reflexes.

For the NTS, I would use an *in vivo* method to assess dendritic development. Based on my findings using the *in* vitro approach in Chapter 4, BDNF is a likely mediator of dendritic development. In addition, targeting a specific cell phenotype is essential, given the NTS heterogeneity and differential effects of BDNF depending on cell type. I would specifically choose the catecholaminergic group, which was previously shown to represent primarily second-order neurons (Appleyard et al., 2007), and has an established mouse model with green fluorescent protein (GFP) expressed under the control of the TH promoter (Appleyard et al., 2007). In order to look at the dendritic arbors in intact brainstem sections, however, will require additional steps. It is likely that the density of TH neurons expressing GFP will be too great, which will not allow the dendritic arbors from individual cells to be traced with accuracy. To get around this issue, I would cut thick, horizontal brainstem sections, visualize the TH-GFP expressing cells, then proceed to use eletrophysiological techniques to fill individual spatially segregated TH-GFP cells with a dye such as biocytin, thus exposing the dendritic arbors from spatially separate cells to allow tracing and subsequent quantification. This has two advantages. The first is that cutting horizontal sections allows visualization of the solitary tract. As previously noted, initial dendritic outgrowth from NTS neurons follows the direction of the solitary tract (Kalia et al., 1993b), suggesting that an afferent-derived signal may guide this extension. Horizontal sections would allow visualization of the dendrites in this plane. The second advantage is that additional physiological experiments could be added to correlate changes in dendritic growth with changes in electrophysiological properties, like the emergence of the A-type potassium current (I_A), as was previously described (Kalia et al., 1993b).

I would compare dendrite parameters between control TH-GFP mice and conditional BDNF knock-out: TH-GFP mice from several different time points (i.e. P3, P7, P14). If BDNF from visceral afferents is required for activity-dependent maturation of NTS dendrites, then I would

expect TH neurons from the conditional BDNF knock-out animals to exhibit shorter, less branched dendrites that do not distinctly follow the solitary tract. If there is no obvious effect, I would ensure that BDNF was absent in the NTS. One possibility is that BDNF can move trans-synaptically (Wetmore and Olson, 1995). For example, BDNF from target organs may be taken up from peripheral afferent terminals and transported to central terminals, where it may be released. This seems unlikely given that NG neurons express significant levels of both BDNF mRNA and protein (Jenkins et al., 2007; Vermehren-Schmaedick and Balkowiec, 2009), thus I would expect BDNF to be absent or at least significantly depleted from afferent terminals in the conditional knock-out animals. Another possibility is that the related neurotrophin, NT-4/5 that also binds to TrkB and $p75^{NTR}$, may be upregulated and compensate for the absence of BDNF. This, too, would need to be tested. Finally, I would use an adjacent brainstem section to assess the density of astrocytes. As Chapter 4 demonstrated, the number of astrocytes affects dendritic length *in vitro*. It is entirely feasible that BDNF removal alters the number of astrocytes, thus producing indirect effects on dendrites through astrocyte density.

In order to test whether BDNF mediates activity-dependent maturation of cardiorespiratory reflexes, an *in vivo* system-wide analysis of cardiorespiratory reflexes is required. Assuming there are no issues with the BDNF knock-out model as discussed in the previous paragraph describing NTS maturation, I would use the same targeted-BDNF knock out mouse model. It was previously determined that, during the first two weeks in mice, the aortic baroreflex exhibits a significant increase in reflex gain, while simultaneously adjusting its operating range to account for the normal developmental rise in mean arterial blood pressure (Ishii et al., 2001). If activity-dependent BDNF release from visceral afferents contributes to maturation of the afferent component and, thereby, the entire reflex, then I would expect that baroreflex gain would remain blunted and may not reset in response to the developmental

increase in blood pressure. If there is no effect, and there are no issues with trans-synaptic BDNF or NT-4, for example, then it will be important to correlate the results of the entire reflex function with NTS dendrite maturation. It may be possible that other sites along the reflex loop compensate for a deficit of BDNF in visceral afferents.

Lastly, I would like to point out that the two proposed studies described above do not really touch on the role of glia in BDNF-activity interactions in the intact system. The model for potential interactions between neurons and glia grows increasingly complex (**Fig. 5-2**). Although our knowledge of glial cells is expanding (Barres, 2008), much remains to be elucidated. Directly testing some of the hypotheses surrounding glia will require a greater understanding and possibly the development of new tools for their selective manipulation. For example, the ability to control the precise timing of glial differentiation/proliferation could go a long way towards understanding their role in the maturation of neural circuitry.

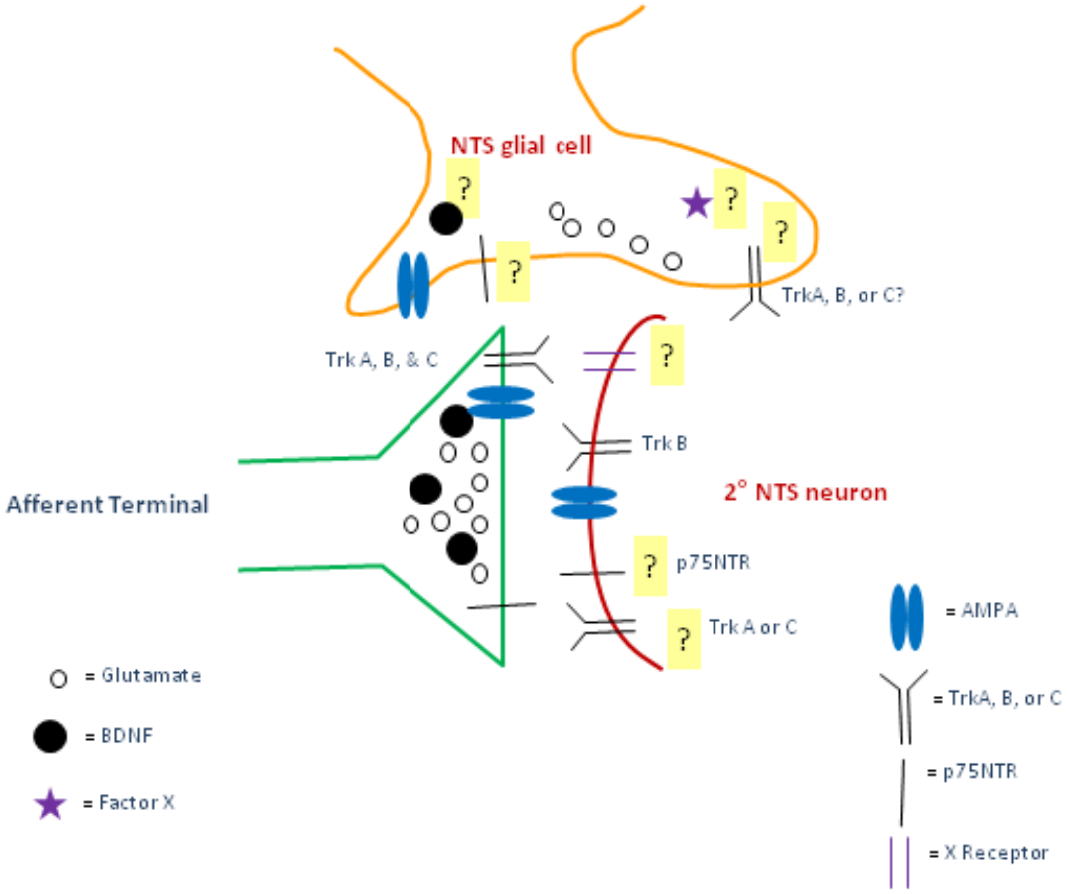

Figure 5-2: Model of the in vivo NTS.

Tripartite synapse demonstrating the immense complexity of possible neuron-glia interactions involving pre- and post-synaptic elements in the intact system.

Conclusions

The work presented in this dissertation provides insight into possible roles of BDNF in the maturation of the sensory portion of cardiorespiratory reflex circuitry. In Chapter 3, I provide detailed characterization of BDNF in aortic baroreceptor pathways, thus enabling this specific reflex to be used as a model in future studies involving mechanisms of activity-dependent BDNF-mediated maturation in the NTS. Moreover, two prerequisites for BDNF-mediated NTS maturation that is dependent on the aortic baroreceptor input are met: 1) BDNF is released in an activity-dependent manner from nodose ganglion neurons stimulated with *in vivo* baroafferent patterns and 2) BDNF is faithfully transported to the central terminals of aortic baroreceptor afferents, where it may be released at synapses with second-order NTS neurons. In experiments described in Chapter 4, I establish that BDNF may mediate dendritogenesis in the NTS *in vivo.* I also unveil a complex interaction between glia and BDNF, and a previously unknown contribution of astrocytes themselves in mediating dendritogenesis. These findings have broad implications for understanding normal maturation in the NTS. Moreover, they may provide clues as to what goes awry in cases of SIDS, where the number of astrocytes more than doubles in the NTS. Given my findings, astrocytes are likely prominent players in establishing normal circuitry during the postnatal period.

References

Althaus HH, Richter-Landsberg C (2000) Glial cells as targets and producers of neurotrophins. Int Rev Cytol 197:203-277.

Andresen MC, Yang M (1989) Arterial baroreceptor resetting: contributions of chronic and acute processes. Clin Exp Pharmacol Physiol Suppl 15:19-30.

Andresen MC, Yang MY (1990) Non-NMDA receptors mediate sensory afferent synaptic transmission in medial nucleus tractus solitarius. Am J Physiol 259:H1307-1311.

Andresen MC, Kunze DL (1994) Nucleus tractus solitarius--gateway to neural circulatory control. Annu Rev Physiol 56:93-116.

Andresen MC, Yang M (1995) Dynamics of sensory afferent synaptic transmission in aortic baroreceptor regions on nucleus tractus solitarius. J Neurophysiol 74:1518-1528.

Andresen MC, Peters JH (2008) Comparison of baroreceptive to other afferent synaptic transmission to the medial solitary tract nucleus. Am J Physiol Heart Circ Physiol 295:H2032-2042.

Andresen MC, Krauhs JM, Brown AM (1978) Relationship of aortic wall and baroreceptor properties during development in normotensive and spontaneously hypertensive rats. Circ Res 43:728-738.

Andresen MC, Doyle MW, Jin YH, Bailey TW (2001) Cellular mechanisms of baroreceptor integration at the nucleus tractus solitarius. Ann N Y Acad Sci 940:132-141.

Apfel SC, Wright DE, Wiideman AM, Dormia C, Snider WD, Kessler JA (1996) Nerve growth factor regulates the expression of brain-derived neurotrophic factor mRNA in the peripheral nervous system. Mol Cell Neurosci 7:134-142.

Appleyard SM, Marks D, Kobayashi K, Okano H, Low MJ, Andresen MC (2007) Visceral afferents directly activate catecholamine neurons in the solitary tract nucleus. J Neurosci 27:13292-13302.

Appleyard SM, Bailey TW, Doyle MW, Jin YH, Smart JL, Low MJ, Andresen MC (2005) Proopiomelanocortin neurons in nucleus tractus solitarius are activated by visceral afferents: regulation by cholecystokinin and opioids. J Neurosci 25:3578-3585.

Arsenault J, Moreau-Bussiere F, Reix P, Niyonsenga T, Praud JP (2003) Postnatal maturation of vagal respiratory reflexes in preterm and full-term lambs. J Appl Physiol 94:1978-1986.

Aylwin ML, Horowitz JM, Bonham AC (1997) NMDA receptors contribute to primary visceral afferent transmission in the nucleus of the solitary tract. J Neurophysiol 77:2539-2548.

Bailey TW, Hermes SM, Andresen MC, Aicher SA (2006) Cranial visceral afferent pathways through the nucleus of the solitary tract to caudal ventrolateral medulla or paraventricular hypothalamus: target-specific synaptic reliability and convergence patterns. J Neurosci 26:11893-11902.

Bailey TW, Appleyard SM, Jin YH, Andresen MC (2008) Organization and properties of GABAergic neurons in solitary tract nucleus (NTS). J Neurophysiol 99:1712-1722.

Balkowiec A, Katz DM (2000) Activity-dependent release of endogenous brain-derived neurotrophic factor from primary sensory neurons detected by ELISA in situ. J Neurosci 20:7417-7423.

Balkowiec A, Katz DM (2002) Cellular mechanisms regulating activity-dependent release of native brain-derived neurotrophic factor from hippocampal neurons. J Neurosci 22:10399-10407.

Balkowiec A, Kunze DL, Katz DM (2000) Brain-derived neurotrophic factor acutely inhibits AMPA-mediated currents in developing sensory relay neurons. J Neurosci 20:1904-1911.

Balland B, Lachamp P, Strube C, Kessler JP, Tell F (2006) Glutamatergic synapses in the rat nucleus tractus solitarii develop by direct insertion of calcium-impermeable AMPA receptors and without activation of NMDA receptors. J Physiol 574:245-261.

Banker GA (1980) Trophic interactions between astroglial cells and hippocampal neurons in culture. Science 209:809-810.

Banker GA, Cowan WM (1977) Rat hippocampal neurons in dispersed cell culture. Brain Res 126:397-342.

Barde YA, Edgar D, Thoenen H (1982) Purification of a new neurotrophic factor from mammalian brain. Embo J 1:549-553.

Barres BA (2008) The mystery and magic of glia: a perspective on their roles in health and disease. Neuron 60:430-440.

Bavis RW, Mitchell GS (2008) Long-term effects of the perinatal environment on respiratory control. J Appl Physiol 104:1220-1229.

Bennett HL, Gustafsson JA, Keast JR (2003) Estrogen receptor expression in lumbosacral dorsal root ganglion cells innervating the female rat urinary bladder. Auton Neurosci 105:90-100.

Biffo S, Offenhauser N, Carter BD, Barde YA (1995) Selective binding and internalisation by truncated receptors restrict the availability of BDNF during development. Development 121:2461-2470.

Biondo B, Magagnin S, Bruni B, Cazzullo A, Tosi D, Matturri L (2004) Glial and neuronal alterations in the nucleus tractus solitarii of sudden infant death syndrome victims. Acta Neuropathol 108:309-318.

Brady R, Zaidi SI, Mayer C, Katz DM (1999) BDNF is a target-derived survival factor for arterial baroreceptor and chemoafferent primary sensory neurons. J Neurosci 19:2131-2142.

Brooks VL, Sved AF (2005) Pressure to change? Re-evaluating the role of baroreceptors in the long-term control of arterial pressure. Am J Physiol Regul Integr Comp Physiol 288:R815-818.

Brown AM (1980) Receptors under pressure. An update on baroreceptors. Circ Res 46:1-10.

Buldyrev I, Tanner NM, Hsieh HY, Dodd EG, Nguyen LT, Balkowiec A (2006) Calcitonin gene-related peptide enhances release of native brain-derived neurotrophic factor from trigeminal ganglion neurons. J Neurochem.

Cajal SR (1911) Histology of the Nervous System of Man and Vertebrates, 1995 translation, 1995 Edition. New York: Oxford University Press.

Chao MV (1994) The p75 neurotrophin receptor. J Neurobiol 25:1373-1385.

Chao MV (2003) Neurotrophins and their receptors: a convergence point for many signalling pathways. Nat Rev Neurosci 4:299-309.

Chapleau MW, Abboud FM (1987) Contrasting effects of static and pulsatile pressure on carotid baroreceptor activity in dogs. Circ Res 61:648-658.

Chapleau MW, Abboud FM (1989) Determinants of sensitization of carotid baroreceptors by pulsatile pressure in dogs. Circ Res 65:566-577.

Chapleau MW, Hajduczok G, Abboud FM (1989) Pulsatile activation of baroreceptors causes central facilitation of baroreflex. Am J Physiol 256:H1735-1741.

Chen CY, Horowitz JM, Bonham AC (1999) A presynaptic mechanism contributes to depression of autonomic signal transmission in NTS. Am J Physiol 277:H1350-1360.

Cheng Z, Powley TL, Schwaber JS, Doyle FJ, 3rd (1997) A laser confocal microscopic study of vagal afferent innervation of rat aortic arch: chemoreceptors as well as baroreceptors. J Auton Nerv Syst 67:1-14.

Cho KW, Blitz IL (1998) BMPs, Smads and metalloproteases: extracellular and intracellular modes of negative regulation. Curr Opin Genet Dev 8:443-449.

Christopherson KS, Ullian EM, Stokes CC, Mullowney CE, Hell JW, Agah A, Lawler J, Mosher DF, Bornstein P, Barres BA (2005) Thrombospondins are astrocyte-secreted proteins that promote CNS synaptogenesis. Cell 120:421-433.

Ciriello J (1983) Brainstem projections of aortic baroreceptor afferent fibers in the rat. Neurosci Lett 36:37-42.

Clark CG, Kline DD, Kunze DL, Katz DM, Hasser EM (2008) The role of brain-derived neurotrophic factor on autonomic and cardiovascular function. In: Society for Neuroscience Abstracts 676.7.

Cline H, Haas K (2008) The regulation of dendritic arbor development and plasticity by glutamatergic synaptic input: a review of the synaptotrophic hypothesis. J Physiol 586:1509-1517.

Cline HT (2001) Dendritic arbor development and synaptogenesis. Curr Opin Neurobiol 11:118-126.

Cragnolini AB, Friedman WJ (2008) The function of p75NTR in glia. Trends Neurosci 31:99-104.

Crair MC (1999) Neuronal activity during development: permissive or instructive? Curr Opin Neurobiol 9:88-93.

Denavit-Saubie M, Kalia M, Pierrefiche O, Schweitzer P, Foutz AS, Champagnat J (1994) Maturation of brain stem neurons involved in respiratory rhythmogenesis: biochemical, bioelectrical and morphological properties. Biol Neonate 65:171-175.

Denis-Donini S, Glowinski J, Prochiantz A (1984) Glial heterogeneity may define the three-dimensional shape of mouse mesencephalic dopaminergic neurones. Nature 307:641-643.

Dijkhuizen PA, Ghosh A (2005) Regulation of dendritic growth by calcium and neurotrophin signaling. Prog Brain Res 147:17-27.

Doan TN, Stephans K, Ramirez AN, Glazebrook PA, Andresen MC, Kunze DL (2004) Differential distribution and function of hyperpolarization-activated channels in sensory neurons and mechanosensitive fibers. J Neurosci 24:3335-3343.

Doyle MW, Andresen MC (2001) Reliability of monosynaptic sensory transmission in brain stem neurons in vitro. J Neurophysiol 85:2213-2223.

Doyle MW, Bailey TW, Jin YH, Andresen MC (2002) Vanilloid receptors presynaptically modulate cranial visceral afferent synaptic transmission in nucleus tractus solitarius. J Neurosci 22:8222-8229.

Drewe JA, Miles R, Kunze DL (1990) Excitatory amino acid receptors of guinea pig medial nucleus tractus solitarius neurons. Am J Physiol 259:H1389-1395.

Elmariah SB, Oh EJ, Hughes EG, Balice-Gordon RJ (2005) Astrocytes regulate inhibitory synapse formation via Trk-mediated modulation of postsynaptic GABAA receptors. J Neurosci 25:3638-3650.

Erickson JT, Conover JC, Borday V, Champagnat J, Barbacid M, Yancopoulos G, Katz DM (1996) Mice lacking brain-derived neurotrophic factor exhibit visceral sensory neuron losses distinct from mice lacking NT4 and display a severe developmental deficit in control of breathing. J Neurosci 16:5361-5371.

Eroglu C, Barres BA (2010) Regulation of synaptic connectivity by glia. Nature 468:223-231.

Esposito D, Patel P, Stephens RM, Perez P, Chao MV, Kaplan DR, Hempstead BL (2001) The cytoplasmic and transmembrane domains of the p75 and Trk A receptors regulate high affinity binding to nerve growth factor. J Biol Chem 276:32687-32695.

Fan W, Andresen MC (1998) Differential frequency-dependent reflex integration of myelinated and nonmyelinated rat aortic baroreceptors. Am J Physiol 275:H632-640.

Fiala JC, Spacek J, Harris KM (2008) Dendrite structure. In: Dendrites, 2nd Edition (Stuart G, Spruston N, Hausser M, eds). New York: Oxford University Press.

Fitzgerald SC, Willis MA, Yu C, Rigatto H (1992) In search of the central respiratory neurons: I. Dissociated cell cultures of respiratory areas from the upper medulla. J Neurosci Res 33:579-589.

Freeman MR (2006) Sculpting the nervous system: glial control of neuronal development. Curr Opin Neurobiol 16:119-125.

Gordon FJ, Leone C (1991) Non-NMDA receptors in the nucleus of the tractus solitarius play the predominant role in mediating aortic baroreceptor reflexes. Brain Res 568:319-322.

Gordon FJ, Sved AF (2002) Neurotransmitters in central cardiovascular regulation: glutamate and GABA. Clin Exp Pharmacol Physiol 29:522-524.

Goritz C, Mauch DH, Pfrieger FW (2005) Multiple mechanisms mediate cholesterol-induced synaptogenesis in a CNS neuron. Mol Cell Neurosci 29:190-201.

Gorski JA, Zeiler SR, Tamowski S, Jones KR (2003) Brain-derived neurotrophic factor is required for the maintenance of cortical dendrites. J Neurosci 23:6856-6865.

Gourine AV, Kasymov V, Marina N, Tang F, Figueiredo MF, Lane S, Teschemacher AG, Spyer KM, Deisseroth K, Kasparov S (2010) Astrocytes control breathing through pH-dependent release of ATP. Science 329:571-575.

Guyenet PG (2006) The sympathetic control of blood pressure. Nat Rev Neurosci 7:335-346.

Guyenet PG, Filtz TM, Donaldson SR (1987) Role of excitatory amino acids in rat vagal and sympathetic baroreflexes. Brain Res 407:272-284.

Halassa MM, Haydon PG (2010) Integrated brain circuits: astrocytic networks modulate neuronal activity and behavior. Annu Rev Physiol 72:335-355.

Hamra M, McNeil RS, Runciman M, Kunze DL (1999) Opioid modulation of calcium current in cultured sensory neurons: mu-modulation of baroreceptor input. Am J Physiol 277:H705-713.

Hartmann M, Brigadski T, Erdmann KS, Holtmann B, Sendtner M, Narz F, Lessmann V (2004) Truncated TrkB receptor-induced outgrowth of dendritic filopodia involves the p75 neurotrophin receptor. J Cell Sci 117:5803-5814.

Heesch CM, Thames MD, Abboud FM (1984a) Acute resetting of carotid sinus baroreceptors. I. Dissociation between discharge and wall changes. Am J Physiol 247:H824-832.

Heesch CM, Abboud FM, Thames MD (1984b) Acute resetting of carotid sinus baroreceptors. II. Possible involvement of electrogenic Na+ pump. Am J Physiol 247:H833-839.

Hermann GE, Van Meter MJ, Rood JC, Rogers RC (2009) Proteinase-activated receptors in the nucleus of the solitary tract: evidence for glial-neural interactions in autonomic control of the stomach. J Neurosci 29:9292-9300.

Horch HW, Kruttgen A, Portbury SD, Katz LC (1999) Destabilization of cortical dendrites and spines by BDNF. Neuron 23:353-364.

Horng SH, Sur M (2006) Visual activity and cortical rewiring: activity-dependent plasticity of cortical networks. Prog Brain Res 157:3-11.

Huang EJ, Reichardt LF (2001) Neurotrophins: roles in neuronal development and function. Annu Rev Neurosci 24:677-736.

Hughes EG, Elmariah SB, Balice-Gordon RJ (2010) Astrocyte secreted proteins selectively increase hippocampal GABAergic axon length, branching, and synaptogenesis. Mol Cell Neurosci 43:136-145.

Ichikawa H, Terayama R, Yamaai T, Yan Z, Sugimoto T (2007) Brain-derived neurotrophic factor-immunoreactive neurons in the rat vagal and glossopharyngeal sensory ganglia; co-expression with other neurochemical substances. Brain Res 1155:93-99.

Inan M, Crair MC (2007) Development of cortical maps: perspectives from the barrel cortex. Neuroscientist 13:49-61.

Ishii T, Kuwaki T, Masuda Y, Fukuda Y (2001) Postnatal development of blood pressure and baroreflex in mice. Auton Neurosci 94:34-41.

Jan YN, Jan LY (2010) Branching out: mechanisms of dendritic arborization. Nat Rev Neurosci 11:316-328.

Jenkins VK, Pricher M, O'Donaughy T, Hsieh HY, Brooks VL, Balkowiec A (2007) Activity-dependent regulation of BDNF expression in nodose ganglia of DOCA-salt hypertensive rats. In: Society for Neuroscience Abstracts 139.11.

Ji Y, Lu Y, Yang F, Shen W, Tang TT, Feng L, Duan S, Lu B (2010) Acute and gradual increases in BDNF concentration elicit distinct signaling and functions in neurons. Nat Neurosci 13:302-309.

Jin X, Hu H, Mathers PH, Agmon A (2003) Brain-derived neurotrophic factor mediates activity-dependent dendritic growth in nonpyramidal neocortical interneurons in developing organotypic cultures. J Neurosci 23:5662-5673.

Jin YH, Bailey TW, Li BY, Schild JH, Andresen MC (2004) Purinergic and vanilloid receptor activation releases glutamate from separate cranial afferent terminals in nucleus tractus solitarius. J Neurosci 24:4709-4717.

Jones JV, Thoren PN (1977) Characteristics of aortic baroreceptors with non-medullated afferents arising from the aortic arch of rabbits with chronic renovascular hypertension. Acta Physiol Scand 101:286-293.

Kalia M (1992) Early ontogeny of the vagus nerve: an analysis of the medulla oblongata and cervical spinal cord of the postnatal rat. Neurochem Int 20:119-128.

Kalia M, Schweitzer P, Champagnat J, Denavit-Saubie M (1993a) Two distinct phases characterize maturation of neurons in the ucleus of the tractus solarius during early development: morphological and electrophysiological evidence. J Comp Neurol 327:37-47.

Kalia M, Schweitzer P, Champagnat J, Denavit-Saubie M (1993b) Two distinct phases characterize maturation of neurons in the nucleus of the tractus solitarius during early development: morphological and electrophysiological evidence. J Comp Neurol 327:37-47.

Kandler K, Gillespie DC (2005) Developmental refinement of inhibitory sound-localization circuits. Trends Neurosci 28:290-296.

Kapfhammer JP (2004) Cellular and molecular control of dendritic growth and development of cerebellar Purkinje cells. Prog Histochem Cytochem 39:131-182.

Katz LC, Shatz CJ (1996) Synaptic activity and the construction of cortical circuits. Science 274:1133-1138.

Kawai Y, Senba E (2000) Postnatal differentiation of local networks in the nucleus of the tractus solitarius. Neuroscience 100:109-114.

Keene SD, Greco TM, Parastatidis I, Lee SH, Hughes EG, Balice-Gordon RJ, Speicher DW, Ischiropoulos H (2009) Mass spectrometric and computational analysis of cytokine-induced alterations in the astrocyte secretome. Proteomics 9:768-782.

Kim S, Chiba A (2004) Dendritic guidance. Trends Neurosci 27:194-202.

King CT, Hill DL (1993) Neuroanatomical alterations in the rat nucleus of the solitary tract following early maternal NaCl deprivation and subsequent NaCl repletion. J Comp Neurol 333:531-542.

Klein R, Conway D, Parada LF, Barbacid M (1990) The trkB tyrosine protein kinase gene codes for a second neurogenic receptor that lacks the catalytic kinase domain. Cell 61:647-656.

Klein R, Nanduri V, Jing SA, Lamballe F, Tapley P, Bryant S, Cordon-Cardo C, Jones KR, Reichardt LF, Barbacid M (1991) The trkB tyrosine protein kinase is a receptor for brain-derived neurotrophic factor and neurotrophin-3. Cell 66:395-403.

Kline DD, Ogier M, Kunze DL, Katz DM (2010) Exogenous brain-derived neurotrophic factor rescues synaptic dysfunction in Mecp2-null mice. J Neurosci 30:5303-5310.

Kunze DL (1981) Rapid resetting of the carotid baroreceptor reflex in the cat. Am J Physiol 241:H802-806.

Kunze DL (1986) Acute resetting of baroreceptor reflex in rabbits: a central component. Am J Physiol 250:H866-870.

Lachamp P, Tell F, Kessler JP (2002) Successive episodes of synapses production in the developing rat nucleus tractus solitarii. J Neurobiol 52:336-342.

Landi S, Cenni MC, Maffei L, Berardi N (2007) Environmental enrichment effects on development of retinal ganglion cell dendritic stratification require retinal BDNF. PLoS One 2:e346.

Lawrence AJ, Jarrott B (1994) L-glutamate as a neurotransmitter at baroreceptor afferents: evidence from in vivo microdialysis. Neuroscience 58:585-591.

Le Roux PD, Reh TA (1994) Regional differences in glial-derived factors that promote dendritic outgrowth from mouse cortical neurons in vitro. J Neurosci 14:4639-4655.

Lein PJ, Beck HN, Chandrasekaran V, Gallagher PJ, Chen HL, Lin Y, Guo X, Kaplan PL, Tiedge H, Higgins D (2002) Glia induce dendritic growth in cultured sympathetic neurons by

modulating the balance between bone morphogenetic proteins (BMPs) and BMP antagonists. J Neurosci 22:10377-10387.

Lessmann V, Brigadski T (2009) Mechanisms, locations, and kinetics of synaptic BDNF secretion: an update. Neurosci Res 65:11-22.

Lessmann V, Gottmann K, Malcangio M (2003) Neurotrophin secretion: current facts and future prospects. Prog Neurobiol 69:341-374.

Lever IJ, Bradbury EJ, Cunningham JR, Adelson DW, Jones MG, McMahon SB, Marvizon JC, Malcangio M (2001) Brain-derived neurotrophic factor is released in the dorsal horn by distinctive patterns of afferent fiber stimulation. J Neurosci 21:4469-4477.

Lin LH (2009) Glutamatergic neurons say NO in the nucleus tractus solitarii. J Chem Neuroanat 38:154-165.

Liu Z, Chen CY, Bonham AC (1998) Metabotropic glutamate receptors depress vagal and aortic baroreceptor signal transmission in the NTS. Am J Physiol 275:H1682-1694.

Liu Z, Chen CY, Bonham AC (2000) Frequency limits on aortic baroreceptor input to nucleus tractus solitarii. Am J Physiol Heart Circ Physiol 278:H577-585.

Loewy AD (1990) Central autonomic pathways. New York: Oxford.

Lom B, Cohen-Cory S (1999) Brain-derived neurotrophic factor differentially regulates retinal ganglion cell dendritic and axonal arborization in vivo. J Neurosci 19:9928-9938.

Lom B, Cogen J, Sanchez AL, Vu T, Cohen-Cory S (2002) Local and target-derived brain-derived neurotrophic factor exert opposing effects on the dendritic arborization of retinal ganglion cells in vivo. J Neurosci 22:7639-7649.

Lu B (2003) BDNF and activity-dependent synaptic modulation. Learn Mem 10:86-98.

Lu B, Pang PT, Woo NH (2005) The yin and yang of neurotrophin action. Nat Rev Neurosci 6:603-614.

Majewska AK, Newton JR, Sur M (2006) Remodeling of synaptic structure in sensory cortical areas in vivo. J Neurosci 26:3021-3029.

Malcangio M, Lessmann V (2003) A common thread for pain and memory synapses? Brain-derived neurotrophic factor and trkB receptors. Trends Pharmacol Sci 24:116-121.

Martin JL, Jenkins VK, Hsieh HY, Balkowiec A (2009) Brain-derived neurotrophic factor in arterial baroreceptor pathways: implications for activity-dependent plasticity at baroafferent synapses. J Neurochem 108:450-464.

Mauch DH, Nagler K, Schumacher S, Goritz C, Muller EC, Otto A, Pfrieger FW (2001) CNS synaptogenesis promoted by glia-derived cholesterol. Science 294:1354-1357.

Mazursky JE, Birkett CL, Bedell KA, Ben-Haim SA, Segar JL (1998) Development of baroreflex influences on heart rate variability in preterm infants. Early Hum Dev 53:37-52.

McAllister AK (2000) Cellular and molecular mechanisms of dendrite growth. Cereb Cortex 10:963-973.

McAllister AK, Lo DC, Katz LC (1995) Neurotrophins regulate dendritic growth in developing visual cortex. Neuron 15:791-803.

McAllister AK, Katz LC, Lo DC (1996) Neurotrophin regulation of cortical dendritic growth requires activity. Neuron 17:1057-1064.

McAllister AK, Katz LC, Lo DC (1997) Opposing roles for endogenous BDNF and NT-3 in regulating cortical dendritic growth. Neuron 18:767-778.

McAllister AK, Katz LC, Lo DC (1999) Neurotrophins and synaptic plasticity. Annu Rev Neurosci 22:295-318.

McCarthy KD, de Vellis J (1980) Preparation of separate astroglial and oligodendroglial cell cultures from rat cerebral tissue. J Cell Biol 85:890-902.

McDougall SJ, Peters JH, Andresen MC (2009) Convergence of cranial visceral afferents within the solitary tract nucleus. J Neurosci 29:12886-12895.

Meijering E, Jacob M, Sarria JC, Steiner P, Hirling H, Unser M (2004) Design and validation of a tool for neurite tracing and analysis in fluorescence microscopy images. Cytometry A 58:167-176.

Mendelowitz D, Reynolds PJ, Andresen MC (1995) Heterogeneous functional expression of calcium channels at sensory and synaptic regions in nodose neurons. J Neurophysiol 73:872-875.

Merrill DC, McWeeny OJ, Segar JL, Robillard JE (1995) Impairment of cardiopulmonary baroreflexes during the newborn period. Am J Physiol 268:H1343-1351.

Merrill DC, Segar JL, McWeeny OJ, Robillard JE (1999) Sympathetic responses to cardiopulmonary vagal afferent stimulation during development. Am J Physiol 277:H1311-1316.

Meyer-Franke A, Wilkinson GA, Kruttgen A, Hu M, Munro E, Hanson MG, Jr., Reichardt LF, Barres BA (1998) Depolarization and cAMP elevation rapidly recruit TrkB to the plasma membrane of CNS neurons. Neuron 21:681-693.

Michael GJ, Averill S, Nitkunan A, Rattray M, Bennett DL, Yan Q, Priestley JV (1997) Nerve growth factor treatment increases brain-derived neurotrophic factor selectively in TrkA-expressing dorsal root ganglion cells and in their central terminations within the spinal cord. J Neurosci 17:8476-8490.

Mifflin SW (1997) Short-term potentiation of carotid sinus nerve inputs to neurons in the nucleus of the solitary tract. Respir Physiol 110:229-236.

Miller AJ, McKoon M, Pinneau M, Silverstein R (1983) Postnatal synaptic development of the rat. Brain Res 284:205-213.

Mowla SJ, Farhadi HF, Pareek S, Atwal JK, Morris SJ, Seidah NG, Murphy RA (2001) Biosynthesis and post-translational processing of the precursor to brain-derived neurotrophic factor. J Biol Chem 276:12660-12666.

Muller CM, Best J (1989) Ocular dominance plasticity in adult cat visual cortex after transplantation of cultured astrocytes. Nature 342:427-430.

Niell CM, Meyer MP, Smith SJ (2004) In vivo imaging of synapse formation on a growing dendritic arbor. Nat Neurosci 7:254-260.

Ohira K, Hayashi M (2009) A New Aspect of the TrkB Signaling Pathway in Neural Plasticity. Curr Neuropharmacol 7:276-285.

Pamidimukkala J, Hay M (2001) Frequency dependence of endocytosis in aortic baroreceptor neurons and role of group III mGluRs. Am J Physiol Heart Circ Physiol 281:H387-395.

Pang PT, Teng HK, Zaitsev E, Woo NT, Sakata K, Zhen S, Teng KK, Yung WH, Hempstead BL, Lu B (2004) Cleavage of proBDNF by tPA/plasmin is essential for long-term hippocampal plasticity. Science 306:487-491.

Parrish JZ, Emoto K, Kim MD, Jan YN (2007) Mechanisms that regulate establishment, maintenance, and remodeling of dendritic fields. Annu Rev Neurosci 30:399-423.

Pecchi E, Dallaporta M, Charrier C, Pio J, Jean A, Moyse E, Troadec JD (2007) Glial fibrillary acidic protein (GFAP)-positive radial-like cells are present in the vicinity of proliferative progenitors in the nucleus tractus solitarius of adult rat. J Comp Neurol 501:353-368.

Pezet S, McMahon SB (2006) Neurotrophins: Mediators and Modulators of Pain. Annu Rev Neurosci.

Pilowsky PM, Goodchild AK (2002) Baroreceptor reflex pathways and neurotransmitters: 10 years on. J Hypertens 20:1675-1688.

Polleux F, Morrow T, Ghosh A (2000) Semaphorin 3A is a chemoattractant for cortical apical dendrites. Nature 404:567-573.

Poo MM (2001) Neurotrophins as synaptic modulators. Nat Rev Neurosci 2:24-32.

Procko C, Shaham S (2010) Assisted morphogenesis: glial control of dendrite shapes. Curr Opin Cell Biol 22:560-565.

Quigley KS, Myers MM, Shair HN (2005) Development of the baroreflex in the young rat. Auton Neurosci 121:26-32.

Radziejewski C, Robinson RC, DiStefano PS, Taylor JW (1992) Dimeric structure and conformational stability of brain-derived neurotrophic factor and neurotrophin-3. Biochemistry 31:4431-4436.

Ramon y Cajal S (1897) Histology of the Nervous System of Man and Vertebrates, 1995 Edition. New York: Oxford University Press.

Rao H, Pio J, Kessler JP (1999) Postnatal development of synaptophysin immunoreactivity in the rat nucleus tractus solitarii and caudal ventrolateral medulla. Brain Res Dev Brain Res 112:281-285.

Reynolds PJ, Fan W, Andresen MC (2006) Capsaicin-resistant arterial baroreceptors. J Negat Results Biomed 5:6.

Rinaman L, Levitt P (1993) Establishment of vagal sensorimotor circuits during fetal development in rats. J Neurobiol 24:641-659.

Rodriguez-Tebar A, Dechant G, Gotz R, Barde YA (1992) Binding of neurotrophin-3 to its neuronal receptors and interactions with nerve growth factor and brain-derived neurotrophic factor. EMBO J 11:917-922.

Sapru HN, Krieger AJ (1977) Carotid and aortic chemoreceptor function in the rat. J Appl Physiol 42:344-348.

Sapru HN, Gonzalez E, Krieger AJ (1981) Aortic nerve stimulation in the rat: cardiovascular and respiratory responses. Brain Res Bull 6:393-398.

Schecterson LC, Bothwell M (1992) Novel roles for neurotrophins are suggested by BDNF and NT-3 mRNA expression in developing neurons. Neuron 9:449-463.

Schecterson LC, Bothwell M (2010) Neurotrophin receptors: Old friends with new partners. Dev Neurobiol 70:332-338.

Scheuer DA, Zhang J, Toney GM, Mifflin SW (1996) Temporal processing of aortic nerve evoked activity in the nucleus of the solitary tract. J Neurophysiol 76:3750-3757.

Schild JH, Clark JW, Canavier CC, Kunze DL, Andresen MC (1995) Afferent synaptic drive of rat medial nucleus tractus solitarius neurons: dynamic simulation of graded vesicular mobilization, release, and non-NMDA receptor kinetics. J Neurophysiol 74:1529-1548.

Schild JH, Clark JW, Hay M, Mendelowitz D, Andresen MC, Kunze DL (1994) A- and C-type rat nodose sensory neurons: model interpretations of dynamic discharge characteristics. J Neurophysiol 71:2338-2358.

Schreihofer AM, Guyenet PG (2002) The baroreflex and beyond: control of sympathetic vasomotor tone by GABAergic neurons in the ventrolateral medulla. Clin Exp Pharmacol Physiol 29:514-521.

Seagard JL, Hopp FA, Drummond HA, Van Wynsberghe DM (1993) Selective contribution of two types of carotid sinus baroreceptors to the control of blood pressure. Circ Res 72:1011-1022.

Segar JL (1997) Ontogeny of the arterial and cardiopulmonary baroreflex during fetal and postnatal life. Am J Physiol 273:R457-471.

Seller H, Illert M (1969) The localization of the first synapse in the carotid sinus baroreceptor reflex pathway and its alteration of the afferent input. Pflugers Arch 306:1-19.

Singh KK, Park KJ, Hong EJ, Kramer BM, Greenberg ME, Kaplan DR, Miller FD (2008) Developmental axon pruning mediated by BDNF-p75NTR-dependent axon degeneration. Nat Neurosci 11:649-658.

Smith BN, Dou P, Barber WD, Dudek FE (1998) Vagally evoked synaptic currents in the immature rat nucleus tractus solitarii in an intact in vitro preparation. J Physiol 512 (Pt 1):149-162.

Soukhova-O'Hare GK, Cheng ZJ, Roberts AM, Gozal D (2006) Postnatal intermittent hypoxia alters baroreflex function in adult rats. Am J Physiol Heart Circ Physiol 290:H1157-1164.

Stevens B (2008) Neuron-astrocyte signaling in the development and plasticity of neural circuits. Neurosignals 16:278-288.

Stevens B, Allen NJ, Vazquez LE, Howell GR, Christopherson KS, Nouri N, Micheva KD, Mehalow AK, Huberman AD, Stafford B, Sher A, Litke AM, Lambris JD, Smith SJ, John SW, Barres BA (2007) The classical complement cascade mediates CNS synapse elimination. Cell 131:1164-1178.

Stornetta RL, Guyenet PG (1999) Distribution of glutamic acid decarboxylase mRNA-containing neurons in rat medulla projecting to thoracic spinal cord in relation to monoaminergic brainstem neurons. J Comp Neurol 407:367-380.

Stornetta RL, Sevigny CP, Guyenet PG (2002) Vesicular glutamate transporter DNPI/VGLUT2 mRNA is present in C1 and several other groups of brainstem catecholaminergic neurons. J Comp Neurol 444:191-206.

Takashima S, Becker LE (1985) Developmental abnormalities of medullary "respiratory centers" in sudden infant death syndrome. Exp Neurol 90:580-587.

Talman WT, Perrone MH, Reis DJ (1980) Evidence for L-glutamate as the neurotransmitter of baroreceptor afferent nerve fibers. Science 209:813-815.

Tashiro Y, Kawai Y (2007) Glial coverage of the small cell somata in the rat nucleus of tractus solitarius during postnatal development. Glia 55:1619-1629.

Teng HK, Teng KK, Lee R, Wright S, Tevar S, Almeida RD, Kermani P, Torkin R, Chen ZY, Lee FS, Kraemer RT, Nykjaer A, Hempstead BL (2005) ProBDNF induces neuronal apoptosis via activation of a receptor complex of p75NTR and sortilin. J Neurosci 25:5455-5463.

Teng KK, Felice S, Kim T, Hempstead BL (2010) Understanding proneurotrophin actions: Recent advances and challenges. Dev Neurobiol 70:350-359.

Thoenen H (1995) Neurotrophins and neuronal plasticity. Science 270:593-598.

Thoren P, Saum WR, Brown AM (1977) Characteristics of rat aortic baroreceptors with nonmedullated afferent nerve fibers. Circ Res 40:231-237.

Todd KJ, Darabid H, Robitaille R (2010) Perisynaptic glia discriminate patterns of motor nerve activity and influence plasticity at the neuromuscular junction. J Neurosci 30:11870-11882.

Vermehren-Schmaedick A, Balkowiec A (2009) Pattern- and promoter-specific regulation of BDNF mRNA expression in nodose ganglion neurons stimulated with physiological patterns of baroreceptor activity. . In: Society for Neuroscience Abstracts 2009, 710.3.

Vilar M, Charalampopoulos I, Kenchappa RS, Reversi A, Klos-Applequist JM, Karaca E, Simi A, Spuch C, Choi S, Friedman WJ, Ericson J, Schiavo G, Carter BD, Ibanez CF (2009) Ligand-independent signaling by disulfide-crosslinked dimers of the p75 neurotrophin receptor. J Cell Sci 122:3351-3357.

Vincent A, Tell F (1997) Postnatal changes in electrophysiological properties of rat nucleus tractus solitarii neurons. Eur J Neurosci 9:1612-1624.

Vincent A, Tell F (1999) Postnatal development of rat nucleus tractus solitarius neurons: morphological and electrophysiological evidence. Neuroscience 93:293-305.

Wang DD, Bordey A (2008) The astrocyte odyssey. Prog Neurobiol 86:342-367.

Wetmore C, Olson L (1995) Neuronal and nonneuronal expression of neurotrophins and their receptors in sensory and sympathetic ganglia suggest new intercellular trophic interactions. J Comp Neurol 353:143-159.

Withers GS, Higgins D, Charette M, Banker G (2000) Bone morphogenetic protein-7 enhances dendritic growth and receptivity to innervation in cultured hippocampal neurons. Eur J Neurosci 12:106-116.

Woo NH, Teng HK, Siao CJ, Chiaruttini C, Pang PT, Milner TA, Hempstead BL, Lu B (2005) Activation of p75NTR by proBDNF facilitates hippocampal long-term depression. Nat Neurosci 8:1069-1077.

Wu GY, Zou DJ, Rajan I, Cline H (1999) Dendritic dynamics in vivo change during neuronal maturation. J Neurosci 19:4472-4483.

Xie PL, McDowell TS, Chapleau MW, Hajduczok G, Abboud FM (1991) Rapid baroreceptor resetting in chronic hypertension. Implications for normalization of arterial pressure. Hypertension 17:72-79.

Yan Q, Radeke MJ, Matheson CR, Talvenheimo J, Welcher AA, Feinstein SC (1997) Immunocytochemical localization of TrkB in the central nervous system of the adult rat. J Comp Neurol 378:135-157.

Yang J, Siao CJ, Nagappan G, Marinic T, Jing D, McGrath K, Chen ZY, Mark W, Tessarollo L, Lee FS, Lu B, Hempstead BL (2009) Neuronal release of proBDNF. Nat Neurosci 12:113-115.

Yen JC, Chan JY, Chan SH (1999) Differential roles of NMDA and non-NMDA receptors in synaptic responses of neurons in nucleus tractus solitarii of the rat. J Neurophysiol 81:3034-3043.

Zhang J, Mifflin SW (1998) Differential roles for NMDA and non-NMDA receptor subtypes in baroreceptor afferent integration in the nucleus of the solitary tract of the rat. J Physiol 511 (Pt 3):733-745.

Zhang LL, Ashwell KW (2001) The development of cranial nerve and visceral afferents to the nucleus of the solitary tract in the rat. Anat Embryol (Berl) 204:135-151.

Zhang W, Mifflin SW (1995) Excitatory amino-acid receptors contribute to carotid sinus and vagus nerve evoked excitation of neurons in the nucleus of the tractus solitarius. J Auton Nerv Syst 55:50-56.

Zhang Y, Barres BA (2010) Astrocyte heterogeneity: an underappreciated topic in neurobiology. Curr Opin Neurobiol 20:588-594.

Zhou XF, Rush RA (1996) Endogenous brain-derived neurotrophic factor is anterogradely transported in primary sensory neurons. Neuroscience 74:945-953.

Zhou XF, Chie ET, Rush RA (1998) Distribution of brain-derived neurotrophic factor in cranial and spinal ganglia. Exp Neurol 149:237-242.

Zhou Z, Champagnat J, Poon CS (1997) Phasic and long-term depression in brainstem nucleus tractus solitarius neurons: differing roles of AMPA receptor desensitization. J Neurosci 17:5349-5356.